THE DEVELOPMENT OF A FUNCTIONAL WHOLE BLOOD ASSAY TO ASSESS THE PRIMING OF PLATELETS BY SURFACE BOUND AGONISTS

by

Colin David Eichinger

A dissertation submitted to the faculty of
The University of Utah
in partial fulfillment of the requirements for the degree of

Doctor of Philosophy

Department of Bioengineering

The University of Utah

May 2016

The University of Utah Graduate School

STATEMENT OF DISSERTATION APPROVAL

The dissertation of **Colin Eichinger**

has been approved by the following supervisory committee members:

Vladimir Hlady	, Chair	**2/18/2016** Date Approved
David W. Grainger	, Member	**2/18/2016** Date Approved
Aaron L. Fogelson	, Member	**2/18/2016** Date Approved
Marc D. Porter	, Member	**2/18/2016** Date Approved
Bruce K. Gale	, Member	**2/18/2016** Date Approved

and by **Patrick A. Tresco**, Chair/Dean of

the Department/College/School of **Bioengineering**

and by David B. Kieda, Dean of The Graduate School.

ABSTRACT

Platelet-surface interactions are a key mediator in a host's response to vascular biomaterials. Directly after implantation, a wide variety of serum proteins are adsorbed onto the surface of vascular devices, many of which activate platelets. Serving as the first step in the coagulation cascade, the local activation of platelets sets off a chain of events that can ultimately determine the fate of implanted vascular devices. Many material engineering approaches have been taken in an effort to reduce this activation; however, the most successful method to date remains the systemic delivery of antiplatelet and anticoagulant agents. The prevalence of antiplatelet pharmaceutics, coupled with a variation in efficacy across a diverse population, has led to an industry focused on the personalized assessment of platelet function.

In this dissertation, methods were developed to address a deficiency in the current approach to platelet function testing. No current assays take into account the transient interactions of platelets with agonist surfaces, interactions that have the capability to prime a platelet population for enhanced adhesion and activation downstream of a stimulus. This phenomenon was leveraged here to create a flow cell in which the upstream priming of a platelet population by a surface-bound agonist could be assessed by downstream capture assay. It was demonstrated that this device is capable of determining the response of a platelet population to a variable priming stimulus, both alone and in the presence of common antiplatelet agents. To further investigate the priming response of platelets, it was

of interest to develop a method by which to pattern multiple proteins on the same surface, thus enabling the measurement of the platelet population response to multiple surface bound agonists. Taking advantage of advances in microcontact printing and modern light microscopy, a new method by which to deposit multiple aligned patterns of agonists on a single substrate was developed. This patterning method was then used to investigate the ability of multiple agonists to prime platelets in flowing blood and observe the synergistic response that platelets exhibit when primed by multiple pathways.

Taken collectively, these experiments contribute to the field of platelet activation by providing a controlled environment in which to study the priming response of platelets following transient exposure to surface bound agonists. This assay provides a platform in which the platelet response to a variety of surface coatings, biomaterials, and antiplatelet agents can be explored, and establishes a foundation for the further investigation of priming pathways in platelets.

TABLE OF CONTENTS

LIST OF FIGURES

LIST OF ABBREVIATIONS

α2β1 ..... integrin α2β1

ADP ..... adenosine diphosphate

AFM ..... atomic force microscopy

ASA ..... acetylsalicylic acid

CCD ..... charge coupled device

COX ..... cyclooxygenase

CPA ..... cone and plate analyzer

CVD ..... cardiovascular disease

DAPI ..... 4',6-diamidino-2-phenylindole

DDI ..... distilled deionized

DIC ..... differential interference contrast

DMEM ..... Dulbecco's modified Eagle medium

DPN ..... dip pen nanolithography

ECM ..... extracellular matrix

FBS ..... fetal bovine serum

GFOGER ..... Gly-Phe-Hyp-Gly-Glu-Arg

GPIb ..... glycoprotein Ib

GPIb-IX-V ..... glycoprotein Ib-IX-V complex

GPIIb/IIIa ..... glycoprotein IIb/IIIa complex

GPVI ..... glycoprotein VI

GPO..... Gly-Pro-Hyp

LTA.....light transmission aggregometry

$P2Y_{12}$.....platelet $P2Y_{12}$ receptor

PBS ..... phosphate-buffered saline

PCI .....percutaneous coronary intervention

PDMS.....polydimethylsiloxane

PKC..... protein kinase C

PLC .....phospholipase C

PPACK.....Phe-Pro-Arg-cholоromethylketone

PRP ..... platelet rich plasma

RGD .....Arginine-Glycine-Aspartate

RICM .....reflectance interference contrast microscopy

TNFα.....tumor necrosis factor

TXA2 .....thromboxane A2

μCP .....microcontact printing

VASP ..... vasodilator stimulated phosphorylation

vWF..... von Willebrand factor

ACKNOWLEDGEMENTS

First and foremost, I would like to thank my research advisor, Dr. Vladimir Hlady, for his unwavering support throughout my graduate career. Under your guidance, I have been continually challenged to become a better scientist and have developed a renewed passion for scientific investigation. I would also like to thank the members of my advisory committee: Dr. David Grainger, Dr. Aaron Fogelson, Dr. Marc Porter, and Dr. Bruce Gale. Your feedback and support have greatly helped shape these research endeavors.

I would be remiss if I did not also acknowledge the considerable contributions that other members of the research community have made to this work. Hlady research group members Dr. Lindsey Corum, Dr. Kate Job, Dr. Tony Hsiao, Dr. Vimal Swarup, Krystin Meidell, Dalton Ostler, Chris Eixenberger, Shekh Rahman, and Holly Grigsby have all assisted in a multitude of ways, including mentorship and guidance, experimental support, and writing assistance. Additionally, I would like to thank the members of the Zimmerman/Weyrich lab, especially Dr. Robert Campbell, for providing human blood samples for this work.

Finally, I would like to thank my family who have been an indispensable source of inspiration and support throughout my educational career.

CHAPTER 1

INTRODUCTION

Cardiovascular disease is currently the leading cause of mortality in the world, and accounts for nearly one in three deaths.[1] In developed nations, this figure increases to over 40 % of all deaths, resulting in a large societal and economic burden.[2] It is estimated that the United States spent over $444 billion on cardiovascular disease (CVD) treatment, medication, and lost productivity in 2010 alone, accounting for 1 in every 6 dollars spent on healthcare.[3,4] Considering the growing rates of obesity and type II diabetes in the United States – coupled with an increasing life expectancy – the incidence of CVD is expected to rise by 10 % over the next 20 years.[5]

CVD often cannot be fully managed by diet and pharmaceutics alone, and surgical intervention remains a final option for patients. The total number of inpatient cardiovascular procedures in the United States exceeded 7.5 million in 2010, often involving the implantation of devices such as catheters, stents, vascular grafts, and heart valves.[6] Coupled with the life-saving efficacy of these devices are complications arising from blood-material interactions.[7,8] In fact, patients receiving implanted vascular devices are at significantly higher risk of thrombotic events irrespective of device success or failure.[9] Platelets in particular interact with proteins adhered to implanted surfaces and greatly increase the risk of device occlusion or embolism.[10,11] As such, it has become

compulsory for patients receiving blood contacting devices to be placed on anticoagulant and/or antiplatelet medications in order to mitigate risks.[12] These medications come with a considerable reduction in quality of life, and their administration often must be sustained for the life of the patient.[13–15] There also exists a significant proportion of the population that can be categorized as low- or nonresponders to commonly administered antiplatelet therapies, necessitating the clinical use of platelet activity tests to tailor therapeutic approaches.[16–18]

This introduction presents an overview of the biology of platelets, their interaction with proteins present on thrombogenic surfaces, and their subsequent adhesion and activation. The concept of platelet priming is introduced, along with potential clinical complications related to implanted medical devices. Additionally, common antiplatelet therapies are reviewed and the implications of low- or nonresponders are addressed. The current methods of testing platelet activity are then discussed and the need for new testing methods is presented. Finally, a rationale for this work and an outline of the three main studies contained in this dissertation are provided.

1.1 Platelets

Platelets are small, anucleate cells that perform the primary function of hemostasis by initiating the clotting process at sites of vessel injury. Derived from large megakaryocytes in the bone marrow, platelets circulate throughout the bloodstream at concentrations of between 150,000 and 400,000 cells per μL of blood.[19,20] The typical lifespan of platelets in circulation is 8 to 9 days, after which they are phagocytosed in the spleen or liver.[21]

Circulating platelets are 2-3 μm in diameter and discoid in shape. While they lack a nucleus and genomic DNA, they do have a dynamic proteome.[19] Genetic information in the form of completed mRNA is inherited from precursor megakaryocytes and contained in the mitochondria. Protein expression is then carried out by the endoplasmic reticulum and ribosomes. Quiescent circulating platelets have low levels of protein translation, whereas this process is upregulated in platelets that have been activated through any of a variety of signaling pathways. Platelets also contain an active actin cytoskeleton which aids in attachment and spreading at sites of injury.

1.1.1 Platelet Function

The primary function of platelets is to identify sites of vessel injury and initiate the clotting cascade. When first encountering a damaged vessel, platelets recognize proteins present in the exposed subendothelium and arrest on the vessel surface.[22–24] In the case of implanted biomaterials, platelets recognize adsorbed blood proteins and attach to the surface of the device.[25–27] Once stationary, platelets undergo a morphological change from their discoid, circulating state to a spread, activated state.[28] This morphological change is accompanied by the activation of a variety of internal signaling pathways as well as the release of the contents of α- and dense granules.[29] The contents of these granules include growth factors, clotting proteins, activation molecules, and adhesion receptors, all of which serve to upregulate the local hemostatic response.[30] This response is a crucial part of hemostasis in the case of a vessel injury, but poses a significant challenge for the biocompatibility of implanted devices. The thrombotic response of platelets can interfere with the function of a device (*e.g.*, the occlusion of a small diameter stent) and greatly

increases the risk of complications such as embolism and stroke.[31,32] As such, the adhesion of platelets to surfaces has been a key focus of research into biomaterial hemocompatibility.

1.1.2 Platelet Adhesion

Platelets adhere to surfaces, both natural and artificial, through interactions between receptors expressed on platelet membranes and molecules present at the surface of interaction. In the case of vessel injury, the two primary proteins of interest are von Willebrand factor (vWF) and collagen, while vWF and fibrinogen are the main mediating factors for artificial surfaces.[33,34] After vessel injury, the extracellular matrix (ECM) of the vasculature is exposed to the circulating bloodstream. Collagen, the most abundant protein in the ECM and an integral part of the vascular basement membrane, then binds with circulating vWF. Short-term interactions with vWF serve to slow down platelets from flow and allow more stable bonds with collagen to occur. Similarly, adsorbed vWF serves to slow platelets near the surface of biomaterials, which then allows stable bonds to form with adsorbed fibrinogen. Figure 1.1 illustrates the main mechanisms of interaction between platelets and both vessel lesions and biomaterials.

1.1.2.1 The Adhesive Role of von Willebrand Factor

Von Willebrand factor is a large (500-20,000 kDa) multimeric protein that circulates in the blood plasma at a concentration of 10 μg/mL.[19] It is also found in the Weibel-Palade bodies of endothelial cells, the α-granules of platelets, and in endothelial ECM, all of which can be released or exposed at sites of injury and promote adhesion.[35–37]

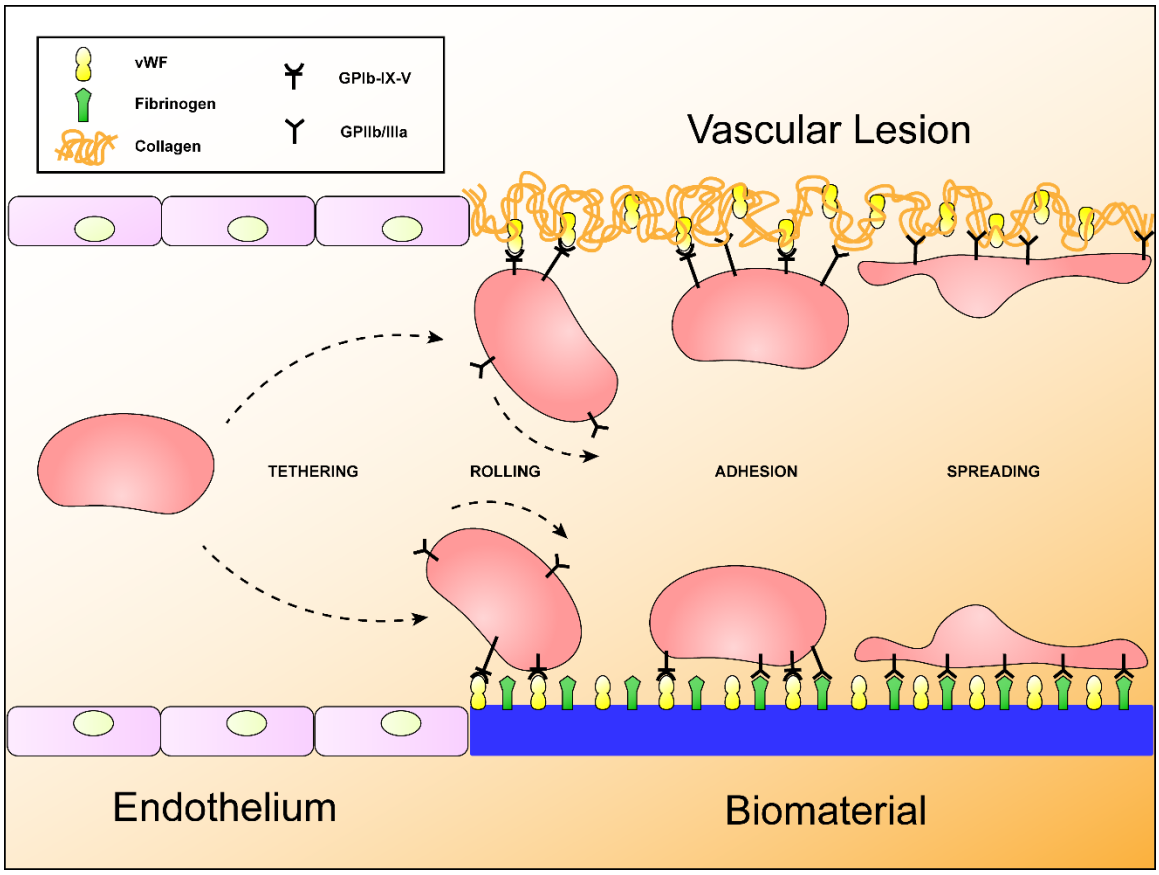

Figure 1.1: Diagram of platelet interactions with vessel lesions and biomaterials. Platelets first tether to the surface and then roll through short-term interactions between GPIb-IX-V and von Willebrand factor. Stronger bonds between GPIIb/IIIa and fibrinogen or collagen allow for stable adhesion and spreading.

VWF binds to platelets through the glycoprotein receptor complexes GPIb-IX-V and GPIIb/IIIa as well as to exposed collagen through the GPIb receptor.[38–40]

The primary role of vWF during platelet adhesion is to slow circulating platelets enough to allow them to form more stable bonds in a process known as "platelet tethering." Soluble vWF does not interact strongly with the platelet GPIb-IX-V receptor complex, but once adsorbed to a surface, exposed to high shear, or bound to collagen, vWF undergoes a conformational change that exposes its A1 domain, enabling platelet binding.[41,42] Interestingly, vWF has also been shown to mediate platelet-surface interactions at low shear rates.[43] Immobilized vWF and the platelet expressed GPIb-IX-V complex have unusual short-term interactions known as catch bonds.[44–46] These bonds are shear strengthening, that is, the bond duration increases as increasing tensile force is applied, allowing platelets to be captured by surfaces from high-shear flow conditions. [34,47–49] Once platelets are slowed down, the diminished bond strength and its high on/off rate, coupled with the torque applied by flowing blood, cause platelets to roll or translocate along the surface. This rolling interaction keeps platelets in the vicinity of the surface and permits stronger bonds to form between platelets and collagen or fibrinogen.

Binding to the GPIb-IX-V complex also serves as an outside-in method of signal transduction, which ultimately results in the activation of platelet GPIIb/IIIa receptors.[50,51] These lead to the arrest and stable adhesion of platelets on procoagulant surfaces through the binding of activated GPIIb/IIIa receptors to the RGD (Arginine-Glycine-Aspartate) sequence in the C1 domain of vWF as well as the RGD sequences in fibrinogen and collagen.[52]

1.1.2.2 The Adhesive Role of Collagen

Collagen is the most abundant protein in the vascular ECM. Platelets can adhere to monomeric collagen, but the fibrillar variants, particularly types I, III, and IV (which give structural support to resident endothelial cells), play a pivotal role in the adhesion of platelets. Platelets have four receptors associated with collagen: GPVI and integrin α2β1, which bind directly to collagen, and GPIIb/IIIa and the GPIb complex, which bind to vWF associated with collagen as described above.[53–55]

Under static conditions, collagen is able to capture and activate platelets without the assistance of cofactors; however, under the conditions of flow that exist in circulation, vWF plays an essential role in supporting platelet adhesion and activation.[56] VWF and collagen have been shown to have a high affinity for one another in their native states.[57,58] This interaction is mediated by the A3 domain of vWF and a 9 residue binding sequence within collagen.[59–61] This close association between vWF and collagen allows for the tethering of platelets to vWF while stronger long-term bonds are formed with collagen.[62]

GPVI is a platelet glycoprotein in the immunoglobulin superfamily that binds directly to collagen through the repeated Gly-Pro-Hyp (GPO) sequence.[63] This low-affinity binding causes the clustering of GPVI receptors and initiates a tyrosine phosphorylation signaling cascade resulting in the activation of integrin α2β1, as well as initiating platelet activation.[64] Integrin α2β1 is a type I transmembrane glycoprotein that typically exists in an inactivated state on the platelet membrane. Once activated by the binding of collagen to GPVI, α2β1 transitions from a low-affinity conformation to a high conformation and binds to the Gly-Phe-Hyp-Gly-Glu-Arg (GFOGER) sequence on collagen through its α2-I domain.[65] These two receptors work collectively in a two-site two-step model to support

the stable adhesion of platelets to exposed subendothelium and initiate further signaling cascades leading to activation.[66]

1.1.2.3 The Adhesive Role of Fibrinogen

Fibrinogen, primarily known for its role in hemostasis as the precursor to fibrin, can also mediate platelet adhesion to implanted surfaces.[67] After the introduction of a blood contacting device, proteins from blood rapidly adsorb to the surface.[68,69] Circulating at a concentration of 1.5-3 mg/mL, fibrinogen makes up approximately 7 % of the blood protein content and due to charge interactions, has a high surface affinity for implanted biomaterials.[70,71] In its native state, fibrinogen does not interact with quiescent platelets; however, once adhered to a surface, it denatures and RGD sites are exposed, leading to platelet recognition and activation.[72–74]

As with collagen, the interplay between vWF (also adsorbed from plasma) and fibrinogen facilitates stable adhesion.[62,75] Once tethered and rolling on the surface, platelets bind to fibrinogen through activated GPIIb/IIIa to form stable adhesions.[76]

1.1.3 Platelet Activation

Platelet activation can occur from a variety of stimuli, including (1) exposure to soluble agonists such as thrombin, adenosine diphosphate (ADP), and platelet activating factor; (2) adhesion to exposed ECM in injured vessels; (3) adhesion to blood proteins adsorbed to artificial surfaces; and (4) physical forces such as high shear stresses. With the exception of shear forces, each of these activation processes is characterized by the binding of an agonist to a specific receptor on the platelet membrane, leading to both intra- and extracellular signaling. Platelet activation is characterized by a number of internal cellular

processes, including the transformation of surface adhesion receptors from resting to active states, the adhesion to and spreading on thrombotic surfaces, and the release of the contents of α- and dense granules.[77,78]

Quiescent platelets have a very low affinity for plasma proteins such as fibrinogen or vWF. During platelet activation, however, the GPIIb/IIIa receptor undergoes a conformational change from a low-affinity to a high-affinity state. This allows the binding of soluble and insoluble factors and aids in the aggregation of platelets at the site of injury. Active GPIIb/IIIa also allows stable bonds to form between platelets and vWF, collagen, and fibrinogen, causing platelets to spread along the surface.[19,79] Spreading is a rapid morphological change in which a discoid shaped platelet extends filopodia across a thrombogenic surface. Early stage spreading platelets are characterized by numerous dendritic extensions, while fully spread platelets take on a more rounded, or 'fried egg' shape. Figure 1.2 is a differential interference contrast (DIC) image that shows platelets in various stages of spreading on a thrombogenic surface.

Accompanying this spreading is the release of the contents of platelet granules. Degranulation occurs when platelet granules merge with the cell membrane and release their contents into the bloodstream, which act to enhance the activation response. Contents of α-granules include the surface receptor P-Selectin; platelet agonists such as vWF, fibronectin, and fibrinogen; as well as prothrombotic agents like platelet factor 4, factor V, and factor XIII, while dense granules contain ADP and calcium, both potent platelet agonists.[80] Through activation and subsequent aggregation on a thrombogenic surface, platelets serve to enhance the clotting response via these chemical signals.

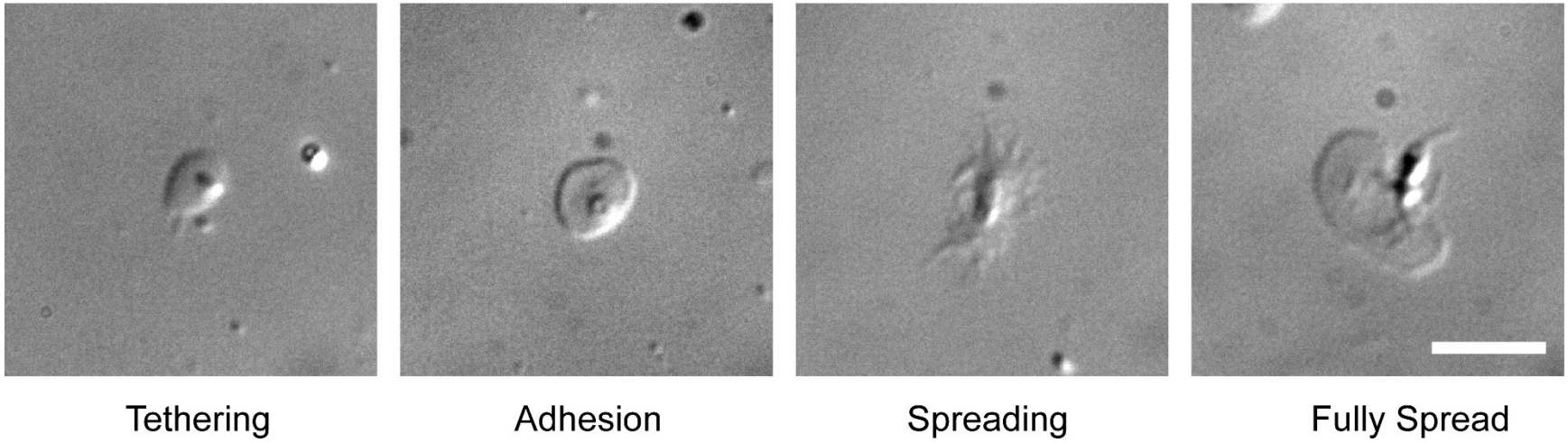

Figure 1.2: DIC images of platelets spreading on a fibrinogen-coated glass surface. Platelets initially tether to the surface, then form stable adhesions through interactions between GPIIb/IIIa and GPIb-IX-V and surface adhered proteins. Next, they extend numerous filipodia which serve to increase surface contacts. Finally, these filipodia coalesce into circular lamellae as the platelet becomes fully spread. Scale bar represents 8 μm.

1.1.4 Platelet Priming

A relatively new concept in the field of platelet biology is that of "priming." This term describes the change in response of an excitable cell type to an agonist that is affected by prior exposure to a mediator. Examples of priming have been previously observed in various cell types such as neutrophils and myocytes, but have only recently been observed in platelets. Recent studies have shown that interactions with certain molecules do not fully activate platelets, but do increase their propensity to become active when exposed to an agonist at a later time. Thus, it is said that these molecules "prime" platelets for activation.[81] A wide variety of molecules have been identified that prime platelets, including proteins, hormones, cytokines, and chemokines.[82] It is also known that the majority of platelets that contact an injury site or biomaterial do not adhere and continue to be swept downstream with the circulation.[75,83] *It is therefore likely that transient interactions between platelets and agonist-covered surfaces create a primed platelet population, a population that has a higher propensity to activate and adhere when exposed to a subsequent downstream stimulus.* Studies done by Corum *et al.* lend support to this theory as they demonstrate that the introduction of a surface adhered platelet agonist is sufficient to prime platelets for enhanced adhesion at a downstream location.[84,85]

Additional support can be found though computer simulation of platelet activation dynamics using models developed by the Fogelson group.[86,87] These models account for many mechanical and chemical interactions between platelets, soluble species, and vessel walls. Designed for small vessels or flow chambers, these models utilize an immersed boundary approach to track hundreds of platelets and their interactions with their surroundings. Also accounted for are fluid concentrations of activating species secreted by

platelets or activating sites on vessel walls. Figure 1.3 shows the result of a simulation in which two platelet activating sites are input into the same model.[88] Interestingly, the downstream site is seen to have a much greater concentration of unbound activated platelets in its vicinity than the upstream one. These results also suggest that the history of transient contact of platelets with an upstream activating region can be carried downstream as an altered or primed state.

The phenomenon of platelet priming has significant clinical implications, especially dealing with the implantation of vascular devices. In addition to material concerns, the two sites of anastomosis in a vascular graft may serve as priming regions for platelets. Platelets entering through the proximal end of a device encounter a disrupted endothelium due to the suturing of the device to the native vessel and may become primed after interacting with exposed agonists. Platelets flowing through the device might then demonstrate an elevated activation response, *regardless of the thrombogenicity of the device surface*. The distal end of the device could therefore serve as a nucleus for enhanced platelet activation. Indeed, it has been shown that in the case of coronary bypass grafts, 89 % of early failures were due to narrowing at the distal anastomosis.[89] A similar trend was also observed in a multicenter prospective study of arteriovenous grafts in which 29 % of cases presented with inflow stenosis, while 100 % of cases exhibited stenosis on the distal end of the device.[90]

Additionally, it has long been known that in the case of vascular grafts implanted in vessels with high shear rates (*e.g.*, aorta, femoral arteries), the material chosen is of little consequence, while in the case of lower shear rates (*e.g.*, coronary arteries), the implanted material is of the utmost importance.[91] The currently accepted theory posits that shear

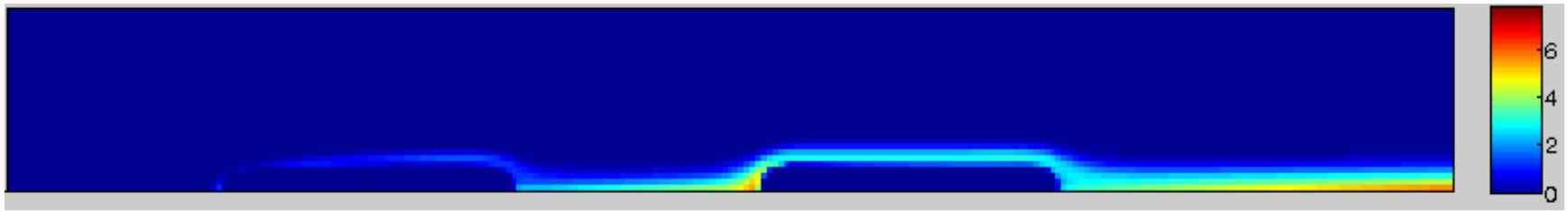

Figure 1.3: Spatial distribution of activated platelets from a two-lesion simulation. The color distribution represents the number of active but unbound platelets after 600 s of flow (from left to right) past two priming regions. Note the higher concentration of active platelets near the downstream priming region and further downstream. (Figure courtesy of Dr. Liederman and Dr. Fogelson[88])

forces, quantified by a term known as the thrombotic threshold velocity, inhibit the formation of thrombi in larger vessels.[92] It might also possible that platelets primed as they enter these grafts are not resident long enough to become fully activated, while those primed as they enter lower shear vessels are given the chance to adhere and activate on the surface of the device, leading to occlusion.

Platelet priming is a recently discovered phenomenon that could have far reaching consequences in the fields of medical device design, vascular surgery, and perioperative care. It has become clear that the spatial distribution of platelet agonists is an important factor in flowing systems and must be taken into account when predicting clinical outcomes.

1.2 Antiplatelet Therapies

Unwanted activation of platelets is a large cause of morbidity and mortality in the Western world. As such, a large amount of effort has been put into developing pharmaceutic interventions to mitigate platelet activation pathways. Three classes of antiplatelet agents are currently approved for clinical use: cyclooxygenase (COX) inhibitors, ADP $P2Y_{12}$ receptor antagonists, and GPIIb/IIIa inhibitors.[93,94]

1.2.1 Cyclooxygenase Inhibitors

This category of antiplatelet agents, of which acetylsalicylic acid (ASA) (Aspirin®, Bayer) is the most common, act by inhibiting COX-1 and COX-2, enzymes that are responsible for the production of potent platelet agonists.[95] COX catalyzes the conversion of arachidonic acid to prostaglandin H_2, which in turn is converted into several compounds

including thromboxane A2 (TXA2). TXA2 activates platelets by binding to a G-protein coupled receptor on the surface of platelets and increasing the expression of GPIIb/IIIa on the cell membrane. ASA functions by diffusing into the catalytic site for the COX enzymes and acetylating a key serine residue, which prevents arachidonic acid from being catabolized.

Low doses of ASA are commonly prescribed either solo or in conjunction with another antiplatelet therapeutic as an approach to prevent secondary ischemic events in individuals receiving implanted vascular devices.[96] In fact, ASA is by and far the most prescribed drug for antiplatelet therapy. Part of ASA's popularity is tied to its mechanism of action; by permanently inhibiting the COX enzymes, its effect can only be reversed by the production of new platelets. Since the average life span of platelets is 8-10 days, only 10-12 % of platelets are replenished every 24 hours. This allows for a once a day dosing scheme, making for an approachable therapy for patients.

1.2.2 $P2Y_{12}$ Inhibitors

This class of antiplatelet agents acts on the platelet receptor for ADP, inhibiting the recognition of this potent agonist. Clopidogrel (Plavix®, Bristol-Myers Squibb) is one such drug that is widely prescribed and functions by binding irreversibly to the $P2Y_{12}$ receptor on the platelet membrane. This orally administered prodrug requires a two-step hepatic conversion to its active metabolite and therefore has a slow onset of therapeutic efficacy. As such, it is often recommended that clopidogrel be combined with ASA treatment to avoid adverse ischemic outcomes. Clopidogrel alone has been shown to be marginally more effective than ASA and is recommended to be prescribed only when there is an

allergy to ASA or an aggressive therapeutic strategy is necessary.[97] Despite its cost and limitations, clopidogrel is currently one of the best-selling antiplatelet agents.[98,99]

Cangrelor (Kengreal™, The Medicines Company) is another drug that acts on the ADP receptor and has only recently been approved by the FDA. This agent is a reversible antagonist of the $P2Y_{12}$ receptor.[100] As an active drug, it has a quick onset and fills a perioperative niche that clopidogrel cannot. Cangrelor is administered intravenously during percutaneous coronary interventions (PCI)s and has been shown to significantly reduce occurrence of myocardial infarction and stent thrombosis when compared to clopidogrel.[101,102]

1.2.3 GPIIb/IIIa Inhibitors

As with cangrelor, GPIIb/IIIa inhibitors are administered intravenously and therefore are only available in a perioperative setting. These drugs target the active conformation of GPIIb/IIIa that allows platelets to bind fibrinogen and von Willebrand factor, leading to platelet activation and aggregation. Three examples of GPIIb/IIIa inhibitors are abciximab (ReoPro®, Eli Lilly), eptifibatide (Integrilin®, Millennium Pharmaceuticals), and tirofiban (Aggrastat®, Medicure).[103] Abciximab is a monoclonal antibody that targets the GPIIb/IIIa receptor and inhibits its function. Eptifibatide is a cyclic heptapeptide and tirofiban is a synthetic nonpeptide, each of which binds reversibly to the GPIIb/IIIa receptor. These drugs have been approved for use during PCIs and the treatment of some acute coronary symptoms.

1.2.4 Inter-Patient Variability in Drug Response

No pharmaceutic therapy is fully efficacious across a diverse population, and ASA and clopidogrel – the two most commonly administered antiplatelet drugs – are no exception. There has been recent research into interpatient variability in response to each of these treatments.[93,104,105] Current figures estimate that therapy with ASA at recommended doses may be ineffectual in up to 30 % of patients.[18,106] This variation can be attributed to compounding inflammatory factors, elevated platelet turnover, and genetic variations of the COX receptors.[107–109] Similarly, the percentage of low responders to clopidogrel is estimated to be between 5 % and 40 % of the population, often attributed to genetic, cellular, and clinical variations.[17,110–112]

Treatment failure with each of these drugs can have serious adverse outcomes, including occlusion of grafts or stents, embolic events, myocardial infarction, and death. Since such a significant proportion of patients experience lower than expected efficacy with these treatments, this presents a huge clinical challenge. *Identification and monitoring of an individual patient's response to a particular antiplatelet therapy is therefore essential in a clinical setting.* Nonresponders in each case can be identified through the use of a variety of platelet function tests and therapy can be adjusted accordingly.

1.3 Platelet Function Tests

Traditionally, basic platelet function tests such as clotting time and aggregometry have been used to diagnose and monitor individuals with bleeding disorders.[113,114] As more research has come to light on the role that platelets perform in thrombosis, however, new applications and diagnostic methods have arisen. Platelet function tests are currently being

used to manage individuals who are taking a variety of antiplatelet drugs in both the acute perioperative and long-term care settings.[115,116] Each of these methods utilizes the current understanding of platelet biology to measure the activation of platelets in response to a provided stimulus and can be divided into four main categories: aggregation tests, shear-based adhesion tests, flow cytometry, and microfluidic assays.

1.3.1 Aggregation Tests

The first platelet function tests were based on the most obvious result of an active platelet population: aggregation. Once activated, platelets will stick to one another through the now high-affinity conformation of GPIIb/IIIa via intermediary plasma molecules such as fibrinogen or von Willebrand factor. The tendency of activated platelets to aggregate is used as a metric of platelet activity in assays such as light transmission aggregometry and VerifyNow® (Accriva Diagnostics).

1.3.1.1 Light Transmission Aggregometry

Light transmission aggregometry (LTA) has long been the gold standard of platelet function testing. LTA was invented in 1962 by Gustav Born, and was initially used to diagnose bleeding disorders.[117] Today, it remains one of the most commonly used tools to assess platelet activity.[118–120] In LTA, a suspension of platelet rich plasma (PRP, isolated from whole blood via centrifugation) is loaded into a cuvette between a light source and a detector. A platelet agonist is added to the cuvette, and the light transmission through the sample is measured over time. As platelets activate and aggregate, the opacity of the solution will decrease and the light transmission through the sample will increase.

Historically, the recorded value was the percentage of total aggregation (versus a sample of platelet poor plasma); however, recently, more sophisticated techniques have led to the interpretation of the dynamics of aggregation curves, allowing for more specific diagnoses.[118] One particular advantage of LTA is the ability to activate platelets with a variety of different agonists, allowing for the study of many activation pathways. Common agonists used include: ADP, collagen, epinephrine, arachidonic acid, and thrombin.[116]

Despite its widespread acceptance and use, LTA has greatly suffered from issues such as standardization of procedures and interpretation of results across laboratories.[121,122] The preparation of the sample (including selection of anticoagulant, isolation of PRP, and handling by laboratory staff) can greatly affect the results generated.[122] As such, there has been a recent effort to standardize the procedure through the publication of specific guidelines.[121,123,124] While LTA can be used to monitor and detect the effects of antiplatelet therapies, the requirement of a large sample volume, long preparation and test times, and specialized equipment make this test less than ideal for a clinical setting.

1.3.1.2 VerifyNow®

The VerifyNow® system (formally Ultegra Rapid Platelet Function Assay, Accriva) is a self-contained point of care test that utilizes the dynamics of aggregation to measure platelet activity. Whole blood from a patient is loaded into a cartridge that contains fibrinogen-coated beads and platelet agonists. This cartridge is then loaded between a light source and detector. Platelets aggregate onto the fibrinogen-coated beads proportionally to the number of GPIIb/IIIa receptors activated by the specific stimulus, and the light transmission through the sample is measured as the beads agglutinate.[125] A proprietary

algorithm is then used to convert the light transmission values into somewhat arbitrary "platelet aggregation units." This method was originally developed to monitor the efficacy of GPIIb/IIIa antagonists such as abciximab and eptifibatide as they will reduce platelet binding to fibrinogen.[126] Since the introduction of the GPIIb/IIIa antagonist test, two more cartridges have been developed, one to monitor ASA and one to monitor clopidogrel.

This system provides the ability to do rapid antiplatelet testing in an operative setting, allowing for the prediction and prevention of adverse cardiovascular events.[127] The system is expensive, however, and certain factors such as hematocrit, plasma fibrinogen levels, and sample handling can influence the results.[126,128] The system is also somewhat limited in scope, as it limits users to the three currently available cartridges and obscures the actual aggregation curves.

1.3.2 Shear-Based Adhesion Tests

Fluid mechanical forces have a significant impact on platelet activation and adhesion, particularly in high-shear locations such as stenoses. The use of elevated shear rates in platelet function tests such as the platelet function analyzer (PFA-100/200®, Siemens) and the IMPACT Cone and Plate(let) Analyzer (Diamed) provides a way to activate a platelet population in the absence of additional agonists.

1.3.2.1 PFA-100/200®

The PFA-100/200® is a shear-activated, cartridge-based platelet assay. It was originally designed to replace or automate bleeding time tests by mimicking an injured blood vessel.[129] In this assay, whole blood is drawn through a membrane with a small (150

μm) aperture which is coated with either collagen and ADP or collagen and epinephrine.[130] These agonists, combined with the elevated shear at the aperture, serve to activate platelets that eventually occlude the membrane. The reduction in flow rate is measured, and the time to occlusion is reported.[120] Since this is a whole blood assay and it requires a small sample size, it is well suited for clinical applications. It is also well suited for the screening of hereditary platelet disorders, particularly von Willebrand disease, due to the incorporation of a high-shear activation component.[130]

The PFA-100/200® systems automate the test and thus eliminate user error; however, care must be taken in sample preparation as results are greatly influenced by a patient's platelet count and hematocrit as well as the anticoagulant used.[118,131] The PFA-100/200® is capable of monitoring antiplatelet therapies; however, recent research has suggested that it is not reliable enough to accurately monitor patients.[132,133] The main drawback to this system, however, is that it is a global measure of platelet activity and is not specific to any particular pathway. This makes it useful as a broad indicator of a patient's platelet activity, but does not provide any information on particular disorders or activation pathways.

1.3.2.2 IMPACT Cone and Plate(let) Analyzer

The IMPACT Cone and Plate(let) analyzer is another device which utilizes shear as the main pathway by which to activate platelets. In this test, whole blood is loaded into a chamber with a stationary polystyrene plate, and an opposing conical surface. The cone is rotated to produce a high-shear environment (1800 s^{-1}) within the sample and platelets are allowed to aggregate on the now plasma-covered polystyrene surface.[134–136] The use of

a cone and plate geometry allows for a constant wall shear to be imparted on the whole sample which is governed by the geometry of the system and the rotational speed of the cone.[137] After a prescribed magnitude and duration of shear, excess blood is washed away and the platelets are stained and imaged in an automated process. The percentage of the well that is covered by platelets and the average size of the aggregates are then measured and recorded. This assay is advantageous since it uses adhered blood proteins to assist in the arrest of activated platelets, thus making a more accurate mimetic environment of an implanted biomaterial. The IMPACT system also uses a small sample volume and is an automated process, lending support for its use in clinical and laboratory settings.

This device is limited by the fact that it currently only uses polystyrene plates (in terms of biomaterials testing applications) and that it is only a broad indicator of platelet function and therefore cannot determine the nature of any particular platelet disorders. The cone and plate geometry is also a poor representative of native vessel geometry, and due to the nature of the assay, real-time data are not available. This test has recently been modified through the addition of platelet agonists so that it can be used to evaluate antiplatelet therapies; however, IMPACT has seen limited results in predicting adverse outcomes in the clinic.[138–141]

1.3.3 Flow Cytometry

Flow cytometric methods offer a highly advanced and specific way to study platelet activation states. In a flow cytometric assay, a cell suspension is passed through a flow cell, between a focused laser and a detector. This detector can measure not only the size of the cells (useful for sorting platelets from red blood cells in a whole blood sample), but also

fluorescence given off by tags attached to the cell surface.[142] Antibodies specific to any of a number of platelet activation markers can be fluorescently conjugated and used to assess a platelet population's state through the presence of these markers on the surface of cells.[143] Two of the most common platelet activation markers measured are P-selectin expression (a sign of α-granule secretion) and the active conformation of GPIIb/IIIa.[144–147] By multiplexing lasers and detectors in the same flow path, multiple activation markers can be studied in parallel in the same sample. This method is quick, easy to use, and high throughput (~20,000 cells/s) so it is useful in gathering detailed information about a platelet population within a sample.

The effect of antiplatelet drugs can be monitored through the use of various combinations of antibodies, agonists, and antiplatelet agents. For example, GPIIb/IIIa antagonists are typically monitored by measuring their receptor occupancy through a number of direct and indirect methods (competitive binding, receptor blocking, secondary binding, etc.).[148–150] $P2Y_{12}$ receptor inhibitors can also be monitored through a vasodilator-stimulated phosphoprotein (VASP) assay, since the phosphorylation of VASP is dependent on the level of activation of the $P2Y_{12}$ receptor.[151,152] Finally, ASA therapy can be monitored through the additional stimulation of a sample with arachidonic acid and comparing with nonstimulated controls.[153]

Despite its versatility in measuring platelet activation status, flow cytometry has significant drawbacks that hinder its use in the clinic. First, the machinery required to perform this analysis is relatively large and expensive. Recent innovations have allowed for the introduction of benchtop flow cytometers; however, these systems are still priced out of the budgets of many primary and secondary care facilities. Additionally, while

performing the assay is relatively straightforward, the sample preparation and interpretation of results is a delicate process and requires a trained and knowledgeable staff.

1.3.4 Microfluidic Methods

Recent advances in the production of microfluidic chambers have led to a resurgence of perfusion devices for the investigation of platelet activity. The original use of perfusion chambers was described by Baumgartner *et al.* in the 1970s.[154,155] This technique consisted of an assay in which blood was perfused through an annulus-shaped Plexiglas chamber past excised sections of denuded endothelium which served to activate and accumulate platelets. Current microfluidic platelet assays operate on the same basic principles as these original perfusion chambers, but can now be rapidly prototyped and highly customized with different geometries, materials, and for different applications.[156,157] The use of a flow cell allows for the creation of a mimetic environment in which to study platelet activation, where factors such as flow rate, wall shear rate, and surface presentation of antigens can be precisely tailored to investigate specific pathways.[85,158,159] The miniaturization and multiplexing of flow channels also allows for the investigation of many separate conditions in parallel while maintaining a small sample volume.

There are several commercially available microfluidic platelet assays, as well as several companies providing preassembled flow channels for investigative use.[160,161] Since they are easy to develop, many individual research groups have also created proprietary devices to suit their specific needs.[162–164] Various solution or surface-based agonists can be introduced to these chambers to provoke platelet activation, including soluble factors, surface-bound protein agonists, stenotic high-shear regions, or live endothelial cells.[165,166]

Detection metrics include platelet adhesion to agonists, time to occlusion, levels of soluble activation markers, or platelet activity surface markers (when coupled with flow cytometry). There has also been research done into the effects of antiplatelet agents on platelet activity under flow conditions.[167–169]

Microfluidic techniques offer many advantages over more established methods; however, the specificity of many assays and the underdevelopment of many devices has led to a lack of adoption in clinical settings.[157,170] Due to their ability to recreate elements of the native coagulation environment, however, microfluidics offers a promising approach to the future of clinical diagnostics.

1.4 Dissertation Overview

The research described herein details the development of a platform for *in vitro* simulation of platelet activation by an upstream platelet agonist: a flow assay that mimics a lesion site with variable surface density of platelet-activating molecules in the upstream position, thus mirroring the physiological conditions in patients with lesions on a blood vessel wall or an implanted vascular device.

1.4.1 Rationale

The environment in which platelets become activated *in vivo* is highly complex and dynamic, involving rheological, biomechanical, and soluble-agonist forces.[171] It therefore stands to reason that the most accurate platelet function test will be one that best recreates the natural environment in which platelets become activated. Current platelet functionality assays lack the flexibility required to present specific agonists (alone or in combination) to

a flowing sample of blood and assess the activation response generated. Although aggregometry is capable of providing a large amount of information on platelet functionality, it is entirely solution based, static, and does not take into account surface-presented agonists.[31,172] The VerifyNow® system does take into account surface-adsorbed fibrinogen; however, it lacks flow and relies on artificially introduced solution-based agonists. Both the PFA-100/200® and IMPACT introduce shear forces; however, shear is only one of many factors that influence platelet activation, and as such, these assays can only measure global platelet activity, not a response to any specific agonist. Flow cytometry is a powerful technique with which to evaluate the activation state of platelets, but it is not a self-contained assay and its clinical utility is limited by its expense and complexity.

Current assays also fall short in their ability to predict adverse clinical outcomes based on patient-specific responsiveness to certain antiplatelet therapeutics.[173–175] As the mechanisms for resistance to antiplatelet therapies are not yet fully understood, there exists a great need for an assay that can accurately determine an individual's response to a particular therapeutic approach.

Perfusion chamber methods have come much closer to providing systems that mimic platelet activation conditions *in vivo*. With the advent of microfluidics, it has become routine to create assays in which many factors can be tuned to fit a particular investigative need, including: the presentation of agonists (surface or solution based), the flow and wall shear rate of the system, the surface coating of the walls of the chamber, the wall compliance of the chamber, and the methods used to detect platelet activation. Lacking from current flow assay methods, however, is a way to analyze the dynamics of platelet

priming. This critical and long overlooked step in the platelet activation process could have sweeping consequences in the fields of medical device design and postoperative treatment of patients.

I hypothesize that in order to create a better and more relevant platelet function assay, a system needs to take into account not only the physical environment in which a platelet becomes activated, but the spatial-temporal environment as well. Through the inclusion of the upstream-priming and downstream-activation dynamic, a more relevant antiplatelet monitoring assay can be created.

1.4.2 Dissertation Outline

This dissertation describes the development of a device that presents one or more agonists to a flowing sample of whole blood and measures the platelet activation state downstream of that agonist. Chapter 2 presents the development of a fluidic device in which an agonist is presented to a flowing sample of blood and the activation state of the platelet population is measured with a surface capture assay downstream of that agonist. The assay design consists of a miniaturized array of flow chambers and takes advantage of a phenomenon known as platelet margination in order to increase sensitivity. The device is disposable, requires a small sample volume (< 1 mL of whole blood) per run, and a typical perfusion lasts 5 min, thus making it an ideal candidate for a variety of clinical uses. This assay is verified by titrating the upstream agonist and seeing a varying response in downstream platelet adhesion. The utility of this method is then demonstrated through the introduction of several antiplatelet agents, showing a marked and dose-dependent decrease in platelet activity after administration.

Platelets *in vivo* encounter a complex milieu of surface presented agonists. In order to recreate a more accurate priming environment, it is necessary to be able to create a flow cell in which platelets can be stimulated by more than one agonist pathway. Previously, there was no method by which to accurately print more than one aligned pattern of agonist over a relevant spatial scale. In this assay, the surface presented agonists are patterned on a surface using microcontact printing, so it was of interest to develop a method by which to modify this procedure to allow for the stamping of multiple aligned patterns on the same surface. Chapter 3 details the development of a microcontact patterning method that enables the presentation of multiple patterns of agonists in registry to a flowing sample.

Chapter 4 describes the incorporation of the multiagonist patterning method with the flow cell design in order to present combinations of agonists to flowing whole blood samples. Through the use of this assay, a combinatorial effect is observed in which the total activation of a platelet population stimulated by multiple agonists is seen to be greater than the stimulation of any one agonist alone, suggesting a synergistic relationship between platelet activation pathways.

Finally, Chapter 5 provides a summary, perspective, and future directions for this research.

CHAPTER 2

FUNCTIONAL ASSAY OF ANTIPLATELET DRUGS BASED ON MARGINATION OF PLATELETS IN FLOWING BLOOD[1]

2.1 Introduction

Each year, millions of individuals require surgical intervention to deal with cardiovascular diseases, oftentimes requiring the assistance of a vascular device such as a stent, shunt, or graft.[176] A major failure mode of these devices is the formation of a thrombus, leading to an occlusion of the device or an embolic event. This haemostatic response of the body to foreign materials often necessitates that patients be placed on systemic anticoagulants, many of which result in a considerable loss in quality of life. The development of antiplatelet agents is hindered by the fact that no current *in vitro* platelet activation assay fully takes into account the conditions under which platelets interact with different agonists *in vivo* and the downstream consequences of such interactions. Our group has recently shown that there is a quantitative relationship between transient contacts of platelets with upstream immobilized agonists and downstream platelet adhesion and

---

[1] Adapted with permission from Eichinger, Colin D., Fogelson, Aaron L., and Hlady, Vladimir. "Functional assay of antiplatelet drugs based on margination of platelets in flowing blood." Biointerphases 11, 029805 (2016). Copyright 2016 American Vacuum Society

activation, leading to a new perspective on vascular device failures.[84] This finding was utilized here to design a novel antiplatelet drug efficacy assay that mimics transient platelet encounters with exposed agonists at a blood vessel wall lesion, or with procoagulant proteins adsorbed to the surface of an implanted vascular device.

2.1.1 Platelet Activation and Adhesion

It is commonly accepted that upon encountering a blood vessel injury or biomaterial, platelets initiate the process of repair by recognizing exposed subendothelial proteins via membrane receptors and tethering to the surface.[19,177] Platelets roll along the surface of the injured vessel or material due to short-term interactions of glycoprotein Ib (GPIb) and von Willebrand factor (vWF), then arrest, activate, and aggregate through the interactions of glycoprotein IIb/IIIa (GPIIbIIIa) and fibrinogen or collagen.[22,23,67] Upon adhering, platelets undergo a morphological change and release the contents of their granules, which contain additional activation factors.[28] These processes lead to an amplification of the activation cascade and the formation of a fibrin clot.[50] Most platelets that contact a locus of injury, however, do not immediately adhere at the site of initial contact.[83] Those platelets that have made transient contacts with a procoagulant surface stimulus remain "primed" for downstream activation as they continue to circulate. We have recently demonstrated that a platelet population allowed to transiently interact with a stimulating surface patch has an increased propensity to activate and adhere downstream.[84,85] This phenomenon is largely due to the margination of platelets in flowing blood which was utilized here to create a new type of antiplatelet agent assay that takes into account the upstream history of platelet-agonist interactions.

2.1.2 Antiplatelet Agents

Anticoagulant or antiplatelet therapy is often used during and after the surgical introduction of a vascular device or repair of a damaged blood vessel to reduce the risk of thrombotic complications.[12] A large proportion of patients continue to receive these therapies indefinitely due to the increased risk of thrombosis and embolism associated with damaged vessel walls or with blood contacting implants. Examples of antiplatelet drugs currently prescribed include thromboxane inhibitors (acetylsalicylic acid), GPIIb/IIIa inhibitors (abciximab, eptifibatide, and tirofiban), and ADP inhibitors (clopidogrel, prasugrel, and cangrelor). Despite the prevalence of antiplatelet and anticoagulation agents, the lack of relevant platelet function assays has limited the scope of antiplatelet drugs tests *in vitro*. There is currently no optimal system in which to test the effects of antiplatelet therapies on the dynamics of platelet activation and adhesion in circulation, since current assays for antiplatelet agents tend to approximate only the local effects of vascular injury or procoagulant device surfaces. Practically no current *in vitro* platelet function assay takes into account the upstream priming that can occur in vessel injury conditions. Platelet aggregometry, for example, in which a platelet agonist is added to whole blood or plasma and aggregate formation is recorded, is considered the "gold standard" for platelet functionality assays.[120] Although aggregometry is capable of providing a large amount of information on platelet functionality, it does not provide a circulatory environment that accurately mimics adhesion, activation, and aggregation onto an injured blood vessel wall or an implanted device.[19,118] Other methods, including analysis of activation markers using flow cytometry or aggregation using techniques such as thromboelastography, only detect bulk platelet activation and do not directly assess surface-induced adhesion and

activation.[178]

2.1.3 Platelet Function Assays

Most platelet function assays are unable to model the effects of a specific activating region and actual vessel flow conditions and specific injury site conditions are typically not presented. One exception is the IMPACT cone and plate analyzer (CPA), which was developed to more accurately represent natural haemostasis.[136] In the CPA, a polystyrene plate is used to monitor platelet adhesion and aggregation in a well-defined shear environment. Plasma proteins are allowed to adsorb to the surface of a polystyrene plate from whole blood, creating a thrombogenic surface. The type and amount of plasma proteins that adsorb to the surface are not controlled, however, so no direct correlations between specific plasma proteins and platelet function can be elucidated. Recent years have also seen the rise in use of microfluidic flow cells as essential tools for studying platelet activation and adhesion.[156,179] Gutierrez *et al.* used extracellular matrix (ECM) coated substrates to investigate the influence of elevated shear rates on platelet adhesion with respect to the GPIIb/IIIa receptor.[165] Similar assays have also been used by Maloney *et al.* to investigate patient-specific responses to antiplatelet therapies.[168]

While these studies have come closer to simulating vessel wall lesion conditions by presenting physiologically relevant substrates to shear and/or ECM activated platelets, the influence of transient contacts between platelets and surface bound agonists has been overlooked. To investigate this phenomenon, we have developed a flow-based method to test the downstream activation of platelets after specific upstream stimulation of platelets by transient contacts with mimetic procoagulant agonists. The surface-immobilized procoagulant proteins act as platelet agonists in order to mimic exposed subendothelium in

a blood vessel lesion or a procoagulant surface of an implanted vascular device. Varying the surface density of an upstream agonist can thus mirror a range of pathological conditions in patients with lesions on a blood vessel wall.

2.1.4 Novel Flow Assay

The central premise of the flow assay described here is that by controlling the presentation of an upstream agonist (a so-called "priming" region made of covalently tethered procoagulant proteins), the subsequent activation of platelets can be determined using a downstream platelet "capture" region. This assay is carried out in a miniaturized array of flow chambers through which a small volume of blood is perfused. Figure 2.1 shows the geometry of the upstream agonist priming and downstream capture regions in rectangular flow chambers. Due to the geometry of the flow cell, this assay takes advantage of a margination phenomenon observed in flowing blood in which platelets are concentrated near the vessel wall. Such margination of platelets towards the chamber walls is due to the existence of a red blood cell depletion zone established during flow. Spatial fractionation of platelets ensures a higher number of contacts between the marginated platelet subpopulation and upstream priming and downstream capture regions. This assay requires a small sample volume (< 1 mL of whole blood) per run, and a typical perfusion lasts 5 min, thus making it an ideal candidate for a variety of clinical uses.

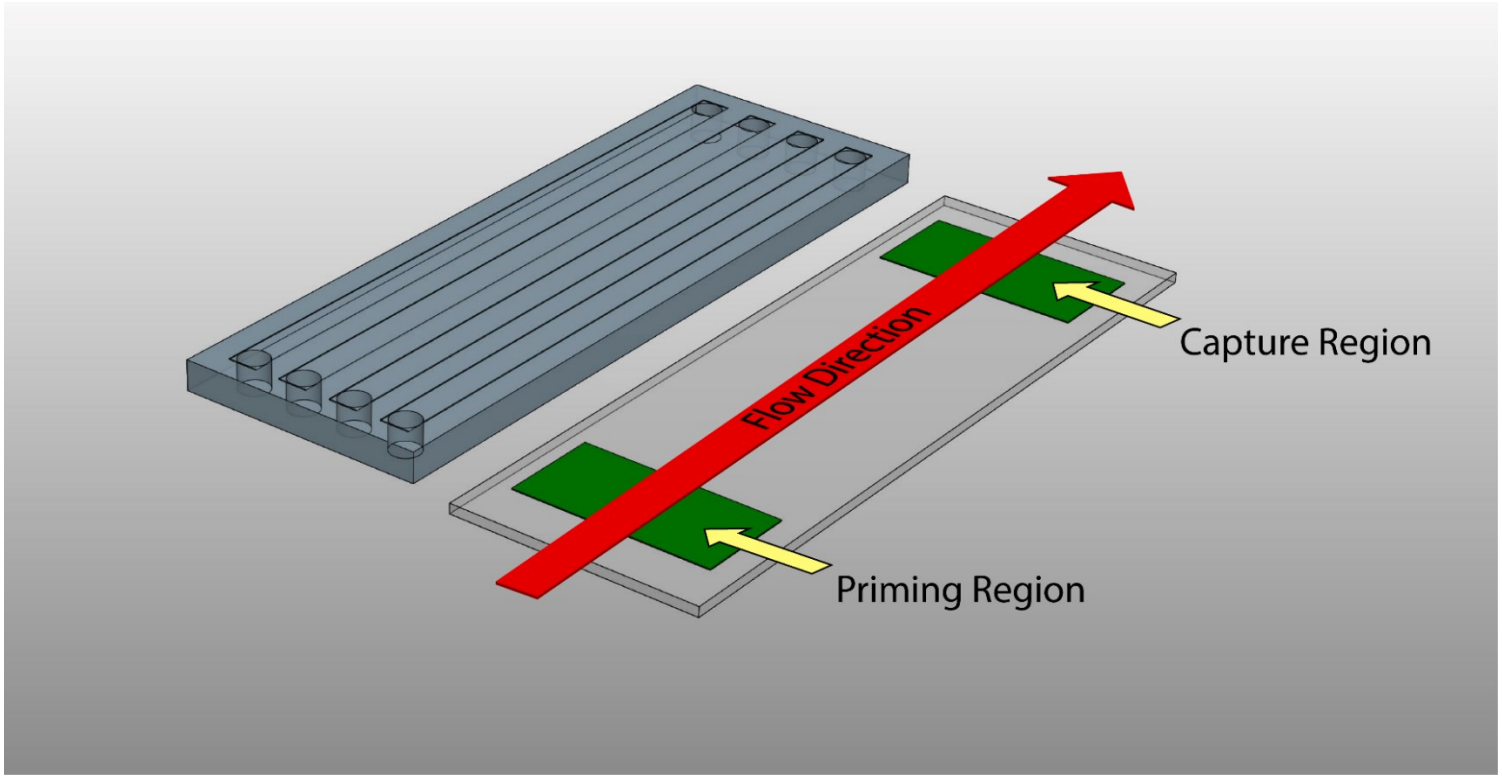

Figure 2.1: Schematic of a flow assay assembly. Protein agonists are deposited on a glass substrate in the priming and capture regions by microcontact printing and covalent attachment of proteins is achieved through the use of a commercial NHS ester chemistry (Nexterion-H®, Schott). A relief-molded PDMS flow channel is inverted on the stamped surface to create the final assembled device. Flow through the device brings blood past the priming region followed by the capture region before exiting the device. Platelets near the substrate surface are therefore able to sequentially interact with two surface-bound agonist regions in a controlled flow environment.

2.2 Methods

2.2.1 Flow Cell Design and Creation

Flow chambers contained an upstream platelet priming area (10 mm in length) and a downstream capture region (also 10 mm in length). Flow channel dimensions were 3 mm wide, 0.1 mm deep, and 70 mm long. Such dimensions were selected to match physiologically relevant venous (~100 s^{-1}) and arterial (500-1000 s^{-1}) shear rates depending on the volumetric flow rate used in perfusion.[180–183] Each device consisted of a parallel array of four flow channels and was designed to fit on a standard 25 mm x 75 mm microscope slide (Figure 2.1). The flow chambers were manufactured through relief molding of polydimethylsiloxane (PDMS) (Sylgard 184, Dow Corning) on patterned polymeric tape. Patterns for the channels were cut out of tape on a xurographic plotter (CE5000-60, Graphtec). These patterns were then transferred to the bottom of a mold and PDMS was cast into the mold at a ratio of 15:1 polymer to crosslinker by weight. The flow chambers were allowed to cure, then released from the mold and cut to final dimensions (25 mm x 75 mm). Fluid vias were bored from the top of the PDMS into the flow channels to provide access for the inlet and outlet of blood.

To create platelet priming and capture regions, patches of fibrinogen were deposited at specific upstream and downstream locations in each flow cell using a microcontact printing (μCP) process described in detail elsewhere.[85,184] Briefly, soft lithographic stamps were created out of PDMS corresponding to random patterns of μm-sized islands of varying surface density coverage. The surface of these stamps was coated with a fibrinogen solution (1 mg/mL in PBS, Haematologic Technologies Inc.) and allowed to dry, then brought into contact with the substrate. The fibrinogen used was highly purified

research grade with a 95% clottable fraction. Purity was verified by the supplier using SDS-PAGE. Covalent linkages between proteins and the glass-based bottom of the flow assay were achieved by using commercially available Nexterion-H® (Schott) slides coated with a PEO-based polymer containing reactive N-hydroxysuccinimide esters.[185,186] After μCP of fibrinogen, the slides were rinsed in DDI water prior to assembly to eliminate any nonbound protein.

The downstream analysis of platelet activation was carried out via a surface capture assay.[84] A printed protein capture region consisting of a 10 mm long patch of 100 % surface density coverage of fibrinogen was covalently immobilized to the surface of the flow cell 45 mm downstream of the priming region. This region served to capture activated platelets from the marginated platelet subpopulation. Figure 2.2 shows a schematic of a flow assay during platelet perfusion, highlighting the μm-sized islands of covalently attached agonist in the priming region at three different surface densities. Devices were assembled by inverting the PDMS fluidic channels onto the stamped Nexterion-H® glass substrate. Capillary forces held the PDMS in place strongly enough to prevent leakage for the duration of the experiments. Prior to all experiments, a solution of human serum albumin (1 mg/mL in PBS, Sigma-Aldrich) was perfused through each flow cell to both coat the PDMS walls of the chamber and backfill any nonstamped regions of the Nexterion-H® slide as adsorbed albumin has been shown to be platelet-inert.[187]

2.2.2 Flow Cell Operation

Whole human blood was drawn from healthy donors into buffered 3.2 % (0.105 M) sodium citrate and was treated with Phe-Pro-Arg-chloromethylketone (PPACK,

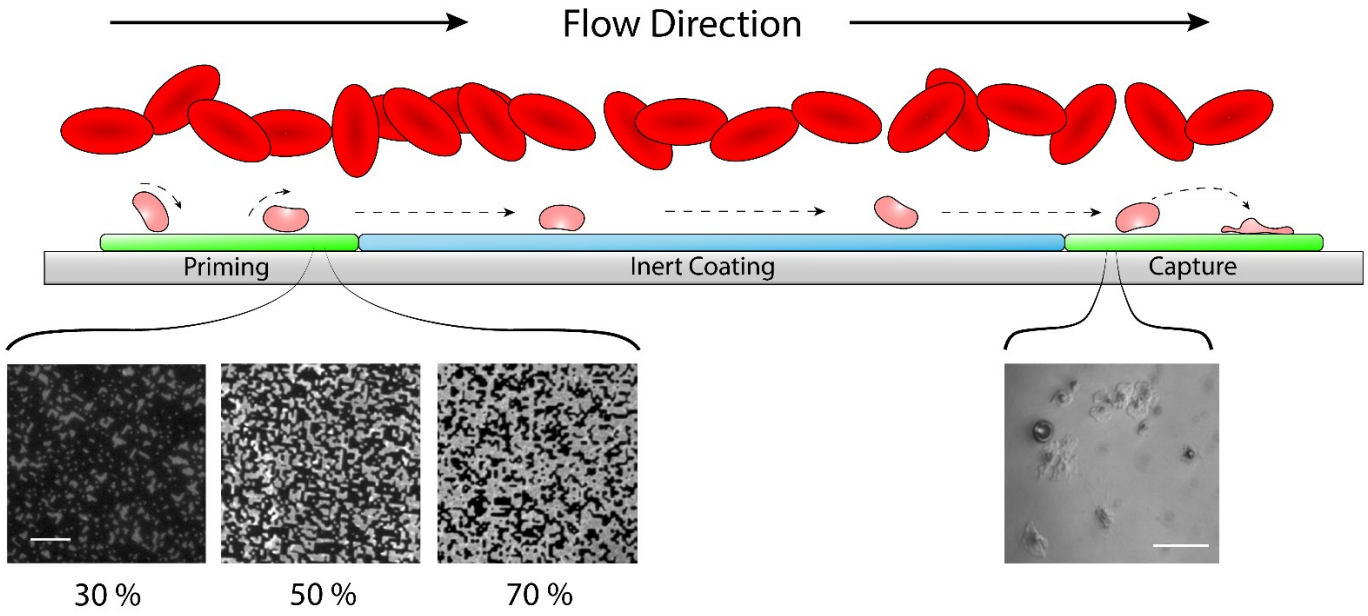

Figure 2.2: Schematic of flow assay function. The presence of red blood cells in flow creates a margination effect which drives platelets towards the chamber walls. An increased number of platelets near the substrate surface relative to the bulk flow increases chances of platelet-surface interactions. Platelets near the substrate transiently roll along the surface and become primed through interactions with agonists. A variable density of printed agonists in the priming region provide a range of probabilities that a platelet contacting the surface in the priming region will interact with a printed agonist. Shown here are fluorescent images of microcontact printed fibrinogen at three different surface coverage densities, 30 %, 50 %, and 70 % (scale bar represents 10 μm). Primed platelets continue to flow downstream along a platelet-inert surface. Primed platelets encountering the downstream agonist patch have an increased propensity to form stable adhesions compared to nonprimed populations. The number of adhered platelets in the capture region is used as an indication of overall priming in the platelet population. The inset image is a representative view of platelets adhered to a fibrinogen capture region (scale bar represents 20 μm).

Haematologic Technologies) to prevent thrombin-induced coagulation. Any additional antiplatelet agent was added at this time as experimental conditions dictated. Blood was kept in a water bath at 37° C for the duration of the experiment, and polyethylene microfluidic tubing connected the flow cell to the vial of blood. Flow was achieved by drawing blood through the device using a syringe-pump (Kent Scientific). A flow rate of 3.6 mL/h produced a shear rate of 200 s^{-1}, which was used in all experiments. Flow was sustained for 5 min, after which the device was rinsed with prewarmed Tyrode's buffer to remove any nonattached cells. Attached cells were fixed in 4 % paraformaldehyde, imaged using a differential interference contrast microscope (DIC) (Diaphot 300, Nikon), and quantified. Adhered platelets were counted in ten randomly selected fields (300 μm x 400 μm) within the downstream capture region.

2.3 Results

2.3.1 Upstream Agonist Titration

Flow cells were created with varying surface coverage densities of fibrinogen in the upstream priming region. Densities of 15 %, 30 %, 50 %, 75 %, 85 %, and 100 % were used. Negative controls of 0 % surface coverage were run both before and after the experiments to ensure that the platelets in the blood sample did not become more active over the course of the experiment. Figure 2.3 shows that the number of platelets adhered to the downstream capture region increased as the surface density of the immobilized agonist in the upstream priming position is increased. This finding indicates that the elevated chances of platelets contacting the upstream agonist led to a greater number of platelets primed for adhesion downstream. These results demonstrate that precise control

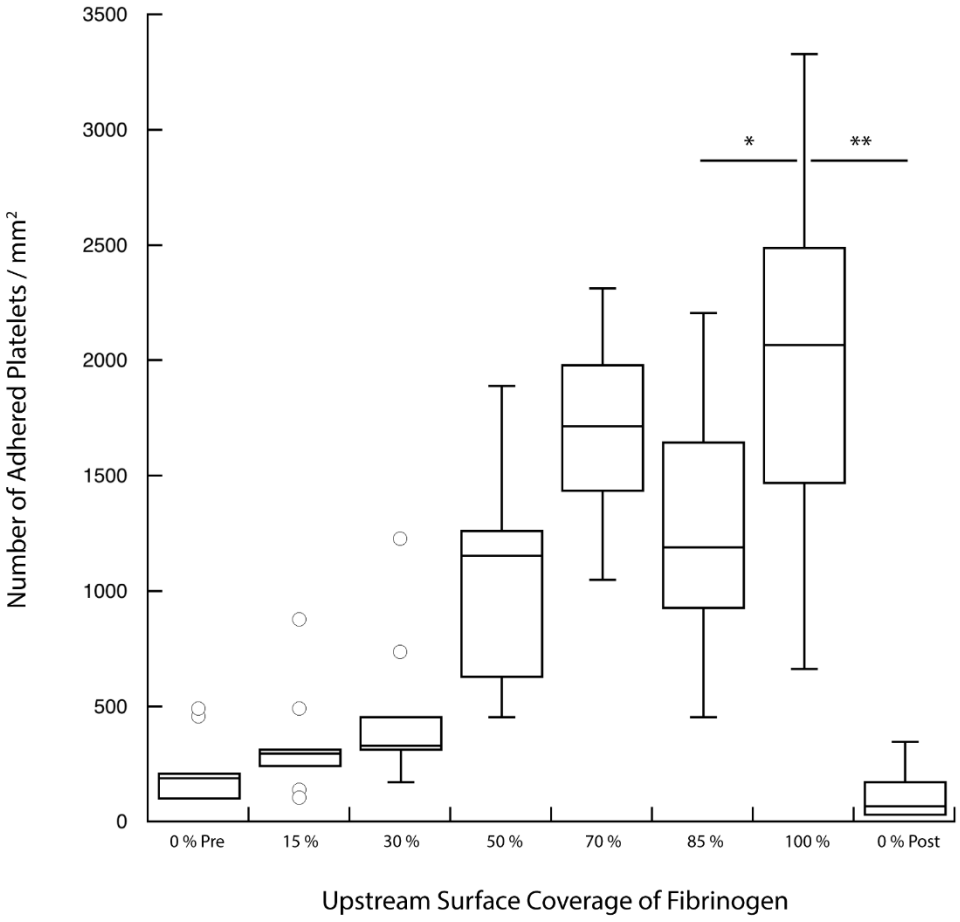

Figure 2.3: Stimulus-dependent response of platelet activation. Platelet adhesion to a downstream fibrinogen capture region is seen to increase as the density of upstream surface bound fibrinogen increases. (**$p < 0.0001$, *$p < 0.05$)

over the relative activation state of a platelet population is achievable and detectable using this device.

2.3.2 Antiplatelet Agents

Two classes of antiplatelet agents were examined for their ability to attenuate platelet activation in response to the upstream agonist. The cyclooxygenase (COX) inhibitor acetylsalicylic acid (ASA) (Aspirin®, Bayer) and the two GPIIb/IIIa inhibitors, eptifibatide (Integrilin®, Millennium Pharmaceuticals) and tirofiban (Aggrastat®, Medicure) were selected as they are all nonprodrug candidates, and thus could be easily added to the blood prior to perfusion.

2.3.2.1 COX Inhibitor

Flow cells were created with 50 %, 85 %, and 100 % coverage of printed fibrinogen in the upstream priming region. Two samples of whole blood were prepared, one untreated, and one treated with 30 μg/mL ASA in whole blood (*i.e.*, the target blood concentration for antiplatelet therapy in adults). Figure 2.4 shows the platelet activation response to varying surface densities of upstream fibrinogen with and without ASA premixed in the perfusate. While an increasing surface density of priming fibrinogen still resulted in increased platelet adhesion, the relative number of adhered platelets significantly decreased in the presence of ASA. These results illustrate the sensitivity of this assay in assessing the efficacy of antiplatelet agents in response to varying levels of platelet activation.

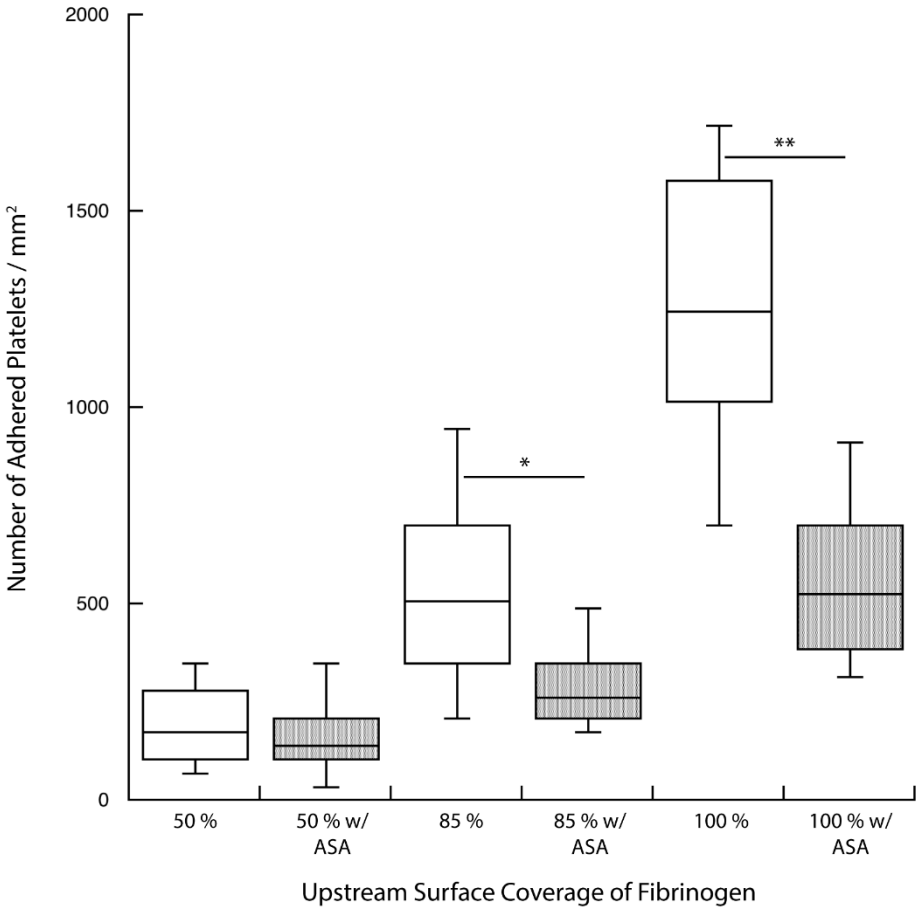

Figure 2.4: Stimulus-dependent response of platelet activation in the presence of acetylsalicylic acid. Acetylsalicylic acid (ASA) is seen to attenuate the platelet activation response. Platelet adhesion to the capture region increases as the density of the upstream priming region increases; however, this rate of increase is diminished in the presence of the recommended therapeutic dose of ASA. (**$p < 0.0001$, *$p < 0.01$)

2.3.2.2 GPIIbIIIa Inhibitors

Another set of experiments was used to test a different class of antiplatelet agents, GPIIbIIIa inhibitors. Specifically, eptifibatide (a cyclic heptapeptide) and tirofiban (a nonpeptide inhibitor) were used. Devices were created with 100 % surface coverage of fibrinogen in both the priming and capture regions. Whole blood mixed with each of these drugs was used as perfusate. Antiplatelet agents were combined with blood at their respective target therapeutic blood concentrations (3 μg/mL, eptifibatide or 0.33 μg/mL, tirofiban) and also at 1/10 of these target concentrations. Figure 2.5 shows the results of the GPIIbIIIa inhibitors on downstream platelet adhesion. Both eptifibatide and tirofiban diminished the number of adhered platelets at their target therapeutic concentration and at 1/10 of that level. At the recommended blood concentration of each of these drugs, results were statistically similar to nonprimed controls (*i.e.*, with no agonist present in the upstream region). This result illustrates the ability of the assay to assess antiplatelet therapies in a dose-sensitive manner.

2.4 Discussion

This novel flow assay, which mimics a physiologically relevant blood vessel wall injury to test platelet function and antiplatelet drug efficacy, was made possible by utilizing a dynamic phenomenon by which transient platelet-agonist contacts prime platelets for enhanced activation and adhesion downstream. The flow assay emulates a procoagulant surface of a vascular device or vessel wall injury by presenting a covalently bound platelet-priming agonist to flowing whole blood. A second patch of an immobilized proadhesive protein downstream of the agonist is used to capture primed platelets. In the present study,

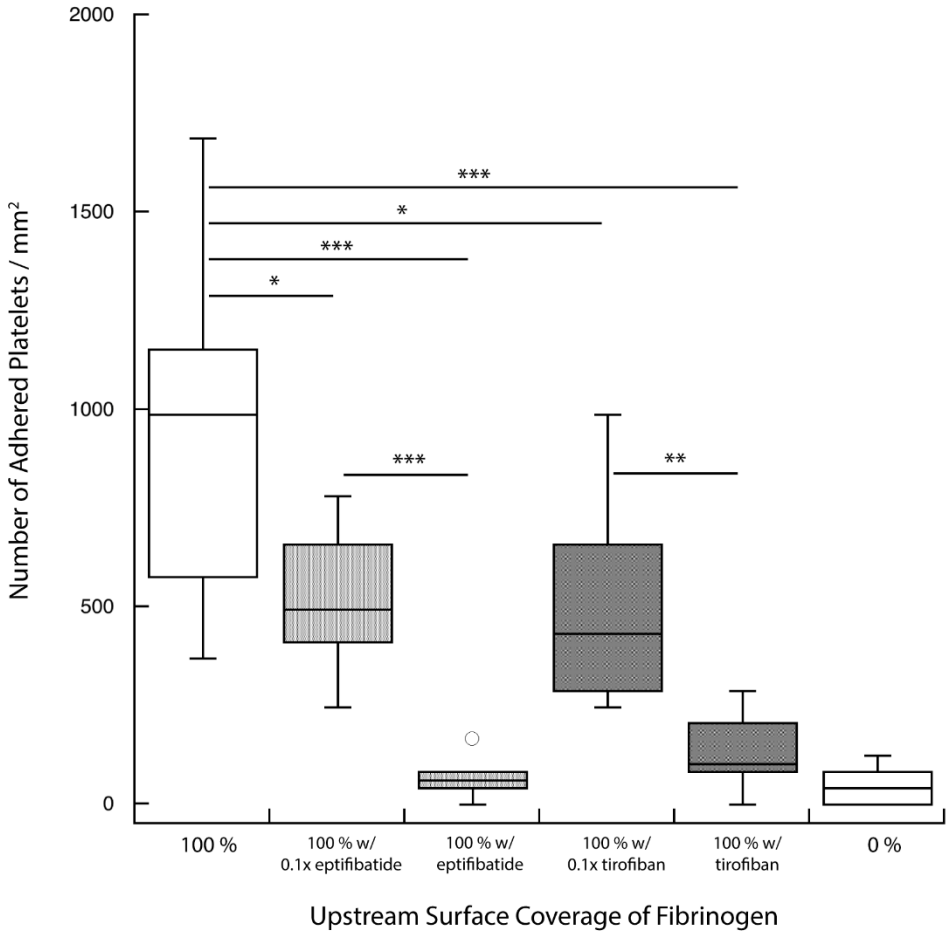

Figure 2.5: Dose-dependent response of platelet activation in the presence of GPIIb/IIIa inhibitors. GPIIb/IIIa inhibitors attenuate the platelet activation response. Both eptifibatide and tirofiban diminish the number of adhered platelets comparable to negative controls at the target therapeutic dose. (***$p < 0.0001$, **$p < 0.001$, *$p < 0.01$)

fibrinogen was used as the protein in the capture region as it has been previously demonstrated to effectively arrest primed platelets[84,85]; however, other capture proteins (*e.g.*, collagen or vWF) could easily be incorporated. This assay would not have the required sensitivity without the phenomenon of platelet margination towards flow chamber walls in laminar flow of whole blood. The dimensions of the flow channels were chosen to increase the chances of a platelet interacting with the chamber walls multiple times by exploiting the margination of platelets and the propensity of platelets once marginated to remain near the chamber walls. Numerous *in vivo* observations and *in vitro* experiments of whole blood flowing in tubes or channels have established the existence of a near-wall region with few to no red blood cells.[188–191] This red cell depletion zone is characterized by an enhanced concentration of platelets compared to their overall bulk concentration in the blood. The red cell depleted and platelet enriched zone comprises the layer of fluid within 2-5 μm of the wall, growing thinner as the hematocrit and shear rate increase. Importantly, platelet margination substantially increases (by 50-fold or more) the rate of platelet contacts with the chamber wall.[155] Computational models of whole blood, which simulate the motion of collections of red blood cells and platelets suspended in plasma, show the temporal development of the red cell depletion zone and the subsequent margination of platelets.[192–194] These studies also show that the red blood cells along the edge of the red cell depletion zone form an effective barrier which strongly inhibits the movement of platelets from the near-wall region back into the core flow.[192,193] In the context of our flow assay, this implies that most of the platelets that contact the upstream priming region will remain within a few microns of the wall during their transit through the chamber to the downstream capture region, and so have a significant chance of contact with the capture

region.

Transient contacts between primed platelets and the capture region result in the arrest of platelets, and the number of arrested platelets has been shown to correlate to the overall activation of the platelet population.[195] Other methods such as FACS analysis of activation-dependent surface markers or β-thromboglobulin plasma levels are more commonly used to assess platelet activation.[142,145,146] Since the fraction of the platelet population that contacts the priming region is rather small (~ 2%), it would be difficult to detect such low numbers of active platelets among the whole platelet population using these methods. Thus, the combination of platelet margination in flow and a downstream capture region allows for the self-selection of activated platelets, making the current assay more sensitive than any of the bulk fluid-based platelet activation assays.

Initially, the surface coverage density of fibrinogen was varied to demonstrate the sensitivity of the assay to increasing levels of platelet priming stimulus. As the percent of surface coverage increased from 0 % to 100 %, the chance that any given platelet flowing past the priming region would contact a fibrinogen patch also increased. The surface coverage density of fibrinogen was seen to have an effect on the activation state of the platelet population, as increased adhesion was observed in the downstream capture region in a dose-dependent manner (Figure 2.3). A similar experiment was repeated in which the upstream surface density of bound fibrinogen was varied in the presence of ASA. The results indicate that ASA was able to decrease the activation of the platelet population relative to nontreated controls. Interestingly, platelet priming was still observed to be dependent on the upstream agonist surface density; however, the number of adhered platelets was diminished. ASA inhibits COX, which in turn halts the formation of

thromboxane A2 (TXA2). By lowering TXA2 levels, a key stimulus for platelet activation was reduced. Other pathways to activation remained open, however, indicated by a continued (albeit decreased) presence of an active platelet population.

The antiplatelet drugs tirofiban and eptifibatide were also tested for their ability to attenuate platelet activation by surface-bound agonists. These drugs inhibit the GPIIb/IIIa receptor on platelets which is presumably responsible for platelet priming by upstream fibrinogen. A dose-dependent response was seen when the concentration of each of these drugs was varied. The number of adhered platelets downstream was significantly reduced even when the drugs were used at 1/10 of their recommended dose, and at the recommended dose, adhesion was reduced to levels of the nonprimed control. These results show the ability of this assay to detect the dose-dependent efficacy of antiplatelet agents.

2.5 Conclusion

In summary, these experiments demonstrate the newfound ability to investigate specific platelet priming pathways through the use of an upstream agonist, downstream surface capture assay. The ability of antiplatelet agents to attenuate this response was also shown, suggesting the utility of this flow assay for the screening of current and future antiplatelet therapies. Interpatient variations in drug sensitivity has been a well-documented challenge surrounding this class of drugs; therefore, the ability to detect the minimum effective therapeutic dose on a patient by patient basis would have large impact on the personalized prescription of such pharmaceutics.

CHAPTER 3

MULTIPROTEIN MICROCONTACT PRINTING WITH MICROMETER RESOLUTION[2]

3.1 Introduction

Cells in their natural environments maintain contact with each other and with extracellular matrix through molecular recognition events. These events regulate cellular behavior and cell differentiation. Understanding the relationship between the molecular recognition events and their effects is ever more important in tissue engineering and regenerative medicine. With the increasing use of biomaterials in medicine, better ways to interface such materials with cellular systems are being sought using biomimetic strategies; that is, creating an artificial environment similar to the natural environment of cells in a given tissue. One such approach is to deposit precise spatial patterns of proteins on a material that serve to accomplish a biological goal. Recently, protein patterned surfaces have been used to control cell adhesion[196–200] and to direct the growth of neurons.[201–205] With the understanding that the cellular interactions with ECM are complex, a method that allows for the precise transfer of multiple independent protein patterns on the same surface

---

[2] Adapted with permission from Eichinger, Colin D., Hsiao, Tony W., and Hlady, Vladimir. "Multiprotein microcontact printing with micrometer resolution." Langmuir 28.4 (2012): 2238-2243.

becomes necessary. Despite advances toward this goal, no current techniques exist with the resolution necessary to pattern surfaces with multiple proteins at the cellular scale over a sufficiently large area.

There exist numerous ways to pattern surfaces with proteins, each with inherent advantages and disadvantages. The three main methods used today are dip-pen nanolithography (DPN),[206–208] inkjet printing,[209–211] and microcontact printing (μCP).[184,212–214] DPN capitalizes on the precision of atomic force microscopy (AFM) to deposit nanoscale patterns of proteins of interest. This system can be multiplexed with many tips, and can be made to deposit multiple proteins in precise registration.[207] Motion of the tips is accomplished with piezoelectric actuators, while coordinates are programmed into a controlling computer, providing for both accuracy and repeatability. Because of the precise optics and computer controllers required, this system is relatively costly. The main downfall of the DPN technique and its application to biological systems, however, is the small scale over which proteins can be deposited. The *x* and *y* range of a typical AFM is limited to a few hundred micrometers; therefore, a large coverage of surface patterns is difficult to achieve in a reasonable amount of time. Multiplexing tips serves to shorten the patterning time; however, it results in a pattern repeated across the surface, not a single unique pattern.

Inkjet printing is a rapid surface patterning technique that lends itself to high throughput applications. This method, well established for the printing of inks, has recently been applied to the patterning of proteins. In inkjet printing, the desired protein solution is loaded into a print cartridge. If multiple proteins are to be used, cartridges are selected that allow for the printing of multiple solutions in parallel. High-resolution jet printers are then

used to deposit a desired protein pattern onto a surface. While this process is rapid and relatively cheap, the nonuniform drying of spotted solutions can lead to inhomogeneous coverage of the desired patterned regions.[215] Additionally, the resolution of these printers is limited by the minimum droplet size they can deposit ~20-30 μm.[209] This resolution limits the application of inkjet printing for cell-pattern interaction studies.

μCP is a more flexible patterning technique. Taking advantage of established photolithographic methods, master dies are made from etched patterns in photoresist or metals. These patterns are transferred to a soft polymeric material through casting and curing of the polymer in the die. Once the cured polymer is peeled off of the template, it can be used as a stamp with which to pattern surfaces with proteins. Polydimethylsiloxane (PDMS) is a typical polymer used to create these stamps and is widely available. By varying the monomer/cross-linker ratio, stamps with a range of elastic moduli can be created, allowing this technique to be tailored to specific applications. With the exception of the exposure and etching of the master template, all other steps in the stamp generation process can be carried out on the benchtop. This method is limited in minimum achievable stamp feature size ~100 nm[214]; however, it provides for any desired pattern of proteins to be deposited over a large area.

All current soft lithographic techniques are limited in their ability to pattern multiple proteins on the same surface. Many groups have addressed this problem with innovations such as multiplexing small arrays,[216] inkjet printing with multiple inks,[217] and microfluidic deposition.[184,218] While these methods do allow for the deposition of multiple proteins on a surface, none allow for large-scale patterning. In order to achieve large area coverage of multiple aligned patterns with small features, stamps need to be used to pattern

the same substrate in serial. This method has been used by multiple groups,[184,219] but has been limited by only a rough degree of alignment, typically achieved by eye. In order to generate increasingly complex patterns, a more precise and repeatable method is necessary.

One proposed application of multiplexed protein patterns can be found in the field of neuronal regeneration. In healthy tissues, astrocytes guide the growth of neurons though a series of molecular cues. When aligned, they express cellular adhesion and guidance molecules in specific spatial orientations so as to guide developing neurons along the same axis.[220] It is thought that by replicating these complex protein patterns, directed neuronal outgrowth can be achieved *in vitro*, an important first step toward neuronal bridging devices. Figure 3.1 shows the essential steps of creating such multiple protein patterns: a high-resolution image of astrocyte expressed laminin (green) and chondroitin sulfate proteoglycan (red) (A) are used to create μCP templates (B) from which the stamps (C) are made to print two proteins (D). In order to replicate these natural patterns, a method is required that allows for the transfer of multiple complex protein patterns to the same surface in precise registration.

Presented herein is a report on a platform that allows for multiplexed μCP of independent patterns with micrometer spatial registration. The device developed consists of an inverted light microscope modified to accept both stamp and substrate. The substrate is affixed to an optically clear stage at the focal distance of the microscope's objective, providing for real-time imaging of the stamping process. This, along with the use of imaging software, allows the user to overlay a live image of a stamp with a previously transferred pattern, thus enabling accurate registration of two or more patterns.

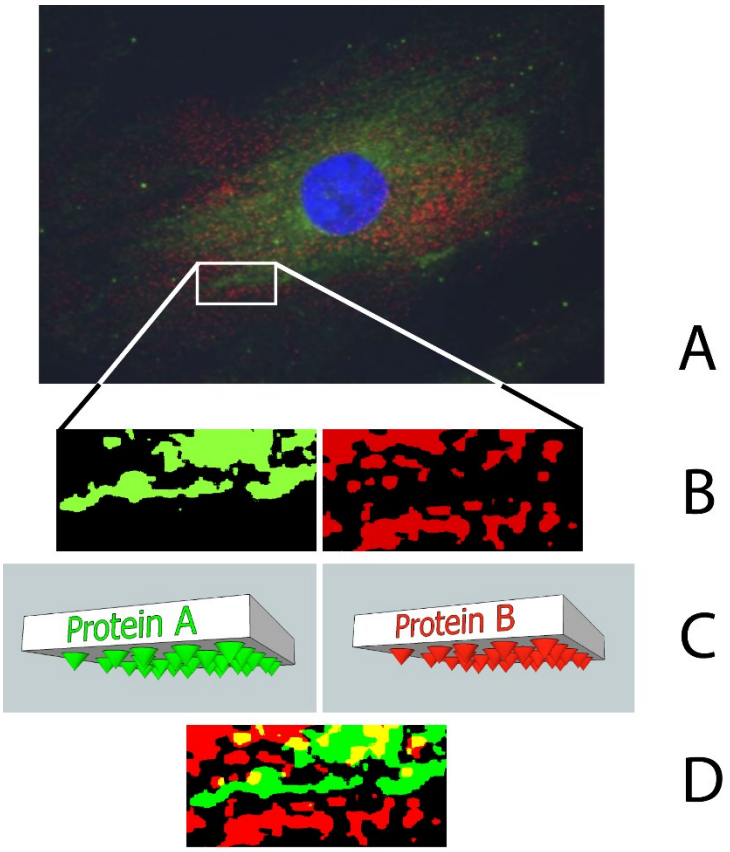

Figure 3.1: Essential steps of creating multiple protein patterns. (A) A high-resolution image of astrocyte expressed laminin (stained green), chondroitin sulfate proteoglycan (stained red), and cell nucleus (stained blue) (courtesy of F. Meng, Tresco's lab, University of Utah). (B) A smaller region of astrocyte membrane is used to create μCP templates for two proteins. (C) These templates are used to prepare two μCP stamps with the same repeating patterns. (D) The stamps are used to print two proteins in registration.

3.2 Methods

3.2.1 Stamping Platform

The multiprotein patterning was carried out using a modified inverted light microscope (Diaphot, Nikon) equipped with a charge-coupled device (CCD) camera (Orca, Hamamatsu) and designed to house both a soft polymeric stamp and a glass substrate (Figure 3.2). The microscope could be run either in bright-field, epi-fluorescence, or reflectance interference contrast microscopy (RICM) modes.[221,222] The stamps were mechanically attached to the microscope stage and could be translated in the *x*, *y*, and *z* directions as well as rotated in Θ_x, Θ_y, Θ_z relative to the substrate for alignment and leveling. The stamp holder consisted of an optical two-axis tilt mount (KMM1, Thorlabs) with a custom rotating glass stage. The holder was attached to the microscope stage via vertical sliding rails, providing a rough vertical adjustment and ensuring the stamp holder was level with respect to the microscope stage. The stamp was held on the glass stage simply using capillary forces, allowing for rapid and easy exchange of stamps and eliminating the need for adhesives or clamps. Additionally, the lack of mechanical clamps prevented deformation of stamp features prior to stamping and preserved the integrity of the pattern. The substrate to be stamped was attached to the outer housing of the microscope's objective lens (Nikon, Fluor 10x, NA 0.5) by a custom engineered stage. This stage allowed for the use of glass coverslips or microscope slides as substrates, thus also facilitating simple substrate exchanges. The stage was optically clear, and the surface to be stamped could be brought into the focal plane of the underlying objective, allowing for real-time *in situ* imaging during the stamping process.

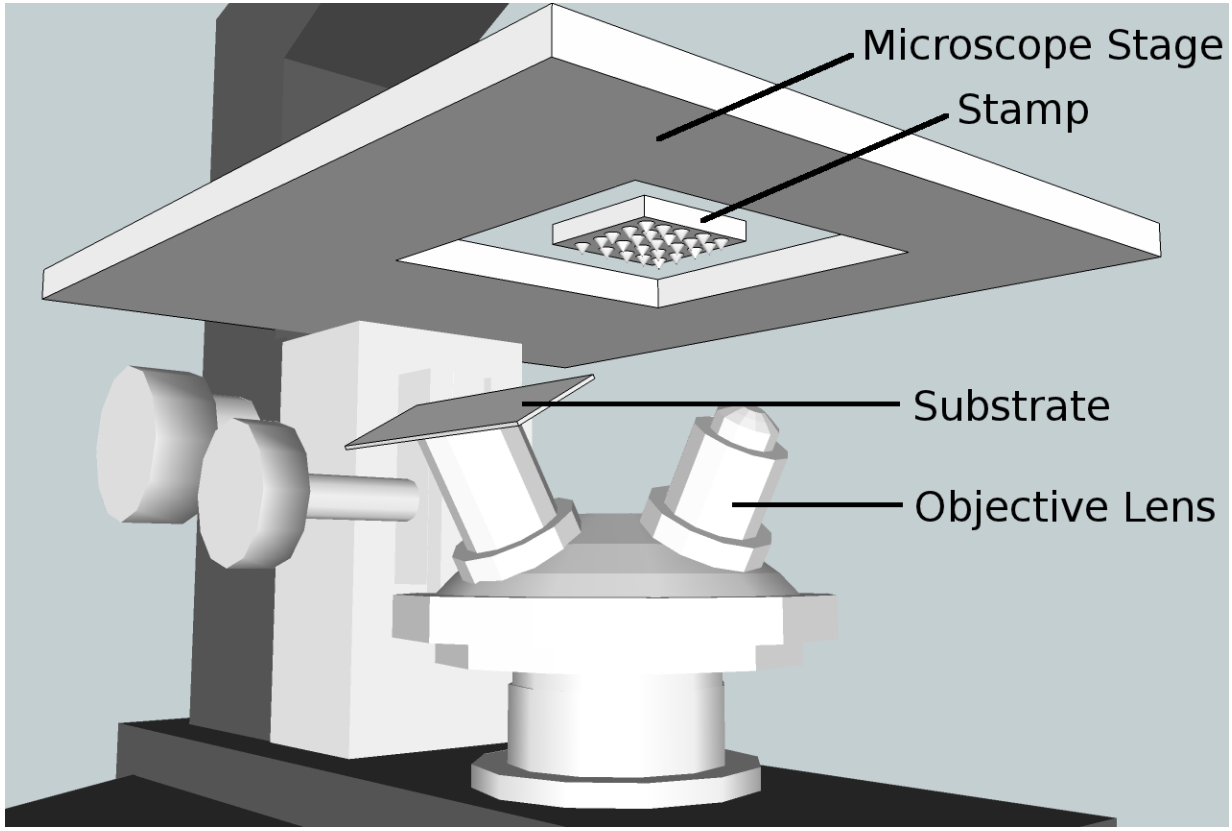

Figure 3.2: Schematic of the multiprotein μCP device. A light microscope was modified to accept stamps and substrates while providing real-time imaging capabilities.

3.2.2 PDMS Stamps

The creation of soft lithographic stamps has been previously described in detail.[213] Briefly, photolithographic techniques were used to transfer template patterns onto chromium-coated fused silica surfaces. A chromium etch was used to provide for relief of features. PDMS (10:1 ratio of base-to-cross-linker by weight) was then cast over the molds and allowed to cure. The PDMS stamps were peeled off of the mold and were cleaned by sonication in a 1 % solution of surfactant Alconox® (Alconox, New York) for 15 min. Stamps were rinsed in ethanol and allowed to dry under nitrogen gas. The stamps were then inked with the desired proteins by depositing 100 μL of protein solution on the feature-side of the stamp and incubating for 30 min. Nonadhered protein was rinsed off with double distilled deionized (DDI) water, and the stamps were dried again under a stream of nitrogen.

3.2.3 Two-protein Stamping Protocol

For illustration, a two-protein stamping protocol is described here; however, it should be noted that this technique could be easily used to create higher order protein patterns. In a two-stamp protocol, the first stamp was placed on the optical two-axis tilt mount and fastened to the stage of the inverted light microscope with its inked side facing toward an objective lens. A substrate to be stamped was attached to the custom stage on the top of the objective (Nikon, Fluor 10x, NA 0.5) (Figure 3.2) and was brought into the focal plane of the objective. The microscope turret was then rotated to retract the substrate stage and to advance the second, so-called “leveling” objective (Nikon Fluor 20x, NA 0.75) below the mounted stamp. Stamp leveling with respect to the substrate was accomplished

by translating and imaging each corner of the stamp and ensuring they were in focus by adjusting the tilt mount (Θ_x, Θ_y) as necessary. Through the use of an objective lens with a shallow depth of field, very precise leveling could be achieved, which was important as features on the elastomeric stamp can deform differently under a nonuniformly applied load. If one portion of the stamp is incident upon the sample first, it will ultimately experience a higher load than the rest of the stamp, which may lead to deformed features or stamp collapse.

The microscope turret was then rotated back to advance the substrate below the stamp. The stage was lowered to bring the stamp into contact with the surface for five min, depositing the protein on the substrate. Using the CCD camera, real-time images of the stamping process were generated. This allowed for recording of the stamping process and, in the case of RICM images, provided quantitative information as to the actual area of the stamp in contact with the surface. When multiple stamped patterns were desired on the same substrate surface, an image of the first stamp was recorded using bright field while the stamp was in contact with the substrate. The first stamp was then retracted, and a second stamp was loaded. The microscope turret was again rotated to advance the leveling objective. The second stamp was leveled in the same manner as the first. The turret was rotated back to again bring the substrate into place. Using the "overlay" function in ImageJ,[223] the recorded image of the first stamp in contact with the surface was layered over the live image from the microscope. Since the substrate remained stationary in the field of view of the camera, the image of the first stamp was representative of the first transferred protein pattern on the substrate. The pattern on the second stamp could therefore be prealigned with the pattern transferred from the first stamp prior to second stamp-

substrate contact. The second stamp was then brought into contact with the surface for 5 min and retracted, resulting in the transfer of the second protein pattern. In this way, surfaces with multiple precisely aligned patterns of proteins were generated. Figure 3.3 shows a schematic of the two-step protocol highlighting the different steps of this process.

Feature deformation and collapse are two inherent problems in μCP[214] and vary based on the physical distribution of pillars used to pattern the substrate. Since the substrate stage was mounted to an objective lens, real-time *in situ* imaging was made possible. This provided for both qualitative and quantitative information during the stamping process. The use of RICM greatly assisted in calibrating the system for each stamp. Using RICM mode, the contact area of the stamp was measured, and the effect of various loading forces on stamp feature deformation was determined. Figure 3.4a shows an RICM image of a random gradient stamp touching a substrate, with contacting features appearing black. Using fluorescently labeled proteins in the stamping process, the resulting patterns on the substrate were visualized using epifluorescence microscopy. Figure 3.4b shows an example of a transferred AlexaFluor 488-labeled laminin (Invitrogen) from the same gradient stamp. Using proteins conjugated with different fluorophores, multiple patterns of proteins on the same surface were viewed independently, and alignment of the patterns was verified.

3.2.4 Cell Adhesion Experiments

Primary P1 CD rat astrocytes were seeded onto patterned coverslips at a sub-monolayer density of approximately 4000 cells/cm^2. The cells were cultured at 37° C and 5 % CO_2 for 48 h in Dulbecco's modified Eagle medium (DMEM)/F12 media (Gibco) supplemented with 10 % fetal bovine serum (FBS; Sigma). Astrocyte cultures were fixed

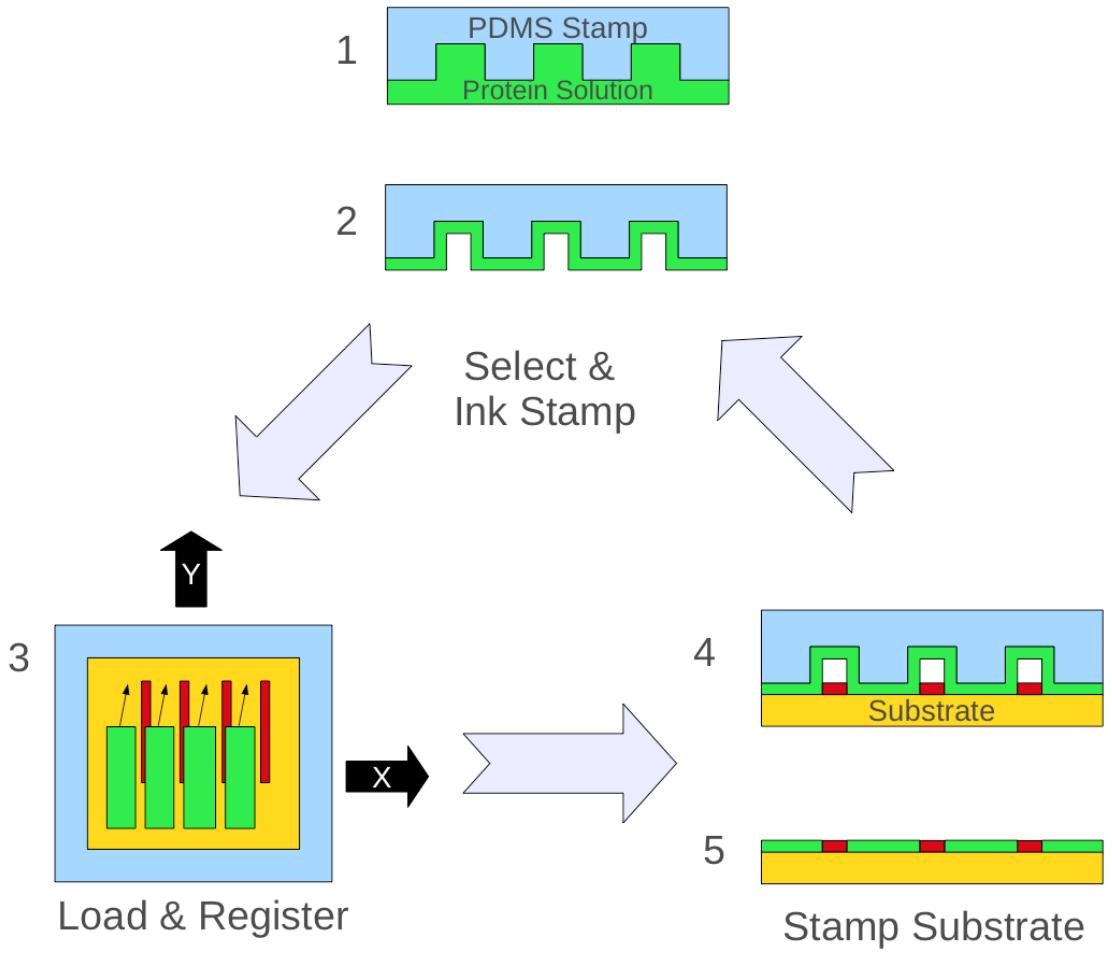

Figure 3.3: Schematic of the multiprotein μCP process. A stamp is inked and dried (1–2) then loaded and leveled using the leveling objective. The substrate stage is advanced with the microscope turret, and the stamp is aligned with the previous pattern (3). The stamp is then brought into contact with the surface and the protein pattern is transferred (4–5). This process is repeated to deposit multiple patterns of proteins.

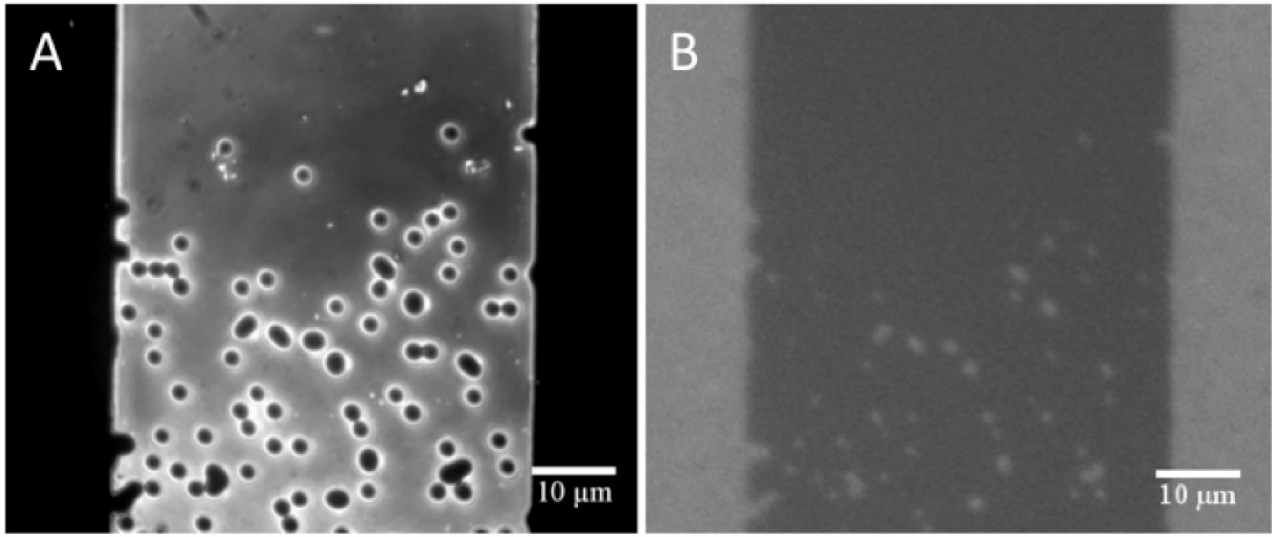

Figure 3.4: Examples of *in situ* microscopy available in the multiprotein μCP process. (A) RICM image of a gradient patterned stamp in contact with a substrate. (B) Fluorescence microscopy image of a transferred laminin (AlexaFluor 488-labeled) protein pattern from a gradient stamp.

with 4 % paraformaldehyde for 15 min. Fixed samples were treated with 4',6-diamidino-2-phenylindole (DAPI; Invitrogen) in a 1:100 dilution in phosphate-buffered saline (PBS) for 15 min to stain for cell nuclei. Samples were then rinsed in DDI water, dried, and mounted with Fluoromount-G (Southern Biotech) for imaging using a fluorescence microscope (Nikon Eclipse E600, Plan 20x, NA 0.75). Cell alignment with respect to alternating patterns of laminin (Invitrogen) and aggrecan (Sigma-Aldrich) was calculated by taking the angle of the longest chord drawn through the nucleus of each cell relative to the patterned lanes using Image Pro Plus (Media Cybernetics). Astrocytes cells present in aggregates were excluded to eliminate cell–cell interactions from two-protein pattern effects.

3.3 Results

To determine the positional error introduced by the leveling procedure, the reproducibility of the microscope turret was investigated. The turret was rotated between the sample stage objective and leveling objective 20 times, and an image of a reticle was taken each time. These images were used to calculate the variation in set position inherent to the microscope turret. The variation was found to be ±1.96 μm in the *x* direction and ±1.23 μm in the *y* direction.

The registration capability of the device was demonstrated by aligning two stamps: the first stamp was based on a randomized 20 % coverage pattern generated using Mathematica's (Wolfram) random function with the smallest feature size being 1 μm^2, while the second stamp was its inverse.[85] Figure 3.5a represents a subsection of the template used to generate the 20 % coverage stamp, and Figure 3.5b shows a bright field

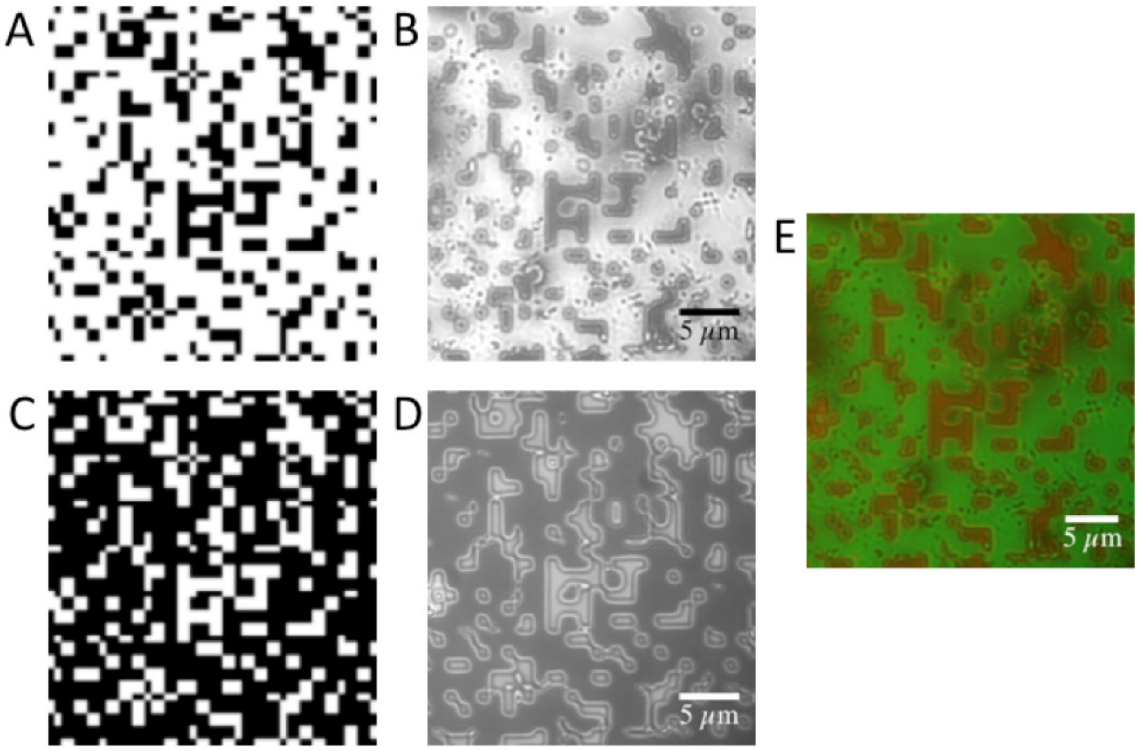

Figure 3.5: The registration capability of the multiprotein μCP process. (A) A subsection of a random 20 % coverage pattern. (B) Bright field image of a randomized 20 % coverage stamp. (C) A subsection of the complementary 80 % coverage pattern. (D) Bright field image of a complementary 80 % coverage stamp. (E) Overlay of the two stamps as seen by operator during the alignment step. False color was added for contrast.

image of the corresponding portion of the stamp. Figures 3.5c and 3.5d shows the same for the complementary 80 % coverage stamp. Figure 3.5e shows an overlay of an image of the 20 % stamp with the live CCD feed of the 80 % stamp during alignment. Colors are added to provide contrast between the features of each stamp.

The precision in printing two different proteins was demonstrated through the use of stamps that were patterned with 15 μm lanes spaced 25 μm apart. Figure 3.6 shows the printing of AlexaFluor 488-labeled laminin using the first stamp and AlexaFluor 592-labeled aggrecan using a second stamp with identical features on the same substrate surface at various inter-lane spacings. Figure 3.6a shows lanes printed with an intended space of 0 μm between them, while Figure 3.6b shows lanes printed with an intended space of 5 μm between them. Actual distances were 1.18 ± 0.25 μm (Figure 3.6a) and 4.76 ± 0.24 μm (Figure 3.6b), calculated by taking the average intensity profile across the gap between lanes and finding the full width at half-maximum value for each.

Astrocytes were cultured over a two-protein pattern of laminin and aggrecan lanes and over appropriate controls (laminin only or aggrecan only patterns). Cells were observed to interact with the underlying protein layers and preferential adhesion and alignment to the laminin lanes was observed. Figure 3.7 shows the alignment of astrocytes cultured on laminin and aggrecan lanes. Alignment along the axis of the laminin lanes was observed in samples that contained laminin patterns either with or without aggrecan, while this alignment was absent for samples containing only aggrecan lanes (Figure 3.7b). Figures 3.7c and 3.7d show histograms of astrocyte alignment relative to the axis of the underlying protein patterns.

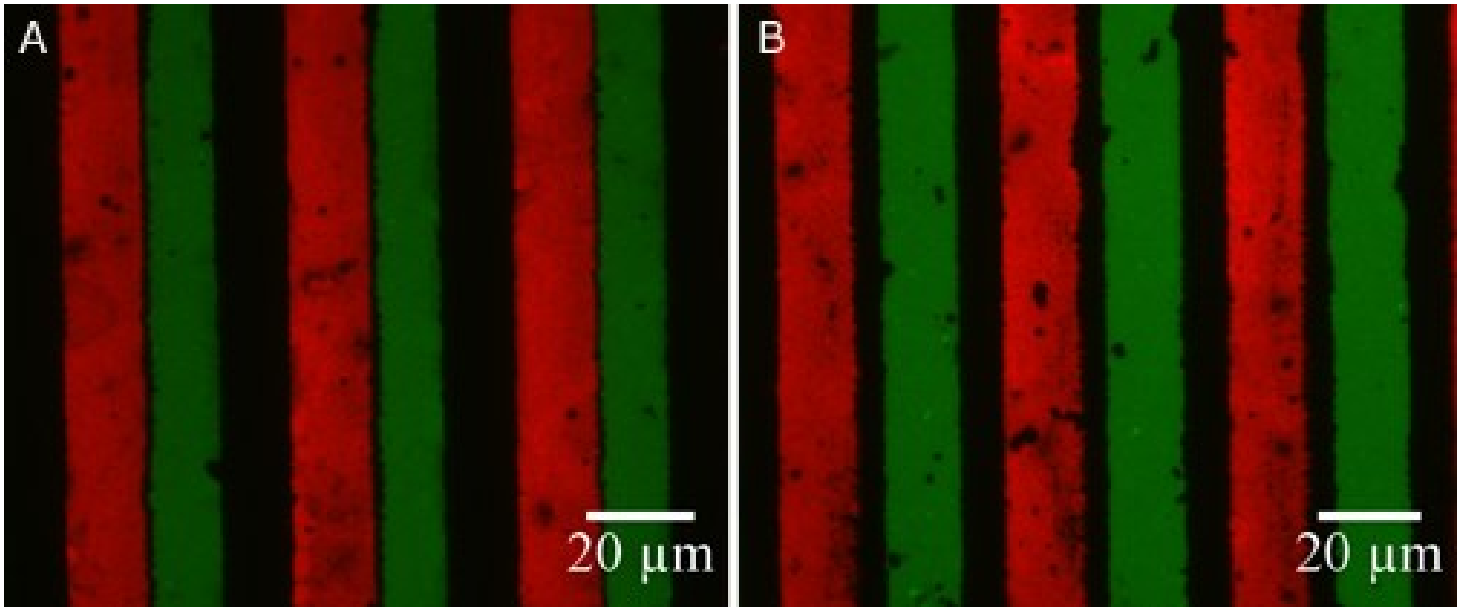

Figure 3.6: Lane patterns printed with the multiprotein µCP process. Lane patterns were printed with laminin (AlexaFluor 488-labeled) and aggrecan (AlexaFluor 592-labeled). (A) Intended lane spacing of 0 µm. (B) Intended lane spacing of 5 µm.

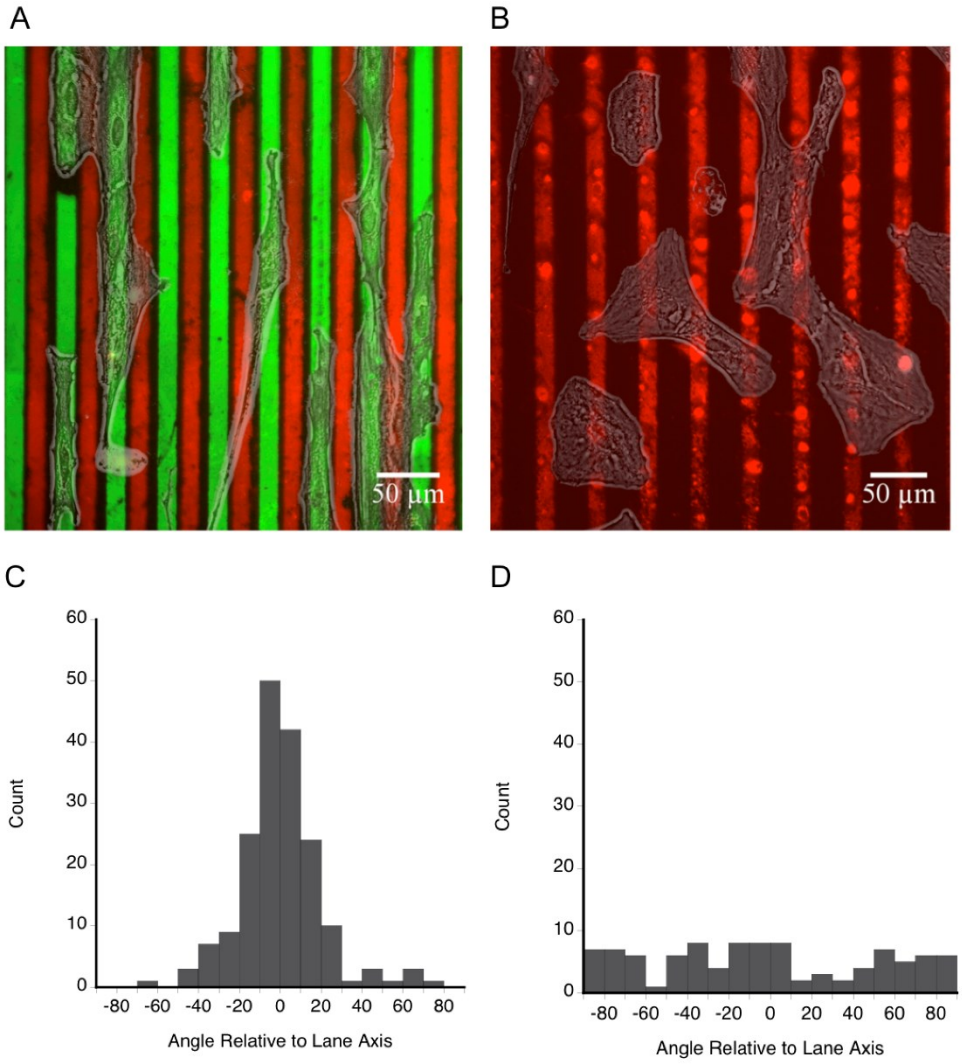

Figure 3.7: Alignment of cells on printed multiprotein patterns. (A,B) Fluorescence images were produced from the sequential stamping of laminin (green, AlexaFluor 488-labeled) and aggrecan (red, AlexaFluor 592-labeled) using two lane stamps with bright field overlay of cultured astrocytes. Astrocytes were seen to interact with the underlying laminin pattern but not the underlying aggrecan pattern. (C) Histogram showing the alignment of astrocytes cultured on laminin and aggrecan lanes relative to underlying pattern (n = 179). (D) Histogram showing the alignment of astrocytes cultured on aggrecan lanes relative to underlying pattern (n = 97).

3.4 Discussion

When aligning multiple stamps, it is important to eliminate motion in the system to ensure the image taken of the first stamp in contact with the surface continually represents the distribution of the first transferred protein species. In printing multiple proteins, the greatest source of alignment error is introduced in the leveling process. During leveling, the microscope turret is rotated between the attached substrate and a separate objective lens. This mechanical system has an intrinsic amount of deviation at each of these set positions. Any deviation in the position of the turret will cause an offset between the image of the first pattern and the actual location of the transferred protein pattern. This will cause the second protein pattern to be deposited slightly out of alignment with the first. The amount of error introduced in this step is within the tolerance of the designed application of the system. It is important to note, however, that for certain stamps, leveling is less of a concern. Depending on the distribution of features on the stamp, variations in pressure across the stamp can have either profound or little effect on the fidelity of pattern transfer. Additionally, the elastic modulus of PDMS can be tailored to reduce the need for stamp leveling. For stamp systems in which pressure variations have little effect, the leveling step can be skipped and thus reduce error in pattern transfer.

As illustrated in Figure 3.5, this technique can be used to precisely register multiple patterns of proteins. The image in Figure 3.5e shows what the user observes while aligning a second stamp with a previously transferred pattern. The first stamp is loaded and brought into contact with the substrate. An image of this stamp in contact with the substrate (Figure 3.5b) is used in conjunction with the live image of a second stamp (Figure 3.5d) to ensure the two patterns are in registry before stamping. In this example, the features from the 20

% random coverage stamp can be seen through the holes in the live image of the complementary stamp (Figure 3.5e). Once the patterns are aligned, the second stamp is brought into contact with the surface, thus transferring the second pattern of proteins. This demonstrates the precision afforded by this method in the *x*, *y*, and rotational degrees of freedom. Higher order patterned systems can be easily created with the same degree of accuracy.

The precise control of alignment allows for the transfer of multiple protein patterns to the same surface in registry. Figure 3.6 demonstrates the control over spacing between printed lane patterns. Both laminin (AlexaFluor 488) and aggrecan (AlexaFluor 592) were used as they are two proteins of interest in the study of neuronal guidance in spinal cord injury bridging devices. Images of each species were obtained separately using appropriate filters that were then combined to form the final image. Precision in alignment is demonstrated by the proximity of stripes in the x-direction and the rotational orientation. Spacing between lanes was controlled with an accuracy of ~1 μm at two different spacings, 0 and 5 μm.

This pattern is fundamentally different from current two-protein patterns in that it is continuous over a large area (1 cm^2) and the two species were precisely deposited in register with one another. Conventional large area, two-protein patterns were previously generated by backfilling one of the proteins, which might have resulted in nonspecific binding and interactions with previously deposited protein layers.[198] Other multiprotein patterns have been generated through the stamping of a single substrate in serial; however, no known current methodologies have the precision and repeatability demonstrated by this method. The current method allows for the presence of nonpatterned space within a

multiprotein system, which conventional methods cannot produce.

Astrocytes cultured over laminin and aggrecan lanes were seen to interact with the underlying protein patterns. Cells were observed to preferentially adhere to laminin lanes (versus nonstamped and aggrecan lanes), and aligned along the axis of the pattern. This was expected, as laminin lanes have been previously shown to induce alignment in cultured astrocytes.[220] Aggrecan, typically implicated in inhibiting neuronal guidance, was not seen to play a significant role in modifying astrocyte behavior versus nonstamped controls. The interaction of cells with the underlying protein patterns demonstrates the transfer of an active protein species to the surface in a controlled pattern and validates this method as a surface-patterning tool.

3.5 Conclusion

Presented here is the description of a technique developed for the deposition of multiple independent protein patterns on the same surface. The integration of live-imaging capabilities makes possible the precise alignment of multiple stamps and introduces valuable imaging tools *in situ*. The capabilities of this method to align and print multiple protein patterns in precise registration have been demonstrated, as has the bioactivity of these transferred patterns. The verification of this technique addresses a previously unmet need in the field of μCP.

CHAPTER 4

DETECTION OF SYNERGY IN PLATELET PRIMING PATHWAYS USING MULTIPLE SURFACE BOUND AGONISTS IN FLOW

4.1 Introduction

Current platelet function tests fall short in their ability to predict adverse clinical outcomes. This is partially due to the complexity of currently available methods and the effect that confounding factors like patient hematocrit, sample handling, and anticoagulant selection have on results.[120,122,126,131] This can also be attributed to the fact that no current platelet function assay takes into account the priming effect in platelets. Platelets encountering a damaged vessel or a biomaterial interact with a complex milieu of agonist molecules, and it has been shown that the majority of platelets that become incident on an agonist surface do not end up making stable adhesions.[83] It has also been demonstrated that a variety of agonist molecules can elicit a priming response from platelets.[81,82] Previous work has shown that a surface-bound agonist is capable of priming platelets for enhanced adhesion downstream (see Chapter 2); however, the effect that multiple priming agonists have on a platelet population has not been studied.[84,85] This chapter documents the integration of a multiagonist priming region into a platelet function assay and posits the existence of a synergistic effect between platelet priming pathways.

4.1.1 Transient Contacts

When a platelet initially becomes incident on a biomaterial or damaged vessel, it first forms an adhesive bond with von Willebrand factor (vWF) that is either adsorbed to the material surface or associated with collagen in the vascular extracellular matrix (ECM).[75] The bond that forms between the GPIb-IX-V complex and vWF is characterized by an extremely quick on-off rate, which allows for the capture of rapidly moving platelets from circulation.[224,225] The shear strengthening nature of this catch bond leads to a stop-start pattern in their motion across the surface.[44,46] Once sequestered from flow, platelets translocate along the surface through the rapid association and disassociation of these bonds.

Due to its critical role in initiating contacts between platelets and surfaces, the nature of this bond has been investigated thoroughly.[226–228] The quick on-off rate of this bond not only allows for the capture of platelets from flow, but also for the rapid disassociation of platelets from the surface. Indeed, it has been observed that the majority of platelets do not make stable adhesions with a surface, but instead return to circulation.[83] This adhesion to, translocation on, and release from an agonist-covered surface likely serves to prime a platelet population for enhanced adhesion and activation at a downstream location.

Numerous recent studies have used microfluidic devices to investigate the interaction between platelets and artificial surfaces, incorporating agonists such as surface-bound proteins and shear. [161,179,229] Very few of these studies, however, have taken into account the transient nature of platelet-surface contacts.[83,230]

4.1.2 Platelet Priming Pathways

Implanted biomaterials and sites of vascular damage are characterized by a complex mixture of adsorbed and exposed molecules including blood plasma proteins and the endothelial ECM. As a platelet rolls across a surface, it is therefore likely that they are exposed to a variety of different agonist molecules such as fibrinogen, vWF, or collagen. Platelets interact with agonists through many different surface receptors, including GPIIb/IIIa, GPVI, integrin α2β1, and the GPIb-IX-V complex, each of which initiates a signal transduction pathway within the platelet. The integrated response of a platelet to each of these stimuli is what determines the final activation state of a platelet.[231]

As with all cells, platelets use common internal signaling pathways which may result in synergistic effects that cannot be anticipated through the study of single agonists alone. Activation pathways, for example, start with unique surface membrane receptors, but use a number of common signal transduction molecules such as phospholipase C (PLC) isoforms, protein kinase C (PKC), and calcium ions (Ca^{+2}), and eventually converge to activate GPIIb/IIIa, form stable adhesions, and release the contents of granules.[232–234] Figure 4.1 illustrates some common elements in platelet adhesion pathways resulting in the activation of GPIIb/IIIa and further amplification events. Given the nature of redundancy in the platelet activation pathway, it is not far-fetched to posit similar redundancies built into the pathways by which platelets become primed. [235,236] It is therefore of interest to be able to stimulate platelets with multiple agonists and measure the priming response elicited.

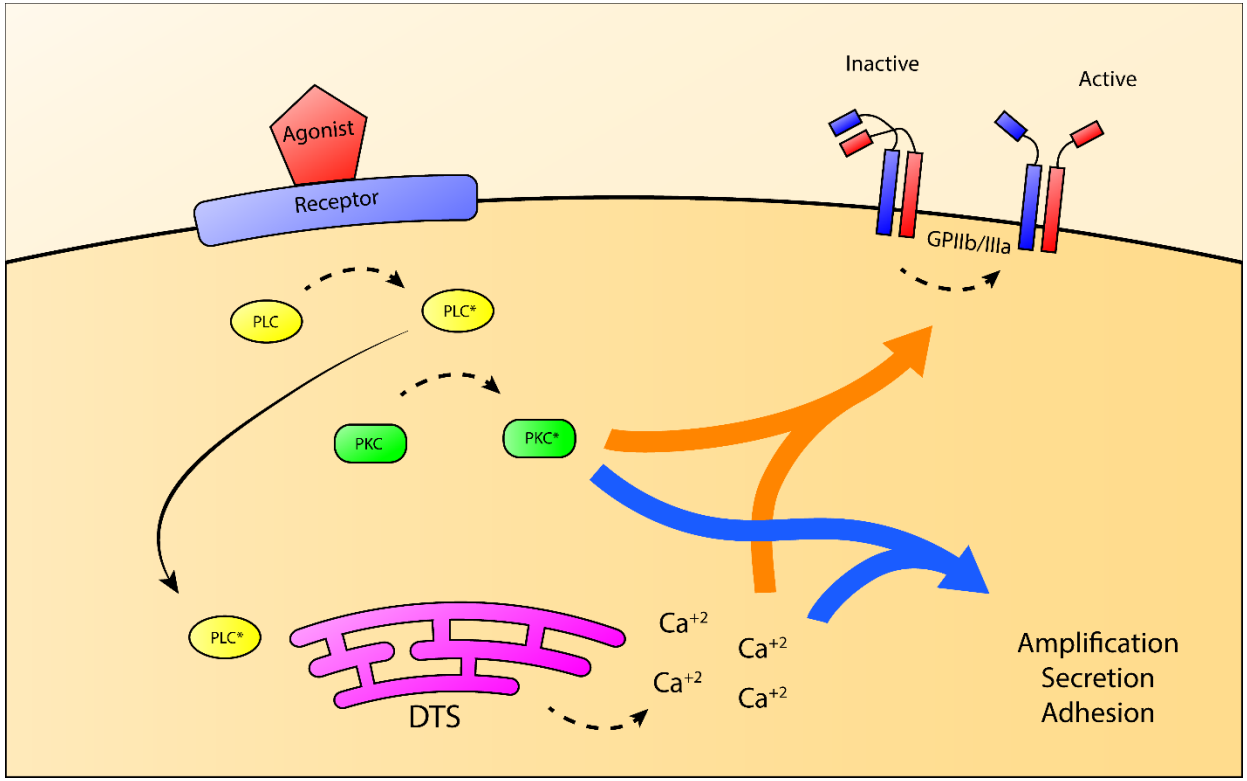

Figure 4.1: Common elements of platelet activation pathways. When an agonist binds to a surface receptor on a platelet, one of a variety of isoforms of phospholipase C (PLC) becomes activated. Active PLC releases cytosolic calcium ions from the dense tubular system, and also catalyzes the activation of protein kinase C (PKC). Both calcium ions and activated PKC are responsible for the conversion of GPIIb/IIIa from a resting to an active state, as well as amplifying other activation pathways, such as the secretion of granules and stable adhesion to surface-presented agonists.

4.2 Methods

4.2.1 Flow Cell Creation

Flow cells were manufactured according to the protocol set out in Section 2.2.1. Briefly, polydimethylsiloxane (PDMS Sylgard 184, Dow Corning) was poured into a flow cell mold at a ratio of 15:1 (polymer to crosslinker by weight) and allowed to cure. Relief for the flow channel features was provided by polymeric tape, which was patterned on a laser cutter (VLS3.60, Universal Laser Systems) and attached to the bottom of the mold. After release from the mold, fluid vias were bored in the flow cells using a biopsy punch (2mm, Robbins Instruments) to allow for inlet and outlet of blood.

Platelet priming and capture regions were created by microcontact printing (μCP) of various platelet agonists. Soft lithographic stamps of varying surface coverage densities were created in a process described in Section 2.2.1 and elsewhere.[85,184] The surface of these stamps was coated with a protein solution and allowed to dry, then inverted onto the substrate. Covalent linkages were formed between the agonists and the glass substrate by a reactive N-hydroxysuccinimide ester chemistry through the use of commercially available Nexterion-H® (Schott) slides.[185,186] Stamps were left in contact with the substrate for 1 hour to ensure the stable adhesion of protein agonists. Priming regions were stamped 5 mm from the inlet to allow for the development of laminar flow, and capture regions were printed 45 mm downstream of the priming regions. The agonist and surface density of the priming regions varied according to experimental conditions; however, capture regions consisted of a plain-field (100 % surface coverage) patch of fibrinogen in all experiments.

Devices were assembled by inverting the PDMS flow channels onto the stamped

glass substrate. After assembly, nonprinted regions on the substrate as well as the walls of the flow channel were passivated by filling the flow channel with a human serum albumin solution (1 mg/mL, Sigma Aldrich) for 1 hour prior to perfusion.

4.2.2 Multiagonist Stamping

Multiprotein μCP was employed to achieve priming regions with multiple agonists. The method described in Chapter 3 was used to print agonist patterns of varying surface density in registry with their complementary pattern. Experimental conditions were as illustrated in Figure 4.2, with the titration of the surface density of one species being offset by a complementary surface density of another. For example, mixtures of two agonist species, A and B, were created in the ratios of 0A:100B, 30A:70B, 50A:50B, 70A:30B, and 100A:0B, as well as unprimed controls. Transfer and alignment of agonist patterns was verified using microscopy of fluorophores conjugated to protein agonists through a succinimidyl ester chemistry (Alexa Fluor 488, 594). Once the multiagonist stamping protocol was established, nonconjugated agonists were used for all priming experiments to avoid interference between fluorophores and platelet binding.

4.2.3 Selective Agonist Blocking

Selective agonist blocking was achieved by incubating the upstream priming region with the appropriate antibody solution for 30 min prior to device assembly. Priming regions were isolated using a custom removable PDMS micro-well to prevent antibody contamination of the rest of the flow channel. Fibrinogen was blocked using goat antihuman fibrinogen (Sigma Aldrich). This antibody has been determined to be pure and

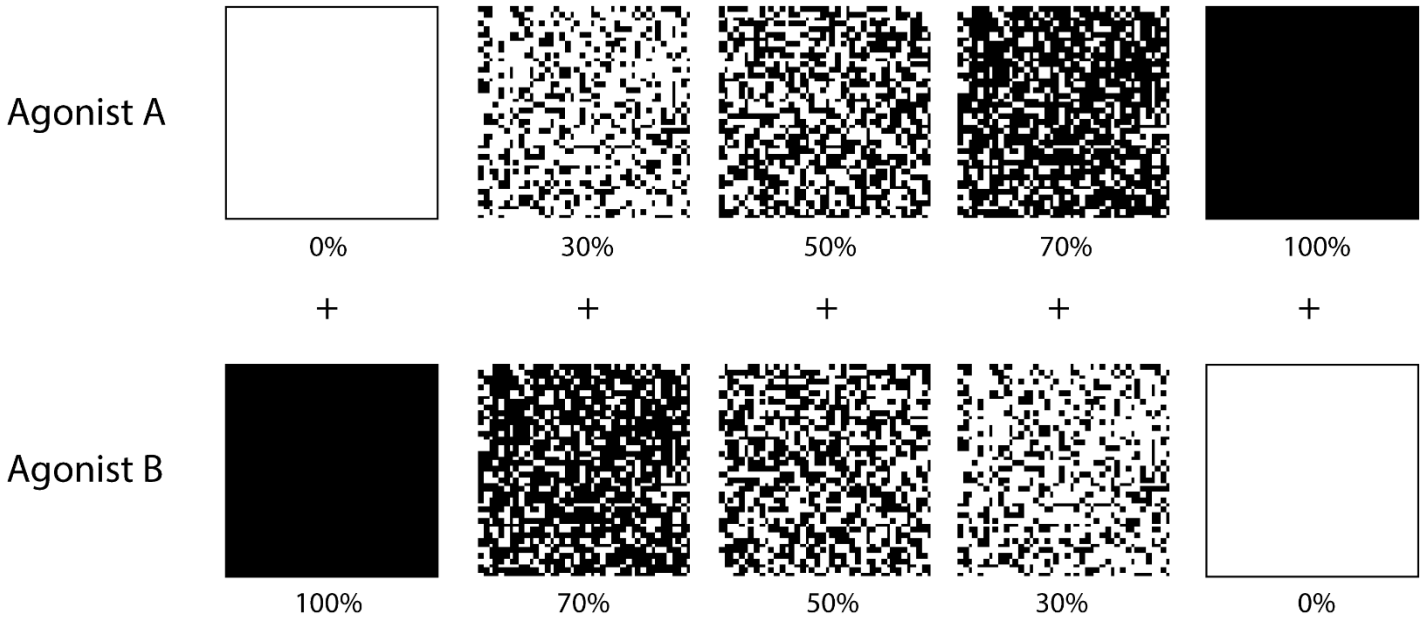

Figure 4.2: Schematic of multi-agonist experimental conditions. Surface coverage density of agonist A was titrated from 0 % to 100 %. The complementary pattern of agonist B was subsequently stamped in registry with the first pattern to create a fully covered field of agonist consisting of discrete components of agonist A and agonist B.

immunospecific for fibrinogen by the supplier, using immunoelectrophoresis against human plasma and fibrinogen. Contaminating antibodies were removed by solid phase adsorption with human plasma proteins. Collagen was blocked using rabbit antihuman collagen type I (Sigma Aldrich). This antibody has been affinity isolated by the supplier to ensure specificity, and was treated to remove any residual lipoproteins. Von Willebrand Factor was blocked using sheep antihuman von Willebrand Factor (Haematologic Technologies Inc.). The purity of the IgG fraction was verified by the supplier to >95 % by SDS-PAGE. The samples were rinsed three times in DDI water following incubation, with care taken to not contaminate areas outside of the priming regions. Devices were then assembled, passivated with albumin, and used immediately.

4.2.4 Flow Cell Operation

Flow cell studies were carried out as described in Chapter 2. Whole blood was collected from healthy human donors into a 0.105 M sodium citrate solution and was anticoagulated with Phe-Pro-Arg-chloromethylketone (PPACK) (Haematologic Technologies) to prevent coagulation. A flow rate of 3.6 mL/h was sustained for 5 min in each experiment to produce a shear rate of 200 s^{-1}. Devices were then rinsed three times with Tyrode's buffer and fixed in a 4 % paraformaldehyde solution. Attached cells were imaged using a differential interference contrast (DIC, Diaphot 300, Nikon) and quantified. Adhered platelets were counted in ten randomly selected fields (300 μm x 400 μm) within the downstream capture region. Statistical significance was established using unpaired t-tests.

4.3 Results

4.3.1 Multiagonist Stamping

Binary-agonist patterns were created at a variety of surface coverage density combinations, including 0A:100B, 30A:70B, 50A:50B, 70A:30B, and 100A:0B, where species A and B represent fibrinogen, vWF, or collagen (see Figure 4.2). Transfer and alignment of the patterns were verified with fluorescent microscopy. Figure 4.3A shows a representative image of a stamped agonist combination with surface coverage densities of 70 % fibrinogen and 30 % collagen. The pattern translational (X, Y) and rotational (Θ) alignment error were measured using image processing software (ImageJ) and results were averaged over 10 samples.[223] Figure 4.3B illustrates the parameters measured in each case. The translational and rotational alignment errors were found to be 0.4 ± 0.1 μm and 0.16 ± 0.03 degrees, respectively.

4.3.2 Agonist Titration

Agonists were titrated from 0 % to 100 % surface density coverage in pairwise combination with complementary patterns of another agonist species. In each case, platelet populations that were presented with two agonists displayed a higher priming response than those presented with the same total surface coverage density of single agonists. Figures 4.4, 4.5, and 4.6 show the number of adhered platelets in the downstream capture region in each experimental condition. The fibrinogen-collagen titration showed a marked increase in adhesion for conditions that presented multiple agonists versus single agonists, the greatest of which was seen to be at a 50A:50B mixture of the two species. The vWF-collagen titration showed a similar response, with a much greater increase in adhesion

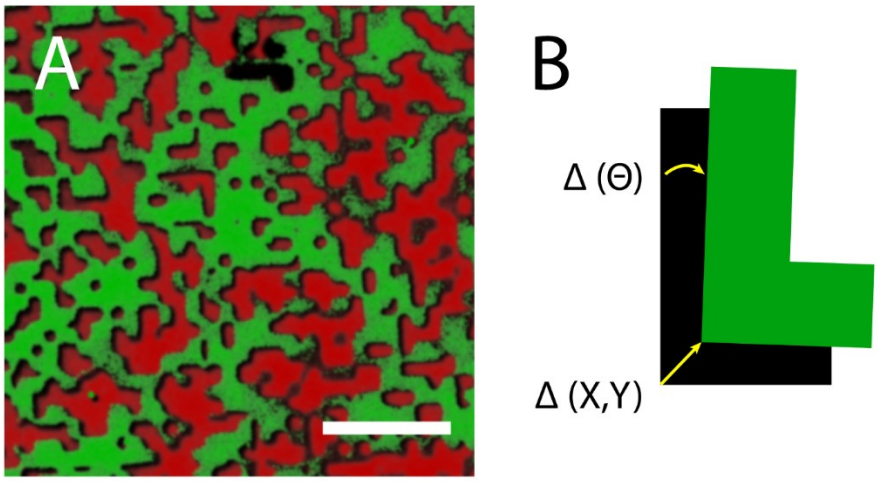

Figure 4.3: Quantification of error in the stamping process. A) Example of a transferred multi-agonist pattern. Fibrinogen (green, Alexafluor 488) was stamped at a 70 % surface density coverage. An inverse pattern stamp was then used to deposit collagen (red, Alexafluor 594) at a surface density coverage of 30 %, precisely aligned with the first pattern. Scale bar represents 10 μm. B) Parameters used to quantify error in the translational (X,Y) and rotational (Θ) alignment of the two stamped agonist patterns.

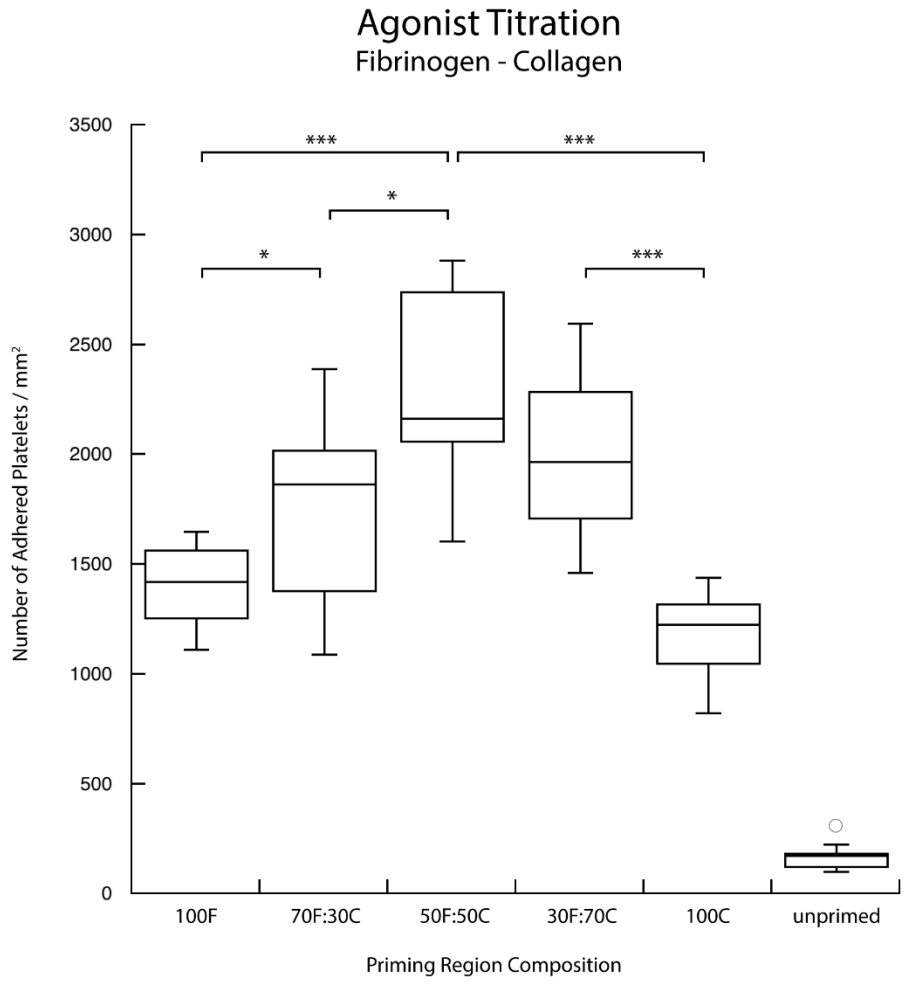

Figure 4.4: Co-presentation of fibrinogen and collagen results in an elevated priming response. Fibrinogen and collagen were presented in various combinations of surface densities. The combination of multiple agonists is seen to produce a priming response that is greater than either of the agonists presented independently. (***$p < 0.0005$, *$p < 0.05$)

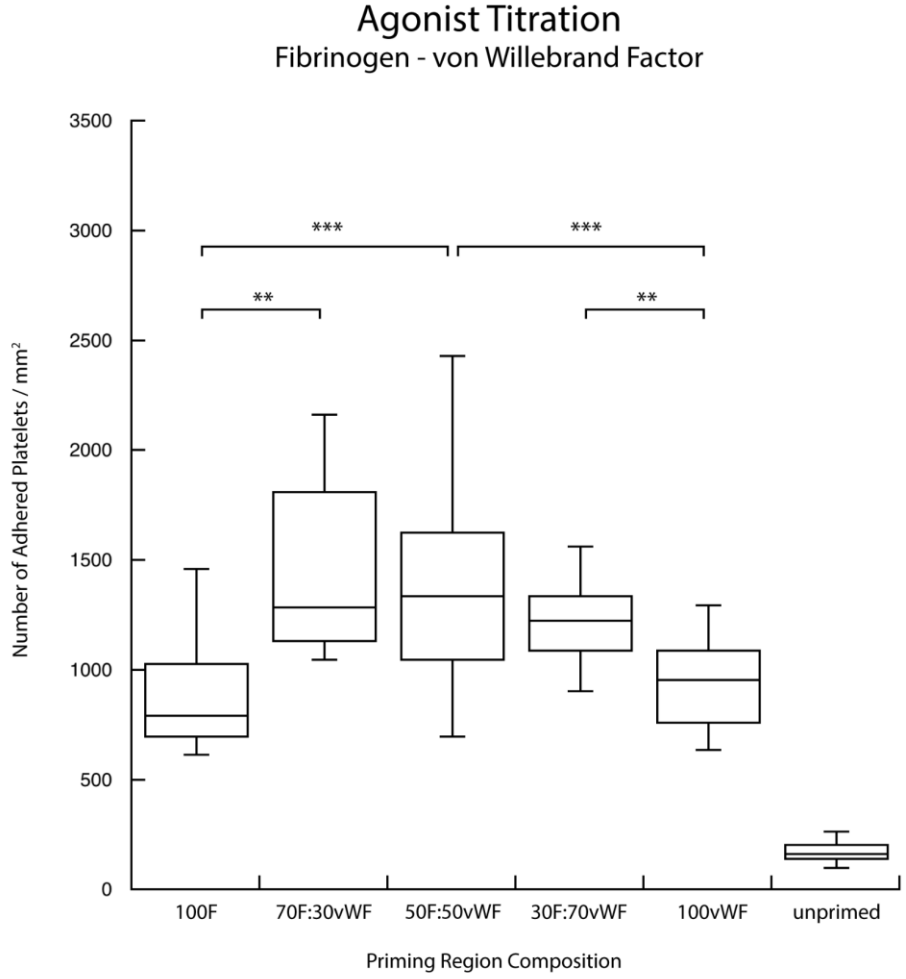

Figure 4.5: Co-presentation of fibrinogen and von Willebrand factor results in an elevated priming response. Fibrinogen and von Willebrand factor were presented in various combinations of surface densities. The combination of multiple agonists is seen to produce a priming response that is greater than either of the agonists presented independently. (***$p < 0.0005$, **$p < 0.005$)

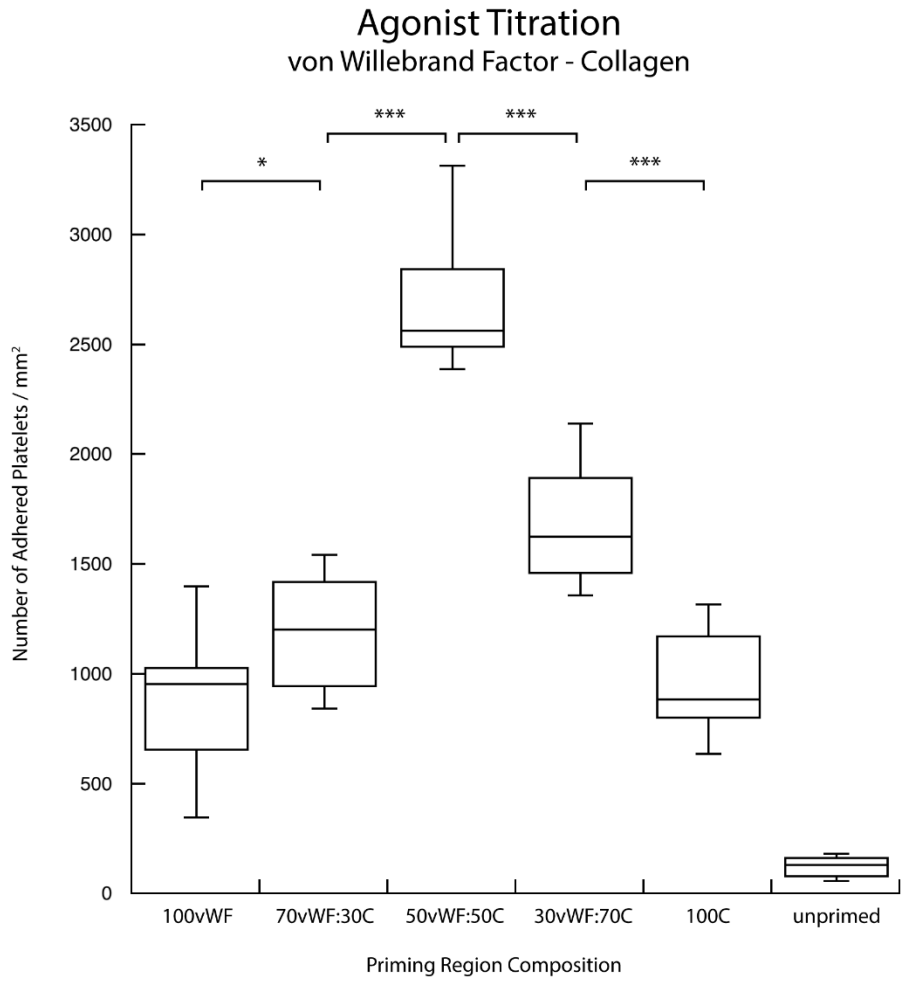

Figure 4.6: Co-presentation of von Willebrand factor and collagen results in an elevated priming response. Von Willebrand factor and collagen were presented in various combinations of surface densities. The combination of multiple agonists is seen to produce a priming response that is greater than either of the agonists presented independently. (***$p < 0.0005$, *$p < 0.05$)

observed at a 50A:50B mixture. In the case of the fibrinogen–vWF combination, the maximum response was harder to determine; however, an increased priming response was still observed for combined agonists over priming with either fibrinogen or vWF alone.

4.3.3 Selective Agonist Inhibition

In this experiment, the pairwise agonist titration was repeated, but one agonist species in the priming region was selectively blocked with the appropriate polyclonal antibody. Figures 4.7, 4.8, and 4.9 show the number of adhered platelets for the blocking of single agonist species in each of the agonist combinations. In each case, the blocking of one of the agonists served to eliminate the enhanced response seen in the titration experiments. A trend, similar to the titration of a single agonist (see Figure 2.3), was observed in every combination of agonist pair and antibody.

4.4 Discussion

Described here is an application of a flow assay that can detect a variable platelet priming response as a result of varying agonist species presentation. This assay utilizes the concept of platelet priming to determine the activation state of a platelet population using a surface capture assay. In the present study, priming regions consisting of variable surface density concentrations of agonist pairs were presented to flowing blood. An enhanced activation response was observed in experimental conditions that presented the flowing blood with multiple agonists when compared to those that presented single agonists.

Stamping of a single pattern of proteins, then backfilling with a second species is the most common way of creating combinations of protein patterns on surfaces; however,

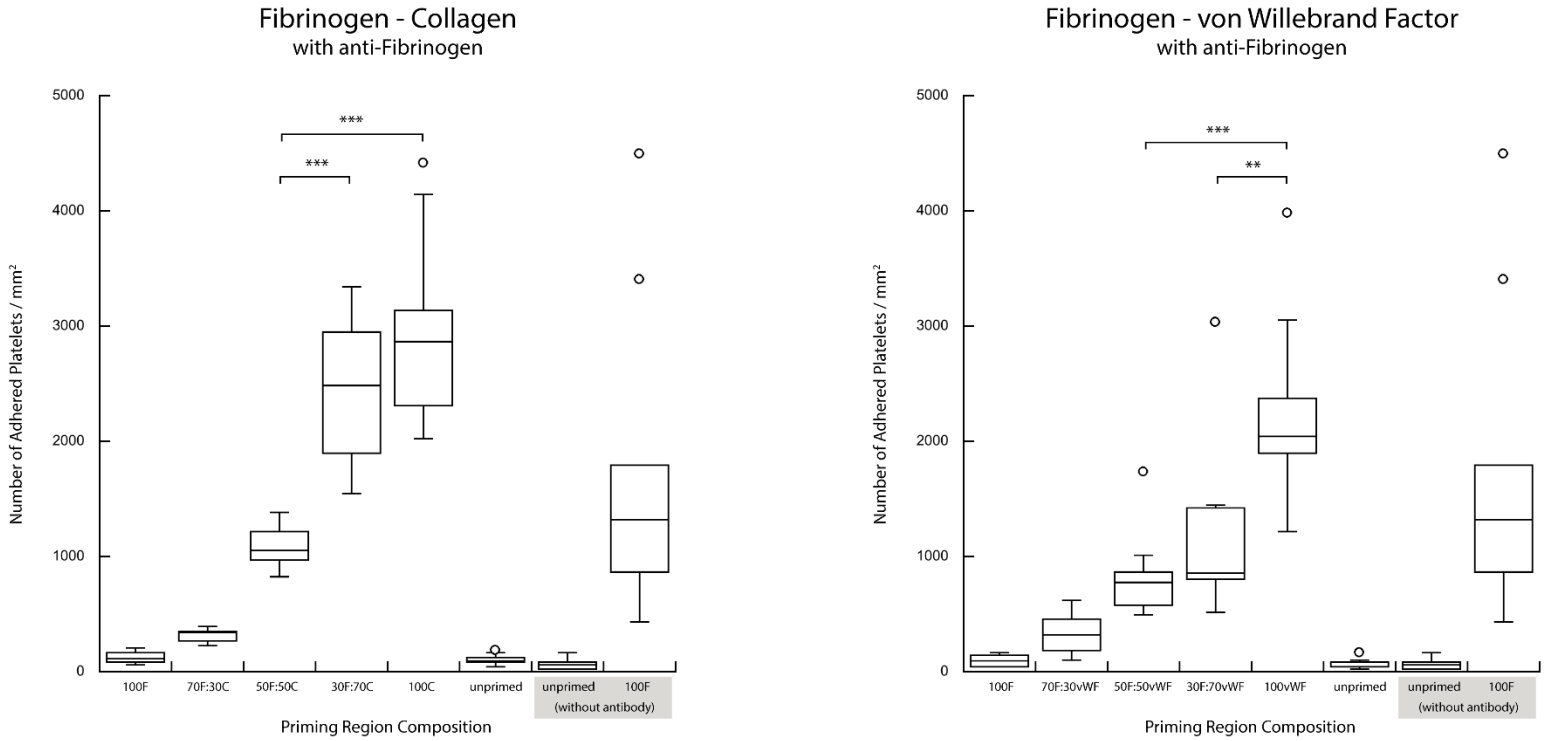

Figure 4.7: Selective blocking of fibrinogen in multi-agonist priming conditions. The selective blocking of fibrinogen in a pairwise combination results in the recovery of a single-agonist titration response. (***$p < 0.0005$, **$p < 0.005$)

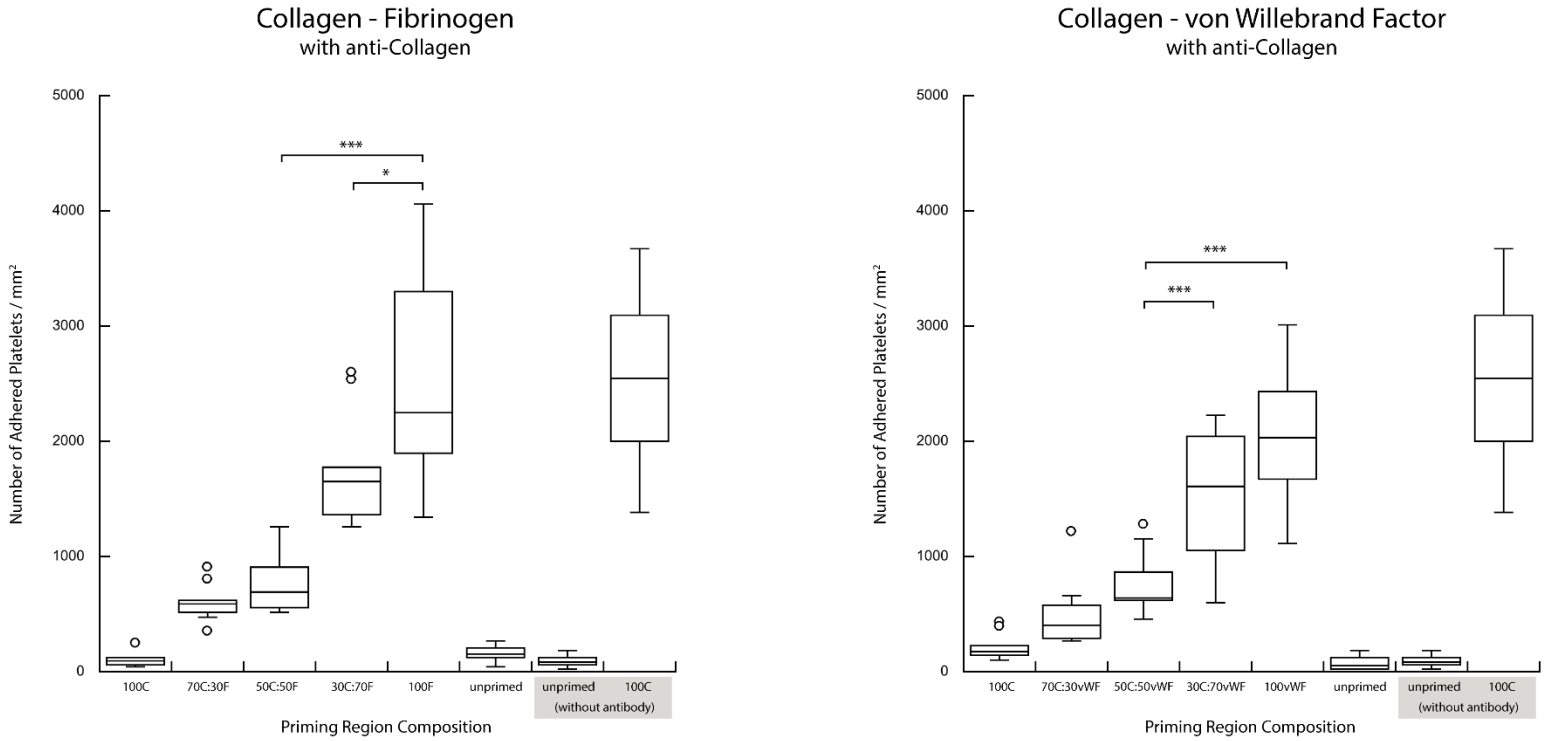

Figure 4.8: Selective blocking of collagen in multi-agonist priming conditions. The selective blocking of collagen in a pairwise combination results in the recovery of a single-agonist titration response. (***$p < 0.0005$, *$p < 0.05$)

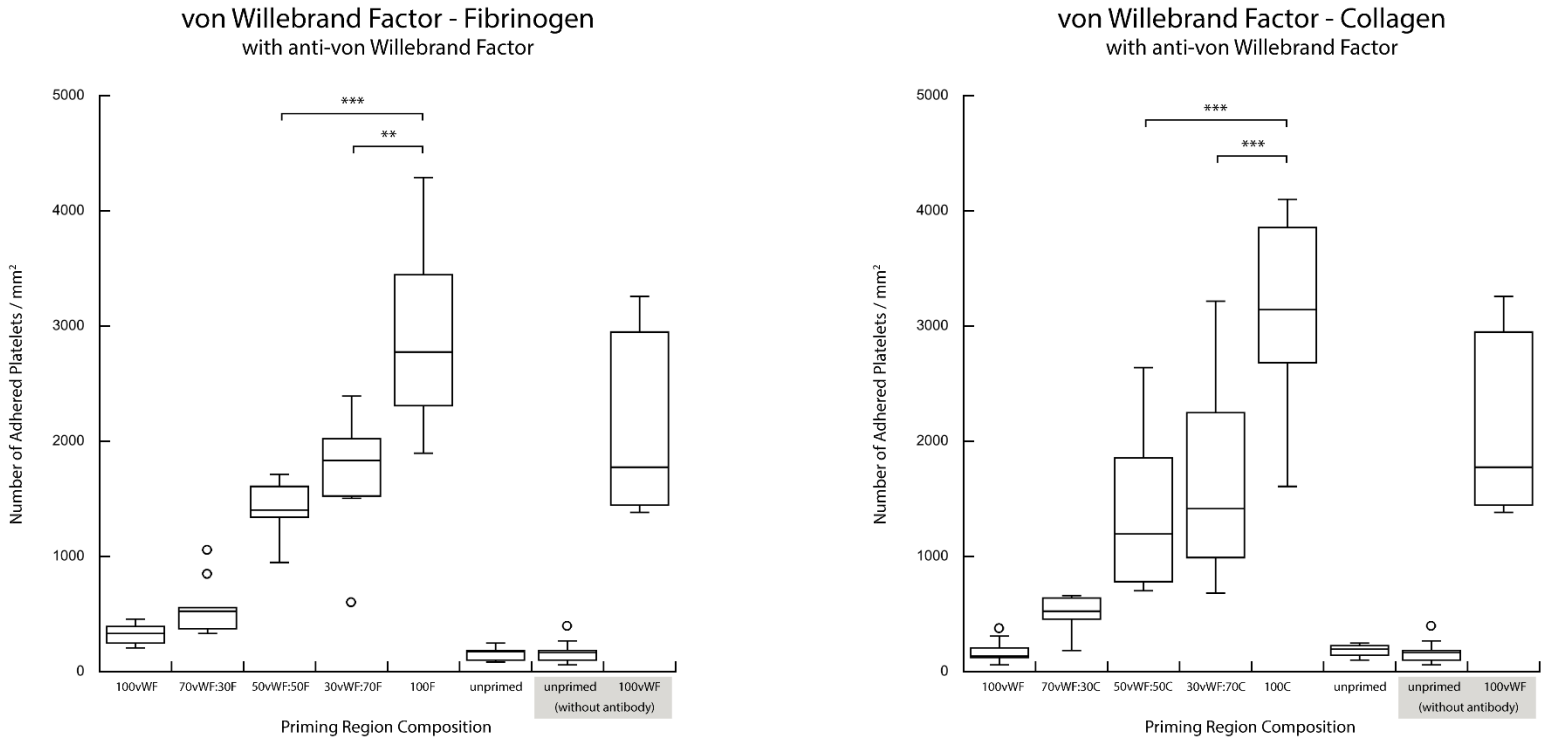

Figure 4.9: Selective blocking of von Willebrand factor in multi-agonist priming conditions. The selective blocking of von Willebrand factor in a pairwise combination results in the recovery of a single-agonist titration response. (***$p < 0.0005$, **$p < 0.005$)

this method was avoided in these experiments due to the affinity that collagen and vWF have for each other.[57,237] This interaction would make it impossible to control the surface densities of each of these species when presented in combination. The creation of multiagonist priming regions therefore took advantage of a previously developed technique to stamp multiple protein patterns in registry on the same surface (Chapter 3).[238] Through the use of this technique, multiagonist regions with varying surface coverage densities of each species were deposited on a glass substrate. Figure 4.2 shows the combinations of agonists used in the experiments, while Figure 4.3A shows an example of a transferred pattern combination. Due to the nature of the stamping process, error can be introduced in both the translational (x and y) and rotational (Θ) alignments of the second pattern with the first (Figure 4.3B). To verify the accuracy of stamp alignment, samples of each agonist were tagged with fluorophores, aligned and stamped on a substrate, then imaged with a fluorescent microscope. Image processing software was used to assess the total error in stamping across 10 test samples. The average stamping error observed was found to be 0.4 ± 0.1 μm of translation and 0.16 ± 0.03 degrees of rotation.

The consequences of error introduced in the stamping process are twofold. First, the total area covered by the stamps will be reduced as gaps are introduced between the two complimentary patterns when they overlap. These gaps will end up backfilled with albumin during the passivation process and therefore should not present any additional priming; however, the maximum priming response may not be achieved in conditions with agonist pairs. Second, the ratio of the surface coverage density between the two agonist species will be different from what is intended. For example, what was previously a 70A:30B ratio could become a 60A:30B ratio if a portion of the B agonist pattern was over-

stamped onto the A agonist pattern. This source of error is unavoidable in this method of stamping; however, it can be minimized by careful and precise alignment during the stamping process and by always depositing the larger of the two surface coverage densities first when generating the upstream priming regions. The translational and rotational errors in pattern alignment observed in stamped agonist samples resulted in minimal over-stamping and gaps in the pattern (Figure 4.3A). The smallest features in these patterns are 1 μm square, with the vast majority of features being much larger, resulting in pattern overlap of very small fractions of the total stamped area. As such, the error in alignment of patterns was deemed acceptable for these applications.

The results of the agonist pair titration experiments suggest that there is an enhanced priming response when multiple agonists are presented to a platelet population simultaneously compared to single-agonist priming conditions. The pairwise combinations had the same theoretical total surface coverage density as the plain field stamps (actual coverage would be less if stamping error is accounted for) and yet as seen in Figures 4.4, 4.5, and 4.6, they demonstrated a significantly higher priming response in each case. These results suggest the existence of a synergistic effect between platelet priming pathways.

Platelet priming depends on the transient interactions of platelets with agonists. In the case of these three agonist species, the receptors involved are the GPIb-IX-V complex and GPIIb/IIIa for vWF, GPVI and integrin α2β1 for collagen, and GPIIb/IIIa for fibrinogen. With the exception of GPIIb/IIIa which has an affinity for both vWF and fibrinogen, each of these agonists acts on a separate platelet receptor. Despite differences in structure and function, these receptors all share similarities in their signal transduction mechanisms. The binding of each of these receptors starts an intracellular signal

transduction chain that begins with the activation of one of a variety of PLC isoforms. Active isoforms of PLC are responsible for releasing cytosolic calcium ion stores from the dense tubular system, and also catalyzing the activation of PKC. Both calcium ions and activated PKC serve to amplify other activation pathways such as granule secretion, platelet morphology change, and the activation of GPIIb/IIIa (Figure 4.1).[235] Recent work has explored the crosstalk between platelet adhesion and activation receptors; however, much is still left to be discovered.[232,233,239,240]

The combination with the most regular pattern of enhanced adhesion was that of fibrinogen and collagen (Figure 4.4). As the surface density of the two species was titrated from 100 % fibrinogen to 100 % collagen, the number of adhered platelets was seen to increase for conditions with two agonists, with a maximum observed at a mixture of 50F:50C. This suggests that the pathways activated when fibrinogen interacts with the GPIIb/IIIa receptor and when collagen interacts with the GPVI and α2β1 receptors act to enhance the priming response in a manner that is not merely dose-dependent on each species. This implies that there is crosstalk between each of these priming pathways, and that the stimulus by multiple agonists serves to enhance the platelet priming response.

The mixture of vWF and collagen displayed a similar trend as the fibrinogen collagen combination, but with a larger enhanced priming response (Figure 4.6). The interplay between vWF and collagen in facilitating stable platelet adhesion *in vivo* has been well documented, so it is of little surprise that this combination exhibited the greatest enhanced priming response. In this case, each agonist has two main receptors by which to interact with platelets, the GPIb-IX-V complex and GPIIb/IIIa for vWF, and GPVI and α2β1 for collagen. Through the interaction of each of these agonists with multiple

receptors, there is a greater likelihood for a synergy between priming pathways within the cell. The redundancy in receptors and priming response is a theme mirrored throughout the coagulation response, and this combination of agonists (which best mimics how platelets interact with a damaged vessel) is no exception.

The receptor pair that showed the lowest levels of enhanced priming was that of vWF and fibrinogen (Figure 4.5). In each combination, the number of adhered platelets was seen to be greater than either vWF or fibrinogen alone, but no trend can be observed between each mixed case. This is surprising, as the interplay in binding to these two molecules is mainly responsible for the adhesion of platelets to artificial surfaces, and thus it is thought that they would exhibit a similar synergy as vWF and collagen which are responsible for adhesion in cases of vascular damage. One possible explanation is that the GPIIb/IIIa receptor shares an affinity for both of these agonists, thus the priming response generated by each of these agonists ends up being shared by the GPIIb/IIIa signaling pathway. For example, a platelet that has contacted a vWF patch and interacted via the GPIIb/IIIa receptor would trigger this priming pathway, thus subsequent contacts with fibrinogen patches would fail to contribute to the priming response. The increased priming response observed, however, may be the result of additional VWF interactions with the GPIb-IX-V complex.

These findings were further investigated through the selective blocking of each of the agonist species. The initial binary priming experiments were repeated in the presence of a polyclonal antibody against one of the two agonists stamped in the priming region. In Figures 4.7, 4.8, and 4.9, the results from these studies can be seen, which show that the enhanced activation response observed in the case of multiagonist priming was eliminated

when platelets were prevented from interacting with one of the species. Instead, results indicative of a typical single-agonist titration experiment were observed; *i.e.*, an increased downstream adhesion response is generated as a result of a greater priming stimulus. For example, when the agonists collagen and fibrinogen were titrated after the priming regions had been incubated with anticollagen, a dose-dependent response to the surface concentration of fibrinogen was observed, regardless of the concentration of stamped collagen. This result mirrors that of a single agonist fibrinogen titration experiment performed earlier (see Figure 2.3). Positive controls performed without the presence of an antibody confirmed the activity of each blocked species. Since the results of these experiments demonstrate a clear dose-dependent response to the nonblocked species, it is not anticipated that there is significant cross reactivity between antibodies and the nontarget agonist. Further verification could be performed using fluorescently tagged antibodies on nontarget antigen surfaces to confirm this assumption. These results demonstrate that the interaction of multiple functional agonists with platelet receptors is required to generate an enhanced priming response.

These experiments confirm that the heightened priming response is the result of the active interaction of platelets with more than one agonist species. Future work to further these findings could use antibodies or small molecule inhibitors to block individual priming pathways (as opposed to blocking the agonists) in order to investigate the role that each receptor plays in the synergistic effects of multiagonist platelet priming. It would also be of interest to see what role antiplatelet agents might play in attenuating the priming response generated by multiple agonist pathways.

4.5 Conclusion

In summary, the results presented in this chapter indicate that the stimulation of more than one priming pathway leads to an activation response that is more than the sum of the parts. Crosstalk between priming pathways likely leads to a synergistic effect which creates a higher activation response in a platelet population than can be generated with a single agonist alone. The existence of synergy between platelet priming pathways is a novel concept that could have broad implications for the fields of platelet activity testing as well as antiplatelet therapeutic evaluation. Since platelets *in vivo* encounter a multitude of agonists at surfaces, the ability to investigate the effects of multiple agonists on platelet priming and activation in a controlled environment is crucial for the understanding of the platelet response to a vascular device or lesion.

CHAPTER 5

SUMMARY AND FUTURE DIRECTIONS

The past 40 years have seen great advancement in the surgical and pharmaceutic treatment of cardiovascular diseases. A wide variety of life saving procedures are now available to patients with vascular deficiencies, including the implantation of heart valves, stents, and shunts. The integration of foreign materials into the body, however, is a process that has long been full of challenges. The implantation of biomaterials into the bloodstream is particularly challenging, as all known materials—save the native endothelium—inherently clot blood.[7,8] Many approaches have been taken in the device design process to reduce the haemostatic response to these materials, including surface coatings engineered to reduce protein adhesion, elute antithrombotic and antiplatelet drugs, and be repopulated by the native endothelium.[68,241–244] The most successful method to date, however, has come from the administration of systemic antiplatelet pharmaceutics. Platelets are of particular interest due to their central role in binding to surface adsorbed proteins and initiating the clotting cascade. To this effect, multiple platelet activation pathways have been identified as targets for therapeutics. Drugs such as cyclooxygenase inhibitors, ADP inhibitors, and GPIIb/IIIa inhibitors have all met with varying degrees of success in preventing adverse outcomes after the surgical introduction of blood contacting devices.[95,99,103,245] Not everyone in the population responds in the same manner to these treatments, however, with

some individuals requiring larger or smaller proportional doses to achieve the desired effect.[246] Additionally, a certain proportion of the population has been identified as nonresponders to common antiplatelet agents such as acetylsalicylic acid (ASA) and clopidogrel.[17,18,109] This variation in response across the patient population has led to a large industry devoted to the assessment of platelet function. Numerous methods have been developed and marketed to test the activity of platelets with and without antiplatelet agents in both the laboratory and clinical settings.[115,120] Despite the wide variety of platelet testing methods, there has been little improvement in predicting and preventing adverse clinical outcomes such as to postoperative device thrombosis.[132,133,141]

5.1 Summary of Work

The goal of the research detailed in this dissertation was to develop new tools with which to test platelet activity and the effects of antiplatelet agents. It is our belief that the local environment in which platelets interact with thrombogenic surfaces is only one factor that determines the activity of a platelet population. To get a more complete picture, the history of the platelets as they flow through the vasculature must be taken into account. Transient, nonadherent interactions with agonist covered surfaces have the ability to prime platelets for enhanced activation and adhesion at locations downstream of the initial stimulus. This principle was leveraged in Chapter 2 to create an assay with which to measure the activation response of a platelet population primed by an upstream agonist. Platelet activity was measured using a surface capture assay, the sensitivity of which was enabled by taking advantage of the phenomenon of platelet margination in flowing whole blood. The increased propensity for platelets to be at and remain near the wall of the flow

chamber due to exclusion by red blood cells made this assay sensitive enough to detect incremental changes in the intensity of the priming stimulus. The surface coverage density of fibrinogen in the upstream priming region was varied in order to increase or decrease the chances that any platelet would encounter an agonist when making transient contacts within the priming region. The number of platelets adhered in the downstream region was quantified and used as a metric of overall platelet activation. A dose-dependent response was observed between the number of adhered platelets and the surface coverage density of the priming region, demonstrating the sensitivity of this device to surface-bound antigens. This experiment was repeated in the presence of ASA, which was mixed with blood prior to perfusion at the recommended concentration for antiplatelet therapy. While a dose-dependent adhesion response to the upstream priming surface coverage was still observed, samples treated with ASA were seen to have significantly fewer platelets adhered than nontreated controls. This experiment demonstrated the ability to detect a stimulus dependent priming response in the presence of an antiplatelet agent. Finally, in this chapter two GPIIb/IIIa inhibitors were tested for their ability to attenuate a platelet priming response. Tirofiban and eptifibatide were both added to whole blood prior to perfusion at their recommended therapeutic concentration and at 1/10 of that level. Flow cells with 100 % surface coverage of fibrinogen were used in each case to elicit the maximum priming response. With both drugs, a dose-dependent response was observed between the concentration of GPIIb/IIIa inhibitor and the number of adhered platelets downstream, demonstrating the sensitivity of this assay in detecting the effects of various concentrations of antiplatelet agents in blood.

These experiments provide a proof of concept for the utility of this flow assay for

laboratory and clinical applications. The ability to detect the priming response of surface bound agonists is of great importance in the development of biomaterials and vascular devices. A platform in which researchers can investigate the priming pathways stimulated by individual agonists will help tease out the complex platelet priming, adhesion, and activation responses that current devices cannot. Additionally, the proof of a priming response to upstream agonists can help in dictating device design criteria, which should take into account the proximity of potential platelet priming sites such as high-shear regions or anastomotic locations. The clinical utility of this assay can be envisioned from the results of the antiplatelet studies. The ability to detect the efficacy of an antiplatelet agent in response to a variable stimulus, and the ability to detect the dose-dependent response from the administration of an antiplatelet agent, demonstrate the potential for this device in monitoring antiplatelet therapies. Using this assay, patients could be tested for their individual response to a prescribed therapeutic regimen, and nonresponders to individual therapeutics could be identified.

One possible concern with the methodology utilized in this assay arises from the use of sodium citrate to reduce the plasma calcium ion concentration in blood samples. Blood is drawn into 0.109 M monosodium citrate, which serves to chelate free calcium ions. Many coagulation factors require the presence of calcium in order to function properly, including the activation of factor X, the conversion of prothrombin to thrombin, and the binding of factors Xa and IXa to the surface of platelets. Through the addition of sodium citrate, coagulation of the blood samples can thus be avoided during blood draw, transport, and handling prior to the introduction of PPACK, a potent thrombin inhibitor.

The assay described here relies on the detection of an active platelet population

through the presence of the active form of GPIIb/IIIa on the surface of platelets. The association of GPIIb and GPIIIa is indeed calcium dependent; however, this process relies on the intracellular ion concentration and is largely independent of the plasma ion concentration.[247] An increase in cytoplasmic calcium concentration is caused by the association of one or more agonists with receptors on the platelet surface which cause a release of ions from the dense tubule system. These ions function to activate GPIIb/IIIa as well as regulate granule release reactions and facilitate stable adhesion and spreading through cytosolic reactions, which are unaffected by the plasma citrate concentrations.

Additionally, the introduction of sodium citrate to blood does not result in the elimination of calcium ions altogether. The dissociation of calcium ions from citrate salts have a pKa of 3.1, resulting in a reduced but measurable concentration of calcium in blood with a normal pH of 7.35.[248] The mean extracellular calcium ion concentration in blood treated with 3.8% sodium citrate was measured by Callan *et al.* and found to be 0.22 ± 0.02 mmol/L.[249] If, in the future, it is desired to study particular aspects of the coagulation cascade that require the presence of extracellular calcium using this assay, it is possible to add back free calcium ions to the blood prior to perfusion, or to eliminate the use of sodium citrate altogether by drawing blood directly into PPACK.

Another possible concern with this approach stems from experiments done by Horbett and Slack, which highlight the differences in adsorption characteristics of fibrinogen to surfaces under various surface and solution conditions.[250,251] In the current studies, the surface is constant in all cases (Nexterion slide H), the surface is patterned via microcontact printing (not solution adsorption), and the concentration of fibrinogen is kept constant across samples, irrespective of surface coverage density. The resulting

conformations of fibrinogen deposited on the priming and capture regions of all assays should therefore be consistent with each other, and are not subject to differences in adsorption kinetics or packing densities.

To further investigate the utility of this device, it was important to develop a method by which to pattern multiple proteins on the same surface so as to measure the response of a platelet population to multiple surface bound agonists. Traditional methods of multiprotein surface patterning such as dip pen nanolithography, inkjet printing, and microcontact printing all suffer from the lack of ability to pattern multiple patterns of proteins in precise registry across a large scale (~1 cm^2).[198] Chapter 3 details the development of a method to overcome these limitations. Taking advantage of advances in microcontact printing that enable micron-scale features, combined with the precise registration and optics of a modern light microscope, a new method by which to stamp multiple aligned patterns was created. In this process, an inverted light microscope was modified to hold both a micropatterned PDMS stamp and a glass substrate. The z-motion of the microscope stage provided the ability to bring the stamp in and out of contact with the substrate, while optics allowed for the visualization of this process in real time. By taking an image while a stamp was in contact with a substrate, the precise locations of features transferred to the substrate from the stamp were recorded. This image was then overlaid on the live image during subsequent stamping steps, which enabled the alignment of additional patterns with the first. In this way, multiple aligned patterns of proteins with micron scale features were created over large areas. Past work has shown that surfaces microcontact printed with proteins can become contaminated by oils or impurities from the PDMS stamp. This source of contamination was reduced in the experiments described in

the previous chapters using a couple of methods. The degree of contamination transferred to a surface has been shown to be a function of curing time of the polymer, with longer cure times resulting in lower amounts of contamination.[252] By allowing the PDMS stamps and microchannels to cure at room temperature as opposed to curing in an oven, a long cure time (> 24 hours) was achieved, thus reducing levels of contamination. Additionally, all new stamps and microchannels were subject to a soak in xylene, which has been shown to be effective in reversibly swelling the polymer and extracting unbound monomers and contaminants.[253] These methods will help in reducing the leeching of oils and monomers from the silicone; however, the elimination of such contamination should be verified using methods such as TOF-SIMS on the final stamped patterns. The development of this method was essential for the recreation of more complex priming environments with which to investigate multiple priming pathways in platelets.

When interacting with vascular lesions or implanted biomaterials, platelets encounter a wide variety of surface-presented agonists. It is logical to presume, with the number of redundancies built in to the platelet activation process, that multiple surface bound agonists could share responsibility for the priming effects observed in platelets. It was therefore of interest to investigate the ability of multiple agonists to prime platelets in flowing blood and observe what, if any, synergistic response platelets might have when primed by multiple pathways. Chapter 4 details experiments in which two agonists in varying surface coverage ratios were used to prime platelets in flowing whole blood. Using the technique developed in Chapter 3, flow cells were created that had two agonists in the priming region. Complementary stamp patterns were used to titrate the amount of each agonist species present, yet keep the total (theoretical) surface coverage density of the

priming region at 100 %. Blood was then perfused through the device as before, and adhered platelets in a downstream capture region were counted as a metric of activation. A synergistic priming effect was observed between pairs of platelet agonists, which resulted in enhanced adhesion in samples that were presented with multiple agonists as opposed to each agonist individually. The observed adhesion response was greater than would be anticipated from combinations of each agonist alone, that is to say, the total adhesion was observed to be greater than the sum of the parts. This phenomenon was verified by repeating each agonist pair titration in the presence of a polyclonal antibody against each species. The presence of a polyclonal antibody against one of the agonist species served to block platelet interaction with that species and prevent its contribution to the priming response. The result in each case was the recovery of a trend that mirrored that of a single agonist titration such as the one observed in Chapter 2.

These experiments demonstrate the sensitivity of this method in detecting the combinatorial response to multiple platelet agonists. The ability of platelets to become primed by transient interactions with surface-bound agonists has only recently been discovered, and the synergistic effects observed from stimulation of multiple priming pathways is a novel concept. This discovery could have implications in the design of biodevices in which the controlled surface presentation of specific molecules is of particular interest. Additionally, the presentation of multiple agonists provides a platform with which to test the effect of antiplatelet agents on the attenuation of individual priming pathways.

Taken collectively, these experiments contribute to the field of platelet activation study by providing a controlled environment in which to investigate the priming response

of platelets after transient exposure to a surface bound agonist. This upstream-priming downstream-activation response can be modified to investigate a wide variety of conditions by varying the strength and composition of the platelet agonist, alone or in the presence of antiplatelet agents. This ability is crucial for the future testing of biomaterials, as the priming effect of surface bound agonists has only recently been realized. The ability to detect the effects of common antiplatelet drugs on a platelet population also suggests a clinical application for these methods in the monitoring of antiplatelet therapies in the perioperative period of cardiovascular procedures. Finally, the development of novel antiplatelet therapies could benefit from the ability to rapidly screen their efficacy in attenuating activation in response to common agonists compared to current standards of care.

5.2 Future Directions

5.2.1 Device Design and Production

Despite the positive results seen from the assay generated for these studies, significant improvements could be made to improve on the design and production of this device. Due to the small number of flow cells needed for these studies, the methods by which fluidic channels were produced remained rudimentary. For example, each flow cell was cast, released, trimmed to size, bored for fluid vias, and assembled by hand. If the production of these devices were to be scaled up, they would benefit greatly from technologies aimed at the mass production, such as large-scale laser cutters, injection molds, or roll to roll processes.[254] Currently, capillary forces are responsible for holding the PDMS flow cell onto the glass substrate, which has proven to prevent leaks over the

duration of these experiments. Commercial devices, however, would need to be shelf-stable for long periods of time, so more advanced bonding methods would need to be employed such as the plasma treatment of contacting PDMS and glass surfaces or chemical adhesive methods. Additionally, other materials besides PDMS, such as poly(methyl methacrylate), polystyrene, or polycarbonate, might be considered in the production of flow channels for their ease in patterning by commercial laser equipment, rigidity for handling concerns, and ability to be bound to substrates.[255,256]

The flow channel design in these studies was kept macroscale, with dimensions of 1 mm x 70 mm x 0.1mm, both for ease in device manufacturing and consistency across all experiments. Future iterations of a similar upstream-priming downstream-adhesion assay could benefit greatly from a reduction in dimension, which would serve to decrease sample size and allow for the investigation of more conditions on a single device. The incorporation of an on-device pumping system or gravity fed flow could also reduce the countertop footprint of the assay and eliminate the need for an external syringe pump, though precise control of the shear rate would have to be investigated. Through the use of a platelet-specific antibody conjugated with a fluorescent tag, such as anti-CD42a or anti-CD61 (either through premixture or introduction in-device) a mechanism could be designed that images and detects platelets similar to an automated plate reader. Such a system would greatly reduce the burden to end-users, as the current method requires imaging and counting of platelets manually.

The surface patterning method developed for multiprotein printing could also be improved from methods used in currently available technologies. Presently, each stamp is leveled and aligned with previous patterns by hand, a tedious and time-consuming process.

Commercial photomask aligning tools have long since solved this problem through automated leveling and alignment techniques with a much higher degree of precision than necessary for these applications. Adaption of these technologies could prove useful for the future of large-scale multiprotein patterning and would serve to assist in the upscale of production of these devices.

5.2.2 Assay Applications

The applications of the assay demonstrated here only scratch the surface of its potential utility. In the current iteration of the device, there remains opportunity for the investigation of other platelet priming pathways. Three common platelet adhesion molecules were investigated in these studies; however, recent work has identified a wide variety of other molecules that act to prime platelets, such as soluble proteins, cytokines, hormones, and prostaglandins, which could provide interesting targets for future studies.[81] The incorporation of molecules such as these into this assay, either through surface immobilization or introduction during flow, would give insight into the priming of platelets by nonadhesion pathways. Experiments could be carried out as described in Chapter 2, with novel agonists stamped in the priming region, or introduced during flow using yet to be developed microfluidic devices. The number of adhered platelets to the capture region could then be assessed, and it is expected that numbers would vary based on the dose of the agonist presented to flowing platelets and the ability of that agonists to produce a priming response in platelets. Shear forces serve as another pathway by which platelets are activated, and could also be easily incorporated into the current design through the introduction of a stenotic priming region.[170,181] The degree of stenosis and length of the

stenotic region, coupled with the volumetric flow rate through the device, could be used to tailor the degree of shear priming stimulus. It is expected that elevated shear forces in an upstream position would serve to prime platelets for enhanced adhesion downstream in a dose-dependent fashion, with both upper and lower limits on this effect.

If the substrate of the device is switched out, the principle of upstream-priming and downstream-adhesion can also be used to test for priming by other agonist surfaces. By linking two devices in serial, one with a biomaterial as a substrate and another with a traditional surface capture assay on glass, the response of a platelet population to plasma proteins adsorbed to a specific material could be investigated. The use of whole blood would enable a protein adsorption response similar to that of an implanted material, and platelets would be allowed to interact with a system mimetic of an implanted biodevice. It is expected that the platelet priming response would depend on the identity and concentration of agonist species adsorbed to the biomaterial surface, which would be a function of the surface properties of the biomaterial itself. This would greatly assist in the development of novel materials and surface coatings for implanted vascular devices. Similarly, vascular lesions could be modeled by growing endothelial cells to confluence on a substrate and then introducing a physical scratch wound to the cell layer.[257] This scratch, when presented to flowing blood similar to assays described previously, could act as a priming region for platelets, and would present surface-bound agonists mimetic to those present in a vascular injury. It is expected that such a mimetic scratch would prime platelets for enhanced adhesion downstream due to the presence of exposed ECM. Finally, when surfaces are recolonized by an endothelial cell population (by design or not), these cells are typically characterized by an inflamed phenotype.[258] The use of tumor necrosis

factor (TNFα) to activate a confluent layer of endothelial cells could be useful as a model by which to characterize the platelet priming response to this environment.[259] Two flow chambers hooked in serial could be used to investigate this phenomenon, with the first chamber used to expose platelets to inflamed endothelial cells, and the second chamber used as a capture assay. It is expected that inflamed endothelial cells will prime platelets for enhanced adhesion downstream relative to native or passive endothelial cells. Work into the development of an endothelial activation flow cell model is currently ongoing.

The antiplatelet agent studies performed demonstrated the ability to detect the effects of two common antiplatelet pathways, yet a third common family, ADP inhibitors, remain uninvestigated. Due to it being a prodrug, cangrelor was excluded from current studies to avoid the need to recruit a patient donor population, especially with a developmental device. Since it is so widely used, however, it remains a prime target for investigation of its efficacy in attenuating platelet activation to surface bound agonists, as a significant proportion of the population demonstrates resistance to its effects. To perform this experiment, it would be necessary to recruit a population currently taking these prodrugs and repeat experiments as described in Chapter 2. It is expected that these drugs will attenuate the platelet priming response in a manner similar to GPIIb/IIIa inhibitors, due to their function of blocking internal activation pathways. There are a variety of other families of antiplatelet agents, including phosphodiesterase inhibitors, protease-activated receptor-1 inhibitors, adenosine reuptake inhibitors, and thromboxane inhibitors, each of which would be of interest for future studies.[260] This assay, with further development, could also prove useful as an efficient and cost-effective way to compare developmental drugs against currently recommended treatments in order to identify promising candidates.

Finally, the multi-agonist studies indicate that platelet priming pathways display a synergistic response that leads to enhanced activation and adhesion downstream of a binary agonist stimulus. These results suggest that there is a combinatorial priming response in platelets that interact with two or more agonists, likely due to crosstalk among intracellular priming pathways.[232,234,240] In these studies, only three common adhesion molecules were used, with each combination displaying similar trends, but varying degrees of synergy. The difference in the synergistic response observed for each of these pairs is thought to arise from the number and type of receptors that platelets have for each of these agonists; however, more studies are needed to confirm this hypothesis. The blocking of individual receptors on the surface of platelets would be a logical next step in teasing out the intricacies of this synergistic response. This experiment could be performed by repeating the agonist titration experiments described in Chapter 4, but in the presence of antigens for individual surface receptors for each agonist. It is expected that a synergistic priming response would still be observed, but this response would be diminished based on each receptor's individual contribution to the synergy. It would also be a logical extension of previous experiments to see how well antiplatelet agents do in attenuating the priming of platelet populations stimulated by multiple agonists. Recent theories have emerged postulating that individual resistance to antiplatelet agents is not due to the inefficacy of the drug, but that platelets are being activated by a pathway outside the target of the antiplatelet agent.[260] For example, if a patient was treated with ASA (which serves to inhibit cyclooxygenase) but had a thrombin-mediated activation stimulus, there might still exist a significant activated platelet population as these two pathways are independent. That individual might then be found to have an active platelet population and be classified

as a nonresponder to ASA treatment. Through the presentation of multiple agonists to platelets in flowing whole blood, the concept of antiplatelet resistance can be further explored through the isolation of individual activation pathways.

APPENDIX

STABILITY OF THE ALBUMIN PASSIVATION LAYER

A possible cause of concern with the current assay design is the stability of the adsorbed albumin layer. If the reactive NHS esters on the glass substrates are not sufficiently backfilled with albumin, blood soluble proteins could adsorb to the surface and create additional agonist regions which might serve to enhance the priming response of the platelet population. The use of albumin to passivate platelet flow cell surfaces has been previously established and validated in our lab.[85,261] Methods to elute proteins from surfaces using surfactants are also well established and were used to further probe the stability of adsorbed albumin.[262,263]

A Nexterion-H® (Schott) slide was printed with a 50 % surface coverage pattern of fibrinogen (unlabeled, 1 mg/mL in PBS, Sigma Aldrich) and then backfilled with fluorescently labeled albumin (1 mg/mL, Sigma Aldrich) (Alexa Fluor® 488, Sigma Aldrich). Figure A.1 shows the presence of adsorbed albumin both in between stamped islands of fibrinogen and in the rest of the flow channel. Figure A.1A shows the pattern immediately postadsorption, while Figure A.1B shows a region at the border of the stamped pattern on the same sample after an 18-hour incubation in 1 % surfactant (Alconox®) solution, followed by a 30-min sonication in a fresh surfactant solution.

The labeled albumin was seen to adhere to the NHS groups left unreacted after the

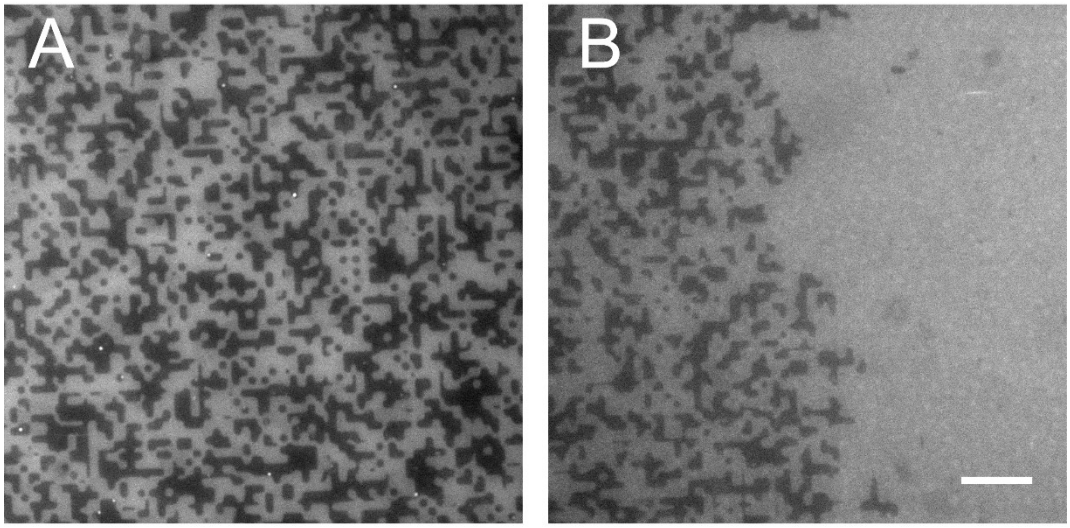

Figure A.1: Stability of the albumin passivation layer. A Nexterion-H® slide was stamped with a 50 % coverage pattern of fibrinogen (unlabeled) and backfilled with albumin (Alexa Fluor® 488). (A) Albumin was observed to interact only with NHS ester groups not previously occupied with stamped fibrinogen. (B) The stability of the pattern was verified after an 18-hour incubation and 30-min sonication in a surfactant solution both in the stamped region (left) and flow channel (right). Scale bar represents 10 μm.

printing of fibrinogen, both in the priming region as well as in the rest of the flow cell. Albumin did not interact with the previously deposited fibrinogen as indicated by the visible pattern in the printed region. The stability of the adhered protein despite an aggressive treatment with surfactant solution lends credibility to the idea that it is covalently attached.

These data show that albumin can be solution adsorbed to the surface of the flow cell and that it does not interfere with previously bound printed proteins. Additionally, the adsorbed protein layer is stable for long periods of time in environments designed to remove nonbound proteins; therefore, the state of the surface is not expected to appreciably change over the short time course of the flow assay experiments (5 min).

REFERENCES

1 M. Heron, *Natl. Vital Stat. Rep.*, 2013, **62**, 1–97.

2 University of Washington, *Inst. Heal. Metrics Eval.*, 2013, 2013.

3 D. Lloyd-Jones, R. Adams, M. Carnethon, G. De Simone, T. B. Ferguson, K. Flegal, E. Ford, K. Furie, A. Go, K. and Greenlund and N. Haase, *Circulation*, 2009, **119**, 119:e21–e181.

4 Centers for Disease Control and Prevention, *Div. Hear. Dis. Stroke Prev.*, 2011.

5 P. A. Heidenreich, J. G. Trogdon, O. A. Khavjou, J. Butler, K. Dracup, M. D. Ezekowitz, E. A. Finkelstein, Y. Hong, S. C. Johnston, A. Khera, D. M. Lloyd-Jones, S. A. Nelson, G. Nichol, D. Orenstein, P. W. Wilson and Y. J. Woo, *Circulation*, 2011, **123**, 933–944.

6 G. A. Mozaffarian D, Benjamin EJ, *Circulation*, 2015, **127**, e6.

7 B. D. Ratner, *J. Biomed. Mater. Res.*, 1993, **27**, 283–287.

8 B. D. Ratner, *Biomaterials*, 2007, **28**, 5144–5147.

9 S. C. Cannegieter, F. R. Rosendaal and E. Briet, *Circulation*, 1994, **89**, 635–641.

10 D. J. Fitzgerald, L. Roy, F. Catella and G. A. FitzGerald, *N Engl J Med*, 1986, **315**, 983–989.

11 F. J. Neumann, I. Ott, M. Gawaz, G. Puchner and A. Schömig, *J. Am. Coll. Cardiol.*, 1996, **27**, 819–824.

12 A. D. Oprea and W. M. Popescu, *Br. J. Anaesth.*, 2013, **111**, i3–17.

13 A. P. Amin, C. Ms, A. Bachuwar, K. J. Reid, A. K. Chhatriwalla, A. C. Salisbury, C. Ms, R. W. Yeh, C. Ms, M. Kosiborod, T. Y. Wang, K. P. Alexander, K. Gosch, D. J. Cohen, C. Ms, J. A. Spertus and R. G. Bach, *J. Am. Coll. Cardiol.*, 2013, **61**, 2130–2138.

14 T. A. Meadows and D. L. Bhatt, *Circ. Res.*, 2007, **100**, 1261–1275.

15 D. Capodanno and D. J. Angiolillo, *Circulation*, 2013, **128**, 2785–2798.

16 R. F. Storey, *Eur. Hear. J. Suppl.*, 2008, **10**, A21–A27.

17 T. A. Nguyen, J. G. Diodati and C. Pharand, *J. Am. Coll. Cardiol.*, 2005, **45**, 1157–1164.

18 G. Krasopoulos, S. J. Brister, W. S. Beattie and M. R. Buchanan, *BMJ*, 2008, **336**, 195–198.

19 A. D. Michelson, in *Platelets*, Academic Press, 2013, pp. 519–545.

20 A. Drouin and E. Cramer, in *Platelets in Thrombotic and Non-Thrombotic Disorders*, eds. P. Gresele, C. Page, V. Fuster and J. Vermylen, Cambridge University Press, Cambridge, 2002, pp. 25–40.

21 L. A. Harker, L. K. Roskos, U. M. Marzec, R. A. Carter, J. K. Cherry, B. Sundell, E. N. Cheung, D. Terry and W. Sheridan, *Blood*, 2000, **95**, 2514–2522.

22 J. A. Ware and B. S. Coller, in *Williams' Hematology*, 1994, p. 1161.

23 D. Blockmans, H. Deckmyn and J. Vermylen, in *Blood Reviews*, eds. V. Fuster, R. Ross and E. Topol, Lippincott-Raven Publishers, 1995, vol. 9, pp. 143–156.

24 D. A. Vorchheimer and R. Becker, *Mayo Clin. Proc.*, 2006, **81**, 59–68.

25 B. Sivaraman and R. A. Latour, *Biomaterials*, 2010, **31**, 1036–1044.

26 S. W. Kim, R. G. Lee, H. Oster, D. Coleman, J. D. Andrade, D. J. Lentz and D. Olsen, *ASAIO J.*, 1974, **20**, 449–455.

27 H. R. Baumgartner, R. Muggli, T. B. Tschopp and V. T. Turito, *Thromb. Haemost.*, 1976, **35**, 124–138.

28 R. Flaumenhaft, J. R. Dilks, N. Rozenvayn, R. A. Monahan-Earley, D. Feng and A. M. Dvorak, *Blood*, 2005, **105**, 3879–3887.

29 R. D. Allen, L. R. Zacharski, S. T. Widirstky, R. Rosenstein, L. M. Zaitlin and D. R. Burgess, *J. Cell Biol.*, 1979, **83**, 126–142.

30 S. R. Hanson and E. I. Tucker, *Biomater. Sci.*, 2013, 551–557.

31 B. D. Ratner, *J. Biomater. Sci. Polym. Ed.*, 2000, **11**, 1107–1119.

32 R. F. Padera and F. J. Schoen, *Biomater. Sci. - An Introd. to Mater. Med. (2nd Ed.*, 2004, 470–493.

33 J. M. Grunkemeier, W. B. Tsai, C. D. McFarland and T. A. Horbett, *Biomaterials*, 2000, **21**, 2243–2252.

34 Z. M. Ruggeri and G. L. Mendolicchio, *Circ. Res.*, 2007, **100**, 1673–1685.

35 H. V Stel, K. S. Sakariassen, P. G. de Groot, J. A. van Mourik and J. J. Sixma, *Blood*, 1985, **65**, 85–90.

36 V. T. Turitto, H. J. Weiss, T. S. Zimmerman and I. I. Sussman, *Blood*, 1985, **65**, 823–831.

37 P. André, C. V. Denis, J. Ware, S. Saffaripour, R. O. Hynes, Z. M. Ruggeri and D. D. Wagner, *Blood*, 2000, **96**, 3322–3328.

38 Z. M. Ruggeri and Ruggeri ZM, *J. Thromb. Haemost.*, 2003, **1**, 1335–42.

39 J. Ware and Z. M. Ruggeri, in *Wiley Encyclopedia of Molecular Medicine*, John Wiley & Sons, London, 2002, pp. 2158–520.

40 M. H. Kroll, T. S. Harris, J. L. Moake, R. I. Handin and A. I. Schafer, *J. Clin. Invest.*, 1991, **88**, 1568–73.

41 S. Goto, D. R. Salomon, Y. Ikeda and Z. M. Ruggeri, *J. Biol. Chem.*, 1995, **270**, 23352–23361.

42 B. Obert, A. Houllier, D. Meyer and J. P. Girma, *Blood*, 1999, **93**, 1959–68.

43 L. Badimon, J. J. Badimon, V. T. Turitto and V. Fuster, *Blood*, 1989, **73**, 961–7.

44 R. K. Andrews and M. C. Berndt, *J. Clin. Invest.*, 2008, **118**, 3009–3011.

45 M. Auton, C. Zhu and M. A. Cruz, *Biophys. J.*, 2010, **99**, 1192–1201.

46 T. Yago, J. Lou, T. Wu, J. Yang, J. J. Miner, L. Coburn, J. A. López, M. A. Cruz, J. F. Dong, L. V. McIntire, R. P. McEver and C. Zhu, *J. Clin. Invest.*, 2008, **118**, 3195–3207.

47 S. Goto, Y. Ikeda, E. Saldívar and Z. M. Ruggeri, *J. Clin. Invest.*, 1998, **101**, 479–486.

48 B. T. Marshall, M. Long, J. W. Piper, T. Yago, R. P. McEver and C. Zhu, *Nature*, 2003, **423**, 190–3.

49 G. Interlandi and W. Thomas, *Proteins Struct. Funct. Bioinforma.*, 2010, **78**, 2506–2522.

50 R. K. Andrews and M. C. Berndt, *Thromb. Res.*, 2004, **114**, 447–453.

51 A. Kasirer-Friede, M. R. Cozzi, M. Mazzucato, L. De Marco, Z. M. Ruggeri and S. J. Shattil, *Blood*, 2004, **103**, 3403–3411.

52 M. Ieko, T. Yasukouchi, M. Kohno, A. Notoya, T. Tarumi, K. Sawada and T. Koike, *Higashi Nippon Dent. J.*, 1997, **16**, 261–270.

53 B. S. Coller, J. H. Beer, L. E. Scudder and M. H. Steinberg, *Blood*, 1989, **74**, 182–192.

54 B. Nieswandt and S. P. Watson, *Blood*, 2003, **102**, 449–461.

55 S. A. Santoro and M. M. Zutter, *Thromb. Haemost.*, 1995, **74**, 813–821.

56 B. Savage, M. Cattaneo and Z. M. Ruggeri, *Curr. Opin. Hematol.*, 2001, **8**, 270–276.

57 M. A. Cruz, H. Yuan, J. R. Lee, R. J. Wise and R. I. Handin, *J. Biol. Chem.*, 1995, **270**, 10822–10827.

58 F. I. Pareti, Y. Fujimura, J. a Dent, L. Z. Holland, T. S. Zimmerman and Z. M. Ruggeri, *J. Biol. Chem.*, 1986, **261**, 15310–5.

59 H. Deckmyn and K. Vanhoorelbeke, *Blood*, 2006, **108**, 3628.

60 T. Lisman, N. Raynal, D. Groeneveld, B. Maddox, A. R. Peachey, E. G, P. G. De Groot, R. W. Farndale, W. Dc and E. G. Huizinga, *Blood*, 2009, **108**, 3753–3756.

61 Z. M. Ruggeri and B. Savage, in *Von Willebrand Factor and the Mechanisms of Platelet Function*, Springer-Verlag, Berlin, 1998, pp. 79–109.

62 Z. M. Ruggeri, J. a Dent and E. Saldívar, *Blood*, 1999, **94**, 172–178.

63 C. G. Knight, L. F. Morton, D. J. Onley, A. R. Peachey, T. Ichinohe, M. Okuma, R. W. Farndale and M. J. Barnes, *Cardiovasc. Res.*, 1999, **41**, 450–457.

64 S. Watson, J. Auger, O. McCarty and A. Pearce, *J. Thromb. Haemost.*, 2005, **3**, 1752–1762.

65 C. G. Knight, L. F. Morton, A. R. Peachey, D. S. Tuckwell, R. W. Farndale and M. J. Barnes, *J. Biol. Chem.*, 2000, **275**, 35–40.

66 S. A. Santoro, J. J. Walsh, W. D. Staatz and K. J. Baranski, *Cell Regul.*, 1991, **2**, 905–13.

67 G. A. Marguerie, E. F. Plow and T. S. Edgington, *J. Biol. Chem.*, 1979, **254**, 5357–5363.

68 J. D. Andrade and V. Hlady, *Adv. Polym. Sci.*, 1986, **79**, 1–63.

69 J. D. Andrade and V. Hlady, *Ann. N. Y. Acad. Sci.*, 1987, **516**, 158–172.

70 J. W. Weisel, *Adv.Protein Chem.*, 2005, **70**, 247–299.

71 C. Fuss, J. C. Palmaz and E. A. Sprague, *J. Vasc. Interv. Radiol.*, 2001, **12**, 677–682.

72 J. S. Bennett, *Ann. N. Y. Acad. Sci.*, 2001, **936**, 340–354.

73 B. Savage and Z. M. Ruggeri, *J. Biol. Chem.*, 1991, **266**, 11227–11233.

74 B. Sivaraman and R. A. Latour, *Biomaterials*, 2010, **31**, 832–839.

75 B. Savage, E. Saldívar and Z. M. Ruggeri, *Cell*, 1996, **84**, 289–297.

76 Y. Ikeda, M. Handa, K. Kawano, T. Kamata, M. Murata, Y. Araki, H. Anbo, Y. Kawai, K. Watanabe, I. Itagaki, K. Sakai and Z. M. Ruggeri, *J. Clin. Invest.*, 1991, **87**, 1234–1240.

77 S. Kamath, A. D. Blann and G. Y. H. Lip, *Eur. Heart J.*, 2001, **22**, 1561–1571.

78 W. Siess, *Physiol. Rev.*, 1989, **69**, 58–178.

79 J. Lefkovits, E. F. Plow and E. J. Topol, *New Engl. J. Med.*, 1995, **332**, 1553–1559.

80 M. F. Hoylaerts, in *Platelets in Thrombotic and Non-Thrombotic Disorders: Pathophysiology*, eds. P. Gresele, C. Page, V. Fuster and J. Vermylen, Cambridge University Press, Cambridge, 2002, pp. 357–368.

81 E. Falcinelli and S. Momi, in *Platelets in Hematologic and Cardiovascular Disorders*, eds. P. Gresele, V. Fuster, J. Lopez, C. Page and J. Vermylen, Cambridge University Press, 2007, pp. 53–78.

82 P. Gresele, E. Falcinelli and S. Momi, *Trends Pharmacol. Sci.*, 2008, **29**, 352–360.

83 M. N. Godo and M. V. Sefton, *Biomaterials*, 1999, **20**, 1117–1126.

84 L. E. Corum and V. Hlady, *Biomaterials*, 2012, **33**, 1255–1260.

85 L. E. Corum, C. D. Eichinger, T. W. Hsiao and V. Hlady, *Langmuir*, 2011, **27**, 8316–8322.

86 A. L. Fogelson, *J. Comput. Phys.*, 1984, **56**, 111–134.

87 A. L. Fogelson and R. D. Guy, *Comput. Methods Appl. Mech. Eng.*, 2008, **197**, 2087–2104.

88 K. Leiderman, The University of Utah, 2010.

89 G. M. FitzGibbon, A. J. Leach, H. P. Kafka and W. J. Keon, *J. Am. Coll. Cardiol.*, 1991, **17(5)**, 1557–1565.

90 A. Asif, F. N. Gadalean, D. Merrill, G. Cherla, C. D. Cipleu, D. L. Epstein and D. Roth, *Kidney Int.*, 2005, **67**, 1986–1992.

91 R. Guidoin, X. Deng and Y. Marois, *ASAIO J.*, 1997, **43**, 239 – 241.

92 L. R. Sauvage, M. W. Walker, K. Berger, S. B. Robel, M. M. Lischko, S. G. Yates and G. A. Logan, *Arch. Surg.*, 1979, **114**, 687–91.

93 D. Capodanno, J. L. Ferreiro and D. J. Angiolillo, *J. Thromb. Haemost.*, 2013, **11**, 316–329.

94 P. Robless, D. P. Mikhailidis and G. Stansby, *Br. J. Surg.*, 2001, **88**, 787–800.

95 C. Patrono, C. Baigent, J. Hirsh and G. Roth, *CHEST J.*, 2008, **133**, 199S–233S.

96 S. R. Messé and B. L. Cucchiara, *UpToDate*, 2015.

97 R. C. Becker, T. W. Meade, P. B. Berger, M. Ezekowitz, C. M. O'Connor, D. A. Vorchheimer, G. H. Guyatt, D. B. Mark and R. A. Harrington, *CHEST J.*, 2008, **133**, 776S–814S.

98 E. J. Topol and N. J. Schork, *Nat. Med.*, 2011, **17**, 40–41.

99 S. P. Jackson and S. M. Schoenwaelder, *Nat. Rev. Drug Discov.*, 2003, **2**, 775–789.

100 J. J. J. van Giezen and R. G. Humphries, in *Seminars in thrombosis and hemostasis*, Stratton Intercontinental Medical Book Corporation, c1974-, New York, 2005, vol. 31, pp. 195–204.

101 A. Pandit, M. R. Aryal, A. A. Pandit, L. Jalota, F. A. Hakim, F. Mookadam, H. R. Lee and I. M. Tleyjeh, *EuroIntervention*, 2014, **9**, 1350–1358.

102 R. F. Storey, R. G. Wilcox and S. Heptinstall, *Platelets.*, 2002, **13**, 407–413.

103 B. S. Coller, *Thromb. Haemost.*, 2001, **86**, 427–443.

104 K.-S. Woo, B.-R. Kim, J.-E. Kim, R.-Y. Goh, L.-H. Yu, M.-H. Kim and J.-Y. Han, *Korean J. Lab. Med.*, 2010, **30**, 460–8.

105 K.-E. Kim, K.-S. Woo, R.-Y. Goh, M.-L. Quan, K.-S. Cha, M.-H. Kim and J.-Y. Han, *Int. J. Lab. Hematol.*, 2010, **32**, 50–55.

106 M. M. C. Hovens, J. D. Snoep, J. C. J. Eikenboom, J. G. van der Bom, B. J. A. Mertens and M. V. Huisman, *Am. Heart J.*, 2007, **153**, 175–181.

107 P. A. Gurbel, K. P. Bliden, R. P. Kreutz, J. DiChiara, M. J. Antonino and U. S. Tantry, *Platelets.*, 2009, **20**, 97–104.

108 N. Zimmermann, M. Kurt, A. Wenk, J. Winter, E. Gams and T. Hohlfeld, *Eur. J. Cardiothorac. Surg.*, 2005, **27**, 606–610.

109 G. Feher, A. Feher, G. Pusch, G. Lupkovics, L. Szapary and E. Papp, *Clin. Genet.*, 2009, **75**, 1–18.

110 V. L. Serebruany, S. R. Steinhubl, P. B. Berger, A. I. Malinin, D. L. Bhatt and E. J. Topol, *J. Am. Coll. Cardiol.*, 2005, **45**, 246–251.

111 C. L. Grines, R. O. Bonow, D. E. Casey, T. J. Gardner, P. B. Lockhart, D. J. Moliterno, P. O'Gara and P. Whitlow, *Circulation*, 2007, **115**, 813–8.

112 T. J. Helton, A. A. Bavry, D. J. Kumbhani, S. Duggal, H. Roukoz and D. L. Bhatt, *Am. J. Cardiovasc. Drugs*, 2007, **7**, 289–297.

113 W. W. Duke, *J. Am. Med. Assoc.*, 1910, **55**, 1185–1192.

114 R. P. Rodgers and J. Levin, in *Seminars in Thrombosis and Hemostasis*, 1990, vol. 16, pp. 1–20.

115 R. Paniccia, R. Priora, A. Liotta and R. Abbate, *Vasc Heal. Risk Manag*, 2015, **11**, 133–48.

116 J. L. Choi, S. Li and J. Y. Han, *Biomed Res. Int.*, 2014, **2014**.

117 G. V. R. Born, *Nature*, 1962, **194**, 927–929.

118 A. D. Michelson, *Circulation*, 2004, **110**, e489–e493.

119 P. Harrison, *Blood Rev.*, 2005, **19**, 111–123.

120 A. D. Michelson, A. L. Frelinger and M. I. Furman, *Am. J. Cardiol.*, 2006, **98**, S4–S10.

121 M. Cattaneo, C. P. Hayward, K. A. Moffat, M. T. Pugliano, Y. Liu and A. D. Michelson, *J. Thromb. Haemost.*, 2009, **7**, 1029.

122 E. A. Femia, M. Pugliano, G. Podda and M. Cattaneo, *Platelets*, 2012, **23**, 7–10.

123 C. P. Hayward, K. A. Moffat, A. Raby, S. Israels, E. Plumhoff, G. Flynn and J. L. Zehnder, *Am J Clin Pathol*, 2010, **134**, 955–963.

124 M. Cattaneo, C. Cerletti, P. Harrison, C. P. M. Hayward, D. Kenny, D. Nugent, P. Nurden, A. K. Rao, A. H. Schmaier, S. P. Watson, F. Lussana, M. T. Pugliano and A. D. Michelson, *J. Thromb. Haemost.*, 2013, **11**, 1183–1189.

125 J. W. Smith, S. R. Steinhubl, A. M. Lincoff, J. C. Coleman, T. T. Lee, R. S. Hillman and B. S. Coller, *Circulation*, 1999, **99**, 620–625.

126 J. W. van Werkum, A. M. Harmsze, E. H. A. M. Elsenberg, H. J. Bouman, J. M. Ten Berg and C. M. Hackeng, *Platelets*, 2008, **19**, 479–88.

127 S. R. Steinhubl, J. D. Talley, G. A. Braden, J. E. Tcheng, P. J. Casterella, D. J. Moliterno, F. I. Navetta, P. B. Berger, J. J. Popma, G. Dangas, R. Gallo, D. C. Sane, J. F. Saucedo, G. Jia, A. M. Lincoff, P. Theroux, D. R. Holmes, P. S. Teirstein and D. J. Kereiakes, *Circulation*, 2001, **103**, 2572–2578.

128 J. C. Wang, D. Aucoin-Barry, D. Manuelian, R. Monbouquette, M. Reisman, W. Gray, P. C. Block, E. H. Block, M. Ladenheim and D. I. Simon, *Am. J. Cardiol.*, 2003, **92**, 1492–1494.

129 S. K. Kundo, E. J. Heilmann, R. Sio, C. Garcia, R. M. Davidson and R. A. Ostgaard, in *Sem. Thromb. Hemostas.*, 1995, vol. 21, pp. 106–113.

130 E. J. Favaloro, *Haemophilia*, 2001, **7**, 170–179.

131 P. Harrison, *Br. J. Haematol.*, 2000, **111**, 733–744.

132 E. J. Favaloro, in *Seminars in Thrombosis and Hemostasis*, 2008, vol. 34, pp. 709–733.

133 A. Bartels, Y. Sarpong, J. Coberly, N. Hughes, J. Litt, J. Quick, J. Kessel, C. Nelson, J. Coughenour, S. L. Barnes, N. S. Litofsky, R. D. Hammer and S. Ahmad, *Surgery*, 2015, **158**, 1012–1019.

134 G. Kenet, A. Lubetsky, B. Shenkman, I. Tamarin, R. Dardik, G. Rechavi, A. Barzilai, U. Martinowitz, N. Savion and D. Varon, *Br. J. Haematol.*, 1998, **101**, 255–259.

135 O. Shenkman, N. Savion, R. Dardik, I. Tamarin and D. Varon, *Thromb. Res.*, 2000, **99**, 353–361.

136 N. Savion and D. Varon, *Pathophysiol. Haemost. Thromb.*, 2006, **35**, 83–88.

137 S. Einav, C. F. Dewey and H. Hartenbaum, *Exp. Fluids*, 1994, **202**, 196–202.

138 G. Spectre, A. Brill, A. Gural, B. Shenkman, N. Touretsky, E. Mosseri, N. Savion and D. Varon, *Platelets*, 2005, **16**, 293–299.

139 S. X. Anand, M. C. Kim, M. Kamran, S. K. Sharma, A. S. Kini, J. Fareed, D. A. Hoppensteadt, F. Carbon, E. Cavusoglu, D. Varon, J. F. Viles-Gonzalez, J. J. Badimon and J. D. Marmur, *Am. J. Cardiol.*, 2007, **100**, 417–424.

140 B. Shenkman, S. Matetzky, P. Fefer, H. Hod, Y. Einav, A. Lubetsky, D. Varon and N. Savion, *Thromb. Res.*, 2008, **122**, 336–345.

141 J. W. van Werkum, H. J. Bouman, N. J. Breet, J. M. Ten Berg and C. M. Hackeng, *Thromb. Res.*, 2010, **126**, 44–49.

142 W. A. Bonner, H. R. Hulett, R. G. Sweet and L. A. Herzenberg, *Rev. Sci. Instrum.*, 1972, **43**, 404–409.

143 A. D. Michelson and M. I. Furman, *Curr. Opin. Hematol.*, 1999, **6**, 342–8.

144 D. J. Weiss and A. Moritz, in *55th Annual Meeting of the American College of Veterinary Pathologists (ACVP) & 39th Annual Meeting of the American Society of Clinical Pathology (ASVCP)*, Elsevier, 2004, vol. 13.

145 S. J. Shattil, M. Cunningham and J. A. Hoxie, *Blood*, 1987, **70**, 307–15.

146 J. L. Ritchie, H. D. Alexander and I. M. Rea, *Clin. Lab. Haematol.*, 2000, **22**, 359–363.

147 C. L. Berman, E. L. Yeo, J. D. Wenceldrake, B. C. Furie, M. H. Ginsberg and B. Furie, *J. Clin. Invest.*, 1986, **78**, 130–137.

148 M. A. Mascelli, E. T. Lance, L. Damaraju, C. L. Wagner, H. F. Weisman and R. E. Jordan, *Circulation*, 1998, **97**, 1680–8.

149 L. K. Jennings and M. M. White, *Am. Heart J.*, 1998, **135**, S179–S183.

150 M. Quinn, A. Deering, M. Stewart, D. Cox, B. Foley and D. Fitzgerald, *Circulation*, 1999, **99**, 2231–2238.

151 B. Aleil, C. Ravanat, J. P. Cazenave, G. Rochoux, A. Heitz and C. Gachet, *J. Thromb. Haemost.*, 2005, **3**, 85–92.

152 B. E. J. Spurgeon, A. Aburima, N. G. Oberprieler, K. Taskén and K. M. Naseem, *J. Thromb. Haemost.*, 2014, **12**, 1733–1743.

153 A. L. Frelinger, M. I. Furman, M. D. Linden, Y. Li, M. L. Fox, M. R. Barnard and A. D. Michelson, *Circulation*, 2006, **113**, 2888–2896.

154 H. R. Baumgartner, *Microvasc. Res.*, 1973, **5**, 167–179.

155 V. T. Turitto and H. R. Baumgartner, *Microvasc. Res.*, 1975, **9**, 335–344.

156 T. V. Colace, G. W. Tormoen, O. J. T. McCarty and S. L. Diamond, *Annu. Rev. Biomed. Eng.*, 2013, **15**, 283–303.

157 C. D. Chin, V. Linder and S. K. Sia, *Lab Chip*, 2012, **12**, 2118.

158 Y. Zheng, J. Chen and J. A. López, *Thromb. Res.*, 2014, **133**, 525–531.

159 S. Zhu, B. A. Herbig, R. Li, T. V Colace, R. W. Muthard, K. B. Neeves and S. L. Diamond, *Biorheology*, 2015, **Preprint**, 1–16.

160 M. Roest, A. Reininger, J. J. Zwaginga, M. R. King and J. W. M. Heemskerk, *J. Thromb. Haemost.*, 2011, **9**, 2322–2324.

161 C. G. Conant, M. A. Schwartz, T. Nevill and C. Ionescu-Zanetti, *J. Vis. Exp.*, 2009, 3–5.

162 E. Westein, S. de Witt, M. Lamers, J. M. E. M. Cosemans and J. W. M. Heemskerk, *Platelets*, 2012, **23**, 501–509.

163 C. G. Conant, M. A. Schwartz and C. Ionescu-Zanetti, *J. Biomol. Screen.*, 2010, **15**, 102–106.

164 M. B. Lucitt, S. O'Brien, J. Cowman, G. Meade, L. Basabe-Desmonts, M. Somers, N. Kent, A. J. Ricco and D. Kenny, *Anal. Bioanal. Chem.*, 2013, **405**, 4823–4834.

165 E. Gutierrez, B. G. Petrich, S. J. Shattil, M. H. Ginsberg, A. Groisman and A. Kasirer-Friede, *Lab Chip*, 2008, **8**, 1486–95.

166 W. S. Nesbitt, E. Westein, F. J. Tovar-Lopez, E. Tolouei, A. Mitchell, J. Fu, J. Carberry, A. Fouras and S. P. Jackson, *Nat. Med.*, 2009, **15**, 665–673.

167 M. H. Flamm, T. V. Colace, M. S. Chatterjee, H. Jing, S. Zhou, D. Jaeger, L. F. Brass, T. Sinno and S. L. Diamond, *Blood*, 2012, **120**, 190–198.

168 S. F. Maloney, L. F. Brass and S. L. Diamond, *Integr. Biol.*, 2010, **2**, 183–92.

169 M. Li, N. A. Hotaling, D. N. Ku and C. R. Forest, *PLoS One*, 2014, **9**.

170 K. B. Neeves, A. A. Onasoga and A. R. Wufsus, *Curr. Opin. Hematol.*, 2013, **20**, 417–23.

171 S. P. Jackson, W. S. Nesbitt and E. Westein, *J. Thromb. Haemost.*, 2009, **7**, 17–20.

172 A. D. Michelson, *Am. J. Cardiol.*, 2009, **103**, 20A–26A.

173 E. Braunwald, D. Angiolillo, E. Bates, P. B. Berger, D. Bhatt, C. P. Cannon, M. I. Furman, P. Gurbel, A. D. Michelson, E. Peterson and S. Wiviott, *Clin Cardiol*, 2008, **31**, I10–6.

174 U. S. Tantry and P. A. Gurbel, *Nat Rev Cardiol*, 2011, **8**, 572–579.

175 C. Pouillot, P. Henry, P. Motreff, E. Van Belle, H. Rousseau, P. Aubry, J. Monségu, P. Sabouret, S. A. O. Connor, J. Abtan, M. Kerneis, C. Saint-etienne, O. Barthélémy, F. Beygui and J. Silvain, *N. Engl. J. Med.*, 2012, **367**, 2100–2109.

176 A. S. Go, D. Mozaffarian, V. L. Roger, E. J. Benjamin, J. D. Berry, W. B. Borden, D. M. Bravata, S. Dai and E. S. Fox, *Circulation*, 2013, **127**, 6–24.

177 S. Kulkarni, S. M. Dopheide, C. L. Yap, C. Ravanat, M. Freund, P. Mangin, K. A. Heel, A. Street, I. S. Harper, F. Lanza and S. P. Jackson, *J. Clin. Invest.*, 2000, **105**, 783–791.

178 J. Boldt, M. Wolf and A. Mengistu, *Anesth. Analg.*, 2007, **104**, 425–430.

179 C. G. Conant, M. A. Schwartz, J. E. Beecher, R. C. Rudoff, C. Ionescu-Zanetti and J. T. Nevill, *Biotechnol. Bioeng.*, 2011, **108**, 2978–2987.

180 S. P. Wu, S. Ringgaard, S. Oyre, M. S. Hansen, S. Rasmus and E. M. Pedersen, *J. Magn. Reson. Imaging*, 2004, **19**, 188–193.

181 P. A. Holme, U. Orvim, M. J. Hamers, N. O. Solum, F. R. Brosstad, R. M. Barstad and K. S. Sakariassen, *Arterioscler. Thromb. Vasc. Biol.*, 1997, **17**, 646–653.

182 R. L. Whitmore, *Rheology of the circulation*, Pergamon Press, Oxford ;New York, 1968.

183 T. G. Papaioannou, E. N. Karatzis, M. Vavuranakis, J. P. Lekakis and C. Stefanadis, *Int. J. Cardiol.*, 2006, **113**, 12–18.

184 A. Bernard, J. P. Renault, B. Michel, H. R. Bosshard and E. Delamarche, *Adv. Mater.*, 2000, **12**, 1067–1070.

185 G. M. Harbers, K. Emoto, C. Greef, S. W. Metzger, H. N. Woodward, J. J. Mascali, D. W. Grainger and M. J. Lochhead, *Chem. Mater.*, 2007, **19**, 4405–4414.

186 C. L. Feng, G. J. Vancso and H. Schönherr, *Adv. Funct. Mater.*, 2006, **16**, 1306–1312.

187 M. Amiji and K. Park, *J. Biomater. Sci. Polym. Ed.*, 1993, **4**, 217–234.

188 G. J. Tangelder, H. C. Teirlinck, D. W. Slaaf and R. S. Reneman, *Am. J. Physiol.*, 1985, **248**, H318–23.

189 P. A. Aarts, S. A. van den Broek, G. W. Prins, G. D. Kuiken, J. J. Sixma and R. M. Heethaar, *Arteriosclerosis*, 1988, **8**, 819–824.

190 A. W. Tilles and E. C. Eckstein, *Microvasc. Res.*, 1987, **33**, 211–223.

191 E. C. Eckstein, A. W. Tilles and F. J. Millero, *Microvasc. Res.*, 1988, **36**, 31–39.

192 L. Crowl and A. L. Fogelson, *J. Fluid Mech.*, 2011, **676**, 348–375.

193 H. Zhao, E. S. G. Shaqfeh and V. Narsimhan, *Phys. Fluids*, 2012, **24**, 11902.

194 D. A. Reasor, M. Mehrabadi, D. N. Ku and C. K. Aidun, *Ann. Biomed. Eng.*, 2013, **41**, 238–249.

195 B. Savage, S. J. Shattil and Z. M. Ruggeri, *J. Biol. Chem.*, 1992, **267**, 11300–11306.

196 M. Mrksich, S. Huang, G. M. Whitesides and D. E. Ingber, *Science*, 1997, **276**, 1425–1428.

197 H. G. Craighead, S. W. Turner, R. C. Davis, C. James, A. M. Perez, P. M. St. John, M. S. Isaacson, L. Kam, W. Shain, J. N. Turner and G. Banker, *Biomed. Microdevices*, 1998, **1**, 49–64.

198 A. S. Blawas and W. M. Reichert, *Biomaterials*, 1998, **19**, 595–609.

199 L. Kam and S. G. Boxer, *J. Biomed. Mater. Res.*, 2000, **55**, 487–495.

200 R. S. Kane, S. Takayama, E. Ostuni, D. E. Ingber and G. M. Whitesides, *Biomaterials*, 1999, **20**, 2363–2376.

201 D. Kleinfeld, K. H. Kahler and P. E. Hockberger, *J. Neurosci.*, 1988, **8**, 4098–4120.

202 P. Clark, S. Britland and P. Connolly, *J. Cell Sci.*, 1993, **105**, 203–212.

203 C. D. James, R. Davis, M. Meyer, A. Turner, S. Turner, G. Withers, L. Kam, G. Banker, H. G. Craighead and M. Issacson, *Trans. Biomed. Eng.*, 2000, **47**, 17–21.

204 V. Hlady and G. Hodgkinson, *Materwiss. Werksttech.*, 2007, **38**, 975–982.

205 G. N. Hodgkinson, P. A. Tresco and V. Hlady, *Biomaterials*, 2008, **29**, 4227–4235.

206 R. D. Piner, J. Zhu, F. Xu, S. Hong and C. A. Mirkin, *Science*, 1999, **283**, 661–663.

207 Y.-S. Lee and M. Mrksich, *Trends Biotechnol.*, 2002, **20**, S14–S18.

208 K. Salaita, Y. Wang and C. a Mirkin, *Nat. Nanotechnol.*, 2007, **2**, 145–155.

209 P. Calvert, *Chem. Mater.*, 2001, **13**, 3299–3305.

210 E. A. Roth, T. Xu, M. Das, C. Gregory, J. J. Hickman and T. Boland, *Biomaterials*, 2004, **25**, 3707–3715.

211 L. R. Allain, D. N. Stratis-Cullum and T. Vo-Dinh, *Anal. Chim. Acta*, 2004, **518**, 77–85.

212 A. Kumar and G. M. Whitesides, *Appl. Phys. Lett.*, 1993, **63**, 2002–2004.

213 Y. Xia and G. M. Whitesides, *Annu. Rev. Mater. Sci.*, 1998, **28**, 153–184.

214 A. Perl, D. N. Reinhoudt and J. Huskens, *Adv. Mater.*, 2009, **21**, 2257–2268.

215 R. D. Deegan, O. Bakajin, T. F. Dupont, G. Huber, S. R. Nagel and T. A. Witten, *Lett. to Nat.*, 1997, **389**, 827–829.

216 Z. Zheng, W. L. Daniel, L. R. Giam, F. Huo, A. J. Senesi, G. Zheng and C. A. Mirkin, *Angew. Chemie - Int. Ed.*, 2009, **48**, 7626–7629.

217 M. S. Hasenbank, T. Edwards, E. Fu, R. Garzon, T. F. Kosar, M. Look, A. Mashadi-Hossein and P. Yager, *Anal. Chim. Acta*, 2008, **611**, 80–88.

218 L. K. Fiddes, H. K. C. Chan, B. Lau, E. Kumacheva and A. R. Wheeler, *Biomaterials*, 2010, **31**, 315–320.

219 A. C. von Philipsborn, S. Lang, A. Bernard, J. Loeschinger, C. David, D. Lehnert, M. Bastmeyer and F. Bonhoeffer, *Nat. Protoc.*, 2006, **1**, 1322–1328.

220 F. Meng, V. Hlady and P. A. Tresco, *Biomaterials*, 2012, **33**, 1323–1335.

221 J. Raedler and E. Sackmann, *Langmuir*, 1992, **8**, 848–853.

222 J. Radler and E. Sackmann, *J. Phys. II*, 1993, **3**, 727–748.

223 M. D. Abràmoff, P. J. Magalhães and S. J. Ram, *Biophotonics Int.*, 2004, **11**, 36–41.

224 T. A. Doggett, G. Girdhar, A. Lawshé, D. W. Schmidtke, I. J. Laurenzi, S. L. Diamond and T. G. Diacovo, *Biophys. J.*, 2002, **83**, 194–205.

225 R. A. Kumar, J. Dong, J. A. Thaggard, M. A. Cruz, J. A. López and L. V McIntire, *Biophys. J.*, 2003, **85**, 4099–109.

226 N. A. Mody, O. Lomakin, T. A. Doggett, T. G. Diacovo and M. R. King, *Biophys. J.*, 2005, **88**, 1432–1443.

227 I. Kang, M. Raghavachari, C. M. Hofmann and R. E. Marchant, *Thromb. Res.*, 2007, **119**, 731–740.

228 B. Fuchs, U. Budde, A. Schulz, C. M. Kessler, C. Fisseau and C. Kannicht, *Thromb. Res.*, 2010, **125**, 239–245.

229 F. Jung, S. Braune and A. Lendlein, *Clin. Hemorheol. Microcirc.*, 2013, **53**, 97–115.

230 N. Ferraz, J. Carlsson, J. Hong and M. K. Ott, *J. Mater. Sci. Mater. Med.*, 2008, **19**, 3115–3121.

231 D. T. L. Jaeger and S. L. Diamond, *Biotechniques*, 2013, **54**, 271–277.

232 B. Nieswandt, W. Bergmeier, A. Eckly, V. Schulte, P. Ohlmann, J. P. Cazenave, H. Zirngibl, S. Offermanns and C. Gachet, *Blood*, 2001, **97**, 3829–3835.

233 B. Ashby, J. L. Daniel and J. B. Smith, *Hematol. Oncol. Clin. North Am.*, 1990, **4**, 1–26.

234 A. R. Hardy, M. L. Jones, S. J. Mundell and A. W. Poole, *Blood*, 2004, **104**, 1745–1752.

235 Z. Li, M. K. Delaney, K. A. O'Brien and X. Du, *Arterioscler. Thromb. Vasc. Biol.*, 2010, **30**, 2341–2349.

236 J. A. López and K. Andrew, *Science*, 1997, **29**, 91–105.

237 T. H. C. Brondijk, D. Bihan, R. W. Farndale and E. G. Huizinga, *Proc. Natl. Acad. Sci. U. S. A.*, 2012, **109**, 5253–5258.

238 C. D. Eichinger, T. W. Hsiao and V. Hlady, *Langmuir*, 2012, **28**, 2238–2243.

239 T. M. Quinton, F. Ozdener, C. Dangelmaier, J. L. Daniel and S. P. Kunapuli, *Blood*, 2002, **99**, 3228–3234.

240 C. L. Yap, S. C. Hughan, S. L. Cranmer, W. S. Nesbitt, M. M. Rooney, S. Giuliano, S. Kulkarni, S. M. Dopheide, Y. Yuan, H. H. Salem and S. P. Jackson, *J. Biol. Chem.*, 2000, **275**, 41377–88.

241 C. J. Wilson, R. E. Clegg, D. I. Leavesley and M. J. Pearcy, *Tissue Eng.*, 2005, **11**, 1–18.

242 M. C. Frost, M. M. Reynolds and M. E. Meyerhoff, *Biomaterials*, 2005, **26**, 1685–1693.

243 G. Mani, M. D. Feldman, D. Patel and C. M. Agrawal, *Biomaterials*, 2007, **28**, 1689–1710.

244 W. He, T. Yong, W. E. Teo, Z. Ma and S. Ramakrishna, *Tissue Eng.*, 2005, **11**, 1574–1588.

245 B. S. Coller, *Annu Rev Med*, 1992, **43**, 171–180.

246 W. Kuliczkowski, A. Witkowski, L. Polonski, C. Watala, K. Filipiak, A. Budaj, J. Golanski, D. Sitkiewicz, J. Pregowski, J. Gorski, M. Zembala, G. Opolski, K. Huber, H. Arnesen, S. D. Kristensen and R. De Caterina, *Eur. Heart J.*, 2009, **30**, 426–435.

247 S. Tsuboi, *J. Biol. Chem.*, 2002, **277**, 1919–1923.

248 N. R. Joseph, *J. Biol. Chem.*, 1946, **164**, 529–541.

249 M. B. Callan, F. S. Shofer and J. L. Catalfamo, *Am. J. Vet. Res.*, 2009, **70**, 472–477.

250 S. M. Slack and T. A. Horbett, *J. Colloid Interface Sci.*, 1988, **124**, 535–551.

251 S. M. Slack, S. E. Posso and T. A. Horbett, *J. Biomater. Sci. Polym. Ed.*, 1992, **3**, 49–67.

252 C. Thibault, C. Séverac, A.-F. Mingotaud, C. Vieu and M. Mauzac, *Langmuir*, 2007, **23**, 10706–10714.

253 J. N. Lee, C. Park and G. M. Whitesides, *Anal. Chem.*, 2003, **75**, 6544–6554.

254 G. M. Whitesides, *Nature*, 2006, **442**, 368–73.

255 A. Alrifaiy, O. A. Lindahl and K. Ramser, *Polymers*, 2012, **4**, 1349–1398.

256 H. Becker and L. E. Locascio, *Talanta*, 2002, **56**, 267–287.

257 C.-C. Liang, A. Y. Park and J.-L. Guan, *Nat. Protoc.*, 2007, **2**, 329–333.

258 A. P. McGuigan and M. V. Sefton, *Biomaterials*, 2007, **28**, 2547–2571.

259 P. P. Nawroth and D. M. Stern, *J. Exp. Med.*, 1986, **163**, 740–5.

260 D. Cox, in *Platelets in Hematological and cardiovascular disorders (A clinical handbook)*, eds. P. Gresele, V. Fuster, J. A. Lopez, C. P. Page and J. Vermylen, Cambridge University Press, Cambridge, 2008, pp. 341–350.

261 L. E. Corum, University of Utah, 2011.

262 M. C. Wahlgren, T. Arnebrant, A. Askendal and S. Welin-Klintström, *Colloids Surfaces A Physicochem. Eng. Asp.*, 1993, **70**, 151–158.

263 P. Claesson, in *Advances in Colloid and Interface Science*, ACS Publications, 1995, vol. 57, pp. 161–227.